RHODES UNIVERSITY
DEPARTMENT OF GEOLOGY

GOLD MINERALIZATION IN AN ARCHAEAN GRANITE-GREENSTONE REMNANT WEST OF MELMOTH, NATAL: ORE GENESIS AND IMPLICATIONS FOR EXPLORATION

by
W D BULLEN

This thesis is submitted in partial fulfilment of the requirements for the degree of Master of Science (Economic Geology), Rhodes University.

22nd December, 1990

Abstract

The previously undifferentiated, "Melmoth Granite-Greenstone Remnant" (MGGR') crops out over an area of about 360 km² in northern Natal, South Africa. The greenstone sequence is comprised mainly of mafic metalavas with lesser serpentinite, talc schist, dacitic tuff, quartz-muscovite schist, quartzite and calc-silicate rocks. The greenstones are intruded by syntectonic trondhjemitic gneisses, late-tectonic granodioritic gneisses and post-tectonic granite dykes. Four phases of deformation and metamorphism are recognized.

Epigenetic, disseminated and quartz vein-hosted gold mineralization is associated with D_2 shearing - a positive correlation existing between the intensity of the shearing, the thickness of the shear zone and the grade of ore it contains. Auriferous quartz veins are distinguished from an earlier generation of barren vein quartz on the basis of mineralogy, texture and relationship to the s-fabric. The mineralization occurs in zones of dilation associated with shear zone refraction. Associated wall rock alteration includes sericitization, argillization and chloritization. An ore genesis model based on the aforementioned parameters, is proposed.

Finally, an exploration programme has been devised in order to locate undiscovered gold deposits in the MGGR. The programme could probably be applied, with minor modifications, to shear zone-hosted gold deposits in other granite-greenstone remnants in northern Natal.

' - Name suggested by writer

CONTENTS

APPENDIX I

Major and Trace Element Contents of Rocks in the Study Area.

APPENDIX II

Gold and Silver Contents of Rocks in the Study area.

LIST OF FIGURES

LIST OF TABLES

1. INTRODUCTION

The Archaean, Melmoth Granite-Greenstone Remnant (MGGR) crops out about 8 km west-northwest of Melmoth, Natal (Fig. 1.1). The remnant was intensely prospected for epigenetic Au mineralization (and associated alluvial deposits) prior to the turn of the last century and a number of small mining operations were established. The two most important workings, which between them produced in excess of 36 kg Au (Du Toit, 1931), are situated in the study area. As far as the writer is aware, no recent work has been carried out on Au mineralization within the MGGR.

Interest in the so-called "Melmoth Goldfield" (Garrard, 1895) around the turn of the last century however, was tempered by a number of factors. These included, amoungst others, the coeval discovery of the Witwatersrand placer deposits in 1886, the 1899-1902 Anglo-Boer War, the financial depression in mining circles as a result of and immediately following the War and the 1905-6 Zulu Rebellion (Gray, 1907) of 1905/6. Prospecting in the MGGR was hindered by a further two factors. Firstly, most of the ground in the Melmoth area was held for speculative purposes only, the holders of the various claims not being interested at all in mining (Gray, 1904). The second problem was that most of the land surrounding Melmoth was privately owned (unlike the rest of Zululand). Prospectors were therefore recquired to purchase a prospecting licence as well as to pay a fee to the farm owner dependant on the size of the area under investigation (Garrard, 1898).

The old mining operations in the Melmoth Goldfield were characterized by mismanagement, incompetance and greed. Systematic development was rarely if ever carried out, attention being focussed largely on pockets of richer ore. Ore reserves were never computed, the workings were poorly laid out and employees were mistreated. The Resident Magistrate (quoted by Garrard, 1895) succinctly summed up the situation saying - "Several of the areas on private lands have every appearance of being payable. Some of these areas would in my opinion have now been worked to advantage with suitable machinery if the Harewood Gold Mining Company (the largest working in the area) had been

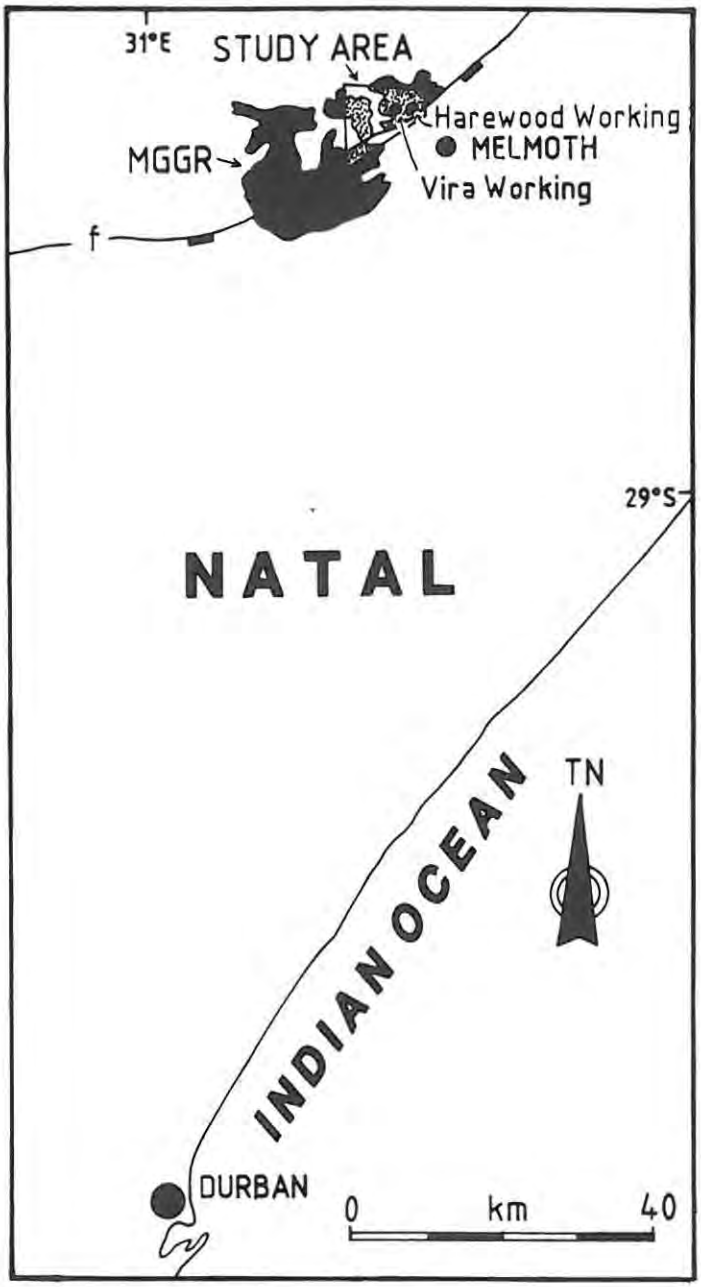

Figure 1.1 Locality map showing the approximate position of the MGGR. The study area, together with the Harewood and Vira Au workings, are indicated.

more satisfactory in the management of its property. This is the only property on which a battery has been erected. It has been worked for several years to a disadvantage, owing to mismanagement on the part of the Directors, and their neglect of their employees, who for several years have as a rule had to institute civil proceedings for the recovery of their wages before obtaining a settlement."

Furthermore, the nature of the mineralization itself was not fully understood. The auriferous quartz reefs, which commonly pinched out with depth, were generally classified as "gash veins" (Gray, 1900) in order to explain their apparently limited vertical extent. The result was that very few searches were made for reef extensions at deeper levels. In addition, it was seldom recognized that the Au was confined to well defined shoots rather than being evenly distributed throughout the reef. Finally some prospectors were even unaware which quartz reefs were Au-bearing and which were barren. For example the prospector in charge of the Times prospect, although aware that two quartz reefs of different ages - one mineralized and the other not - were present on the property, was unable to distinguish between the two (Garrard, 1898).

Au exploitation in the MGGR around the turn of the last century was therefore negatively affected by:

a) adverse political and economic factors.

b) inefficient prospecting and mining procedures.

A study to reassess the economic potential of the MGGR with respect to Au mineralization was therefore initiated by the writer. The derivation of an ore genesis model and the development of a related exploration programme were considered fundamental to the project.

Detailed geological mapping on a scale of 1:10 000 was undertaken throughout the ±35 km² study area in order to familiarize the writer with the geology of the inlier. This represented the first serious attempt to differentiate the various rock types. Particular attention was paid to the Nyani River valley near the western margin of the study area since the valley cuts across strike exposing a complete lithological succession. The area was previously mapped by Matthews in 1979 on a scale of 1:50 000. The amount of detail depicted however was limited and therefore wholly inadequate for the purposes of this project. The two workings enclosed within the study area (Fig. 1.1) were mapped on a scale of 1:1000 in order to elucidate pertinent features. Careful attention was paid to the structure of the area since its effect on mineralization was considered central to the project. Although extensive geological mapping was considered essential,

it must be emphasized that the project was principally an economic study.

Numerous thin-sections were cut for rock and mineral identification purposes as well as to study the effects of metamorphism and deformation. Where practical, polished sections from orebody samples were made. Major and trace element analyses were carried out on the principal lithological units as well as on altered wall rock assemblages adjacent to mineralized quartz reefs (Appendix I). Similar analyses were undertaken on gossanous material in the vicinity of the orebodies. Lastly, the Au and Ag concentrations of the main rock types, altered wall rock (at varying distances away from mineralized veins), gossanous material, auriferous quartz reefs and fault breccia associated with later (post-Natal Group) faulting were determined (Appendix II). It was decided to forego fluid inclusion studies owing to time constraints as well as to the limited value such studies would have in terms of an exploration model. Attention was paid to the effects of metamorphism, particularly in terms of an ore genesis model.

The old Harewood Au working is situated on an eastern spur of N'gwebu Mountain. Numerous shafts, incline shafts and adits were sunk on the reefs albeit in a totally unsystematic fashion. Mining ceased in 1898. The second working, referred to as the "Vira Reef" (Gray, 1910) is situated about 1 km west of the Harewood mine (Fig. 1.1). The Times prospect, which was worked intermittently between 1897 and 1901 (Gray, 1902), also occurs within the study area.

2. REGIONAL GEOLOGY

The MGGR forms part of the Kaapvaal craton which, together with the Zimbabwe craton and Limpopo Mobile Belt constitute the Archaean terrane of Southern Africa. The first two comprise predominantly pre- (possibly), syn-, late- and post-tectonic granitoid intrusives together with associated meta-volcanic and metasedimentary (greenstone) sequences. These acted as a basement upon which later supracrustal successions accumulated. Just over 80 000 km² of the Archaean regions of the Kaapvaal craton is exposed in the northern, western and eastern Transvaal and northern Natal (Anhaeusser, 1976). Greenstone sequences account for 7000 km² of this figure. In terms of average Au yields (in kgAu/km²), greenstone belts in Southern Africa, including those within the Zimbabwe craton, boast figures of around 40 (compared with 5 and 20 for similar successions in Canada and Australia respectively).

The largest, least altered, most extensively exposed and hence best studied greenstone belt in the Kaapvaal craton is the Barberton Mountain Land outcropping in the eastern Transvaal and Swaziland. The Barberton Sequence (Anhaeusser and Viljoen, 1986) has been subdivided into the Onverwacht, Fig Tree and Moodies Groups. The first (and lowermost) consists essentially of mafic and ultramafic lavas (komatiite, komatiitic basalt, high-Mg basalt and tholeiite) overlain by felsic rocks (quartz-sericite-fuchsite schist), banded iron-formation, banded chert and calc-silicate rocks. The last two consist mainly of detrital sediments with subordinate volcanic and pyroclastic members. Production from the more than 350 Au occurrences known in the Barberton Mountain Land for the period 1884 to 1983 totalled around 251 553 kg (Anhaeusser, 1986). Other principal areas of greenstone exposure occur in the vicinity of Sutherland, Pietersburg, Murchison, Muldersdrif and Amalia in the Transvaal. Five isolated greenstone remnants are exposed in Northern Natal (Fig. 2.1) namely, the Dwalile, Assegaai, de Kraalen, Commondale and Nondweni. The first four were loosely correlated with the Barberton Sequence but have recently been ascribed separate formation status (for example - Hunter, in press [a]). The last is regarded as a separate group (Lindström, 1987).

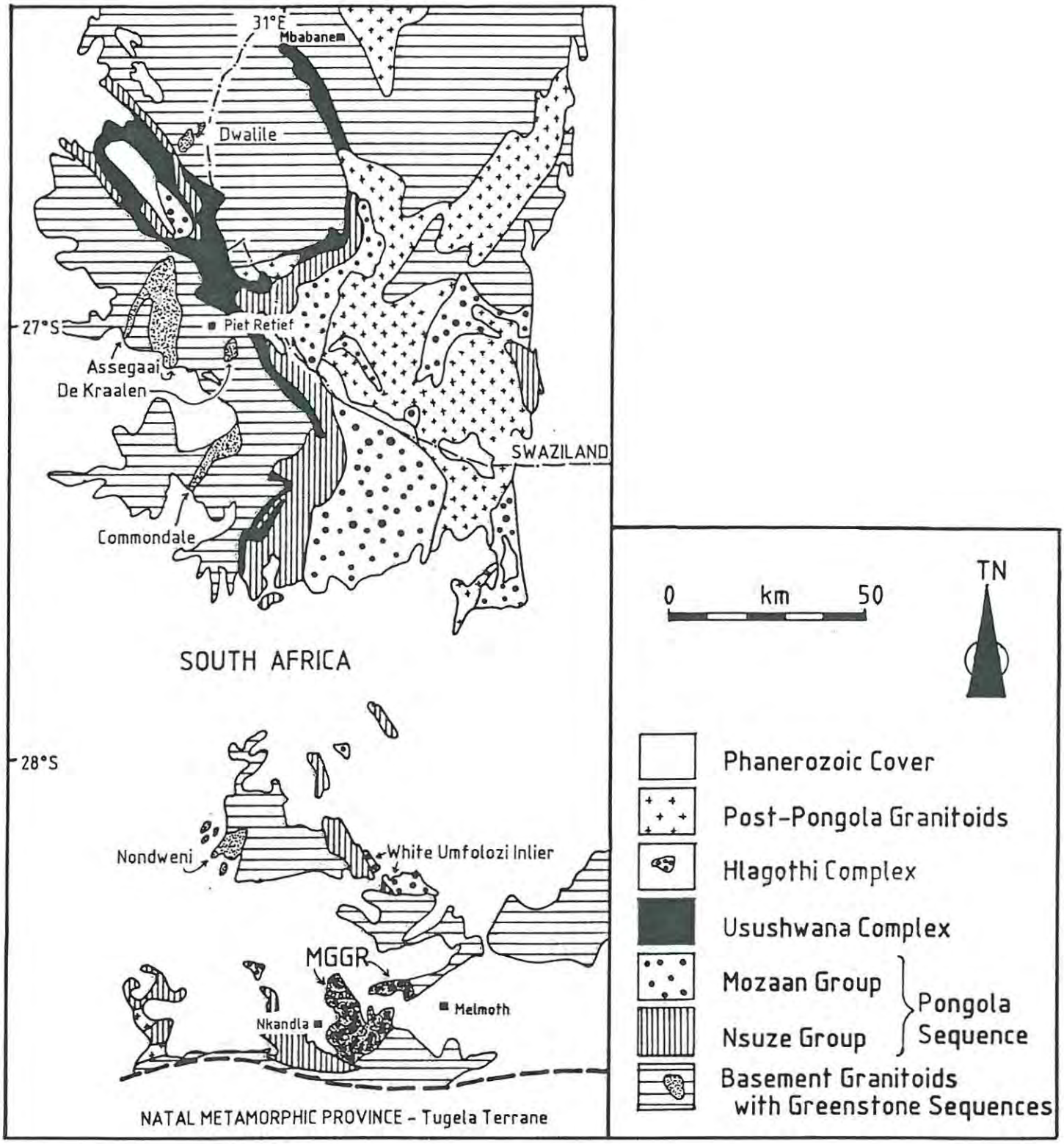

Figure 2.1 Simplified geological map of northern Natal and southwestern Swaziland. The main greenstone remnants and the MGGR are indicated.

The timing of geological events with respect to the evolution of the Kaapvaal craton has been the subject of some debate. A suite of tonalitic and trondhjemitic gneisses termed the "Ancient

Gneiss Complex" (Hunter, 1970) crop out to the south of the Barberton greenstone belt. The Complex was considered, on the basis of geophysics, geochemistry, metamorphic style and structural character, to predate the associated greenstones thus representing an early sialic crust upon which volcanic and sedimentary sequences accumulated. This idea was reiterated by Smith and Hunter (1988). Fouchè (1986), on the basis of extensive geophysical work, envisaged the presence of an extensive homogeneous primordial sialic crust in Southern Africa during the early Archaean. Continuously failing rift systems in the more attenuated portions of the proto-lithosphere provided pathways for the intrusion and extrusion of mantle derived magmas. Anhaeusser (1973) and Anhaeusser and Wilson (1981) however, discounted the presence of an early sialic crust. Instead, the Ancient Gneiss Complex was regarded as a remnant of a previously extensive ensimatic crust which predated granitoid nucleation. As such, the Complex was considered to postdate the initial stages of greenstone development. Field and geochemical evidence point to the derivation of the granitoids from mafic precursors such as those found near the base of the Barberton Sequence (Anhaeusser, 1986).

Age dating in the Barberton Mountain Land has failed to resolve the problem. Hamilton *et al.* (1979) reported Sm-Nd whole rock isochron ages of ≈3510 Ma for the earliest komatiite-dominant volcanic successions. Barton *et al.* (1983) on the other hand provided a maximum Rb-Sr age of 3491 ± 166 Ma for the Ancient Gneiss Complex. The primitive supracrustal sequences and the earliest granitic rocks therefore appeared, within the limits of geochronological error, to be genetically coeval. However, recent U-Pb dating by Compston and Kröner (1988) on zircons from the Ancient Gneiss Complex gave an age of 3644 ± 4 Ma, demonstrating that at least part of the Complex is older than the associated greenstones.

The MGGR is loosely correlated with the Nondweni Group (Lindström, 1987), the type area of which crops out near the village of Nondweni 60 km northwest of Melmoth (Fig. 2.1). The group has been divided into three formations, namely the Magongolozi, Toggekry and Witkop (Versveld *et al.*, 1988). The

first consists predominantly of mafic volcanic rocks. The second comprises largely quartz-feldspar-sericite-biotite schist with minor rhyolite, silicified pillowed basalt and chert. The uppermost Witkop Formation consists largely of pillowed mafic lava flows. (Vein-hosted Au mineralization in this formation was worked on a small scale prior to the turn of the last century). Sm-Nd isotopic dating by Wilson and Carlson (1986) yeilded an age of 3170 ± 50 Ma for the Nondweni greenstone belt. Recent Rb-Sr, Pb-Pb and U-Pb dating by Matthews *et al.* (1989) on the Mvunyana granodiorite which is intrusive into the eastern flank of the belt gave an age of approximately 3.29 Ga. Matthews *et al.* noted further that the Mvunyana intrusive represents the oldest granitoid component so far identified in the Archaean granite-greenstone terrane south of Swaziland, having been intruded during Anhaeusser and Robb's (1981) second magmatic cycle. Isotopic dating of granite-gneisses to the south and southeast of Melmoth produced ages in excess of 3.1 Ga (Matthews, 1988).

Continual underplating of the Kaapvaal proto-crust by tabular granitoid batholiths from about 3.2 Ga resulted in the rapid thickening of the crust culminating in the development of a stable, high-standing crustal plate around 3.0 Ga (Hunter, 1988). Gradual subsidence along the southeast margin of the stabilized Kaapvaal craton from about 3.0 Ga ago led to the accumulation of a thick volcanic and sedimentary package termed the Pongola Sequence (Fig. 2.1). The lower, predominantly volcanic Nsuze Group developed in response to incipient rifting in the more attenuated parts of the Pongola basin (Anhaeusser and Wilson 1981). The group attains a maximium thickness of ca. 8000 m southeast of Piet Rietief (Hunter and Wilson, 1988) but thins rapidly towards the south to less than 2500 m thick in the vicinity of Nkandla west of Melmoth (Button, 1981). The overlying, sedimentary Mozaan Group, which is about 2500 m thick southeast of Piet Retief, is not preserved south of the White Mfolozi inlier. The Usushwana Complex, the intrusive equivalent of the Nsuze Group (Hunter and Wilson, op. sit.), was deposited in a graben-like structure along the western margin of the Pongola basin. Isotopic U-Pb dating on felsic volcanic rocks of the Nsuze Group in Swaziland yielded an age of 2940 ± 22 Ma (Hegner *et al.*, 1984).

Several differentiated, mafic-ultramafic sills intrude the lower part of the Nsuze Group 20 km northeast of Nkandla and again about 10 km north-northeast of Nkandla along the Mhlatuze River (Fig. 2.1). The intrusive package was first recognized by Du Toit (1931) and termed the Hlagothi Igneous Complex. Pb-Pb isotopic dating by Groenewald (1988) yielded ages of between 2980 and 3050 Ma for the Complex. Groenewald regarded the igneous activity as evidence that crustal stability in the southernmost portion of the Kaapvaal Province was attained some time after the deposition of the Pongola Sequence.

The late Proterozoic Natal Metamorphic Province (possibly an eastern extension of the Namaqualand Metamorphic Province) crops out over an extensive area south of Melmoth. Thomas (1989) subdivided the Province into a number of tectono-stratigraphic terranes bounded by major structural discontinuities. The northernmost Tugela terrane is in tectonic contact with the Kaapvaal craton to the north (Fig. 2.1) and was regarded by Matthews (1972) as a deformed and metamorphosed Proterozoic obduction zone. Mafic-ultramafic segments of oceanic crust along with overlying metalavas and pelagic metasediments representing the middle and upper parts of an ophiolite complex, were thrust northwards during the Kibaran orogenic cycle onto the Kaapvaal craton along a basal décollement known as the Mfongosi thrust (Matthews, 1981). The northernmost extent of the various thrust sheets during the late Proterozoic is not known. It is possible however that the Tugela terrane may, at some stage, have overlain the MGGR. The affect of this possible overthrusting on the underlying basement rocks and hence on the associated Au mineralization should not be overlooked.

The MGGR is unconformably overlain by resistant, flat-lying sandstones of the Natal Group. These occupy higher ground and form the scarp-bounded, so-called Melmoth Plateau (Matthews, 1988). Locke (1973), on the basis of palaeontological evidence, considered the sediments to be Devonian in age. The Group consists of a basal conglomerate overlain by a number upward-fining sequences of grit, medium to fine-grained quartzose sandstone and occasionally arkosic sandstone, siltstone and shale (Lindström, 1987). A maximum thickness of ca. 500 m is recorded

near Eshowe (Du Toit, 1931). The Natal Group is unconformably overlain by rocks of the Karoo Sequence.

3. GEOLOGY OF THE MELMOTH GRANITE-GREENSTONE INLIER

The greenstones of the MGGR comprise predominantly actinolite-tremolite(-chlorite) and talc schists together with lesser serpentinite, rhyodacitic tuff, quartz-muscovite/sericite schist, quartzite and calc-silicate rocks (Figs. 3.1 {pocket} and 3.2). All display an east-west trending, steep southerly dipping fabric.

Serpentinites, serpentine-talc rocks and talc schists constitute the ultramafic portion of the greenstone belt. Textural evidence (see section 3.1.2) points to an intrusive origin for these rocks. The actinolite-tremolite(-chlorite) schists are extrusive in origin, derived from both tholeiite and basalic komatiite. Meta-sedimentary and felsic meta-volcanic rocks make up a very small portion of the succession. The overwhelming abundance of mafic and ultramafic rocks suggests that only the lowermost portion of the volcanic pile is preserved.

Three phases of granitoid intrusion are evident. Syntectonic tonalitic gneisses crop out to the north, and late-tectonic granodioritic gneisses to the south, of the greenstone sequence. The latter host a number of late-tectonic granite dykes. The MGGR has in places been intruded by rocks of the mafic to ultramafic Hlagothi Igneous Complex as well as by a number of dolerite dykes of probable Karoo age.

3.1 The Greenstone Sequence

3.1.1 Extrusive Mafic Rocks

Extrusive mafic rocks account for over 70% of the greenstone sequence (Fig. 3.1). All display a typical lower greenschist facies metamorphic assemblage of actinolite-tremolite + (Mg-rich) chlorite + clinozoisite + plagioclase (albite) ± quartz ± epidote. Metamorphic grades increase to amphibolite facies (indicated by the appearance of hornblende) adjacent to granitoid intrusives. The lavas have, on the basis of geochemical evidence, been subdivided into tholeiitic and komatiitic types (Fig. 3.3). Confirmatory evidence, utilizating geochemical, modal and

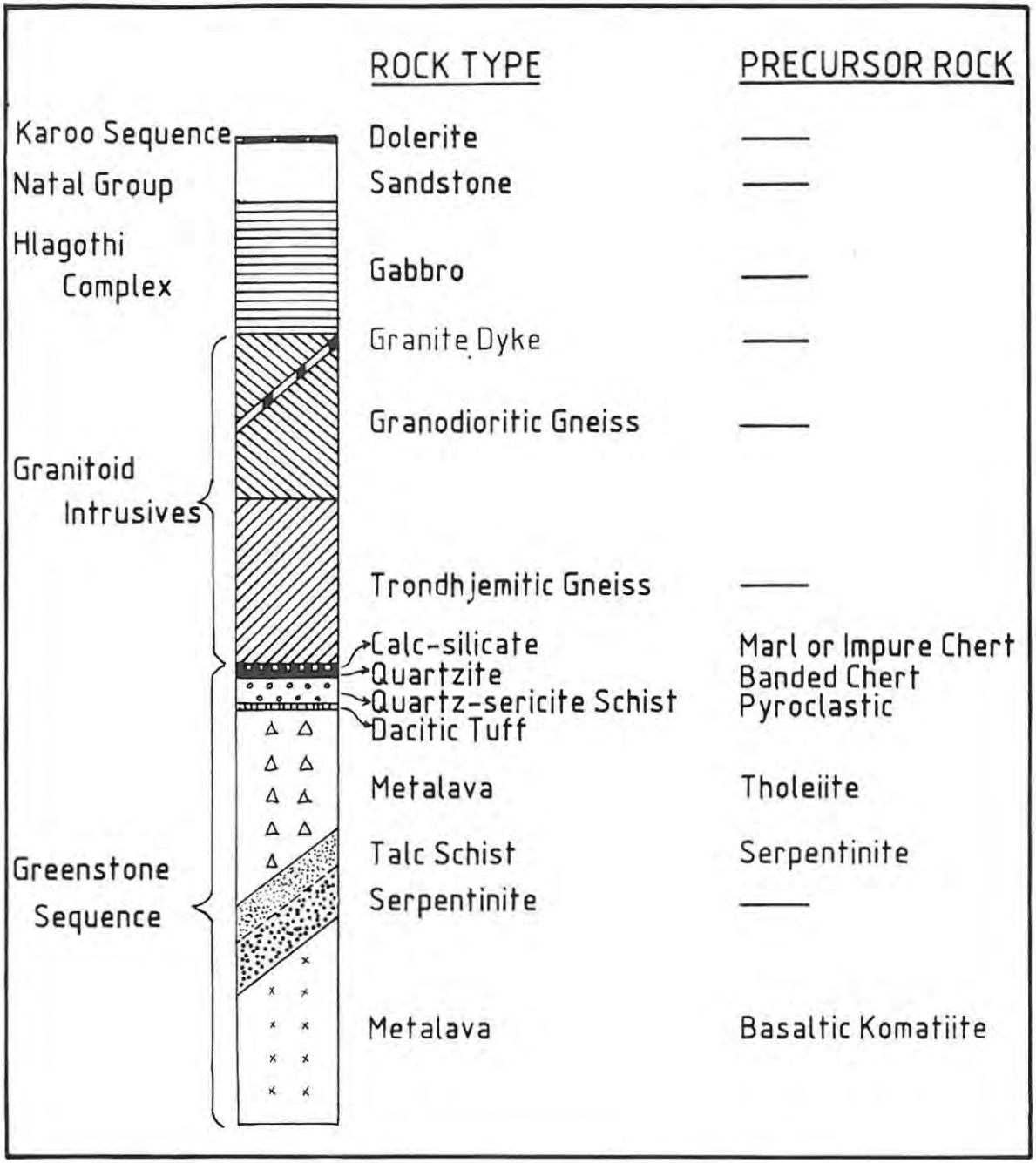

Figure 3.2 Generalized stratigraphic column of the MGGR in the study area. Igneous and sedimentary precursor rocks are indicated.

normative data, is provided in Table 3.1. Condie (1981) suggested that komatiites should show spinifex textures (in order to exclude cumulus, ultramafic rocks). Quench textures were however not observed in the metalavas of the MGGR suggesting that the lavas were erupted in voluminous amounts, thus cooling relatively slowly.

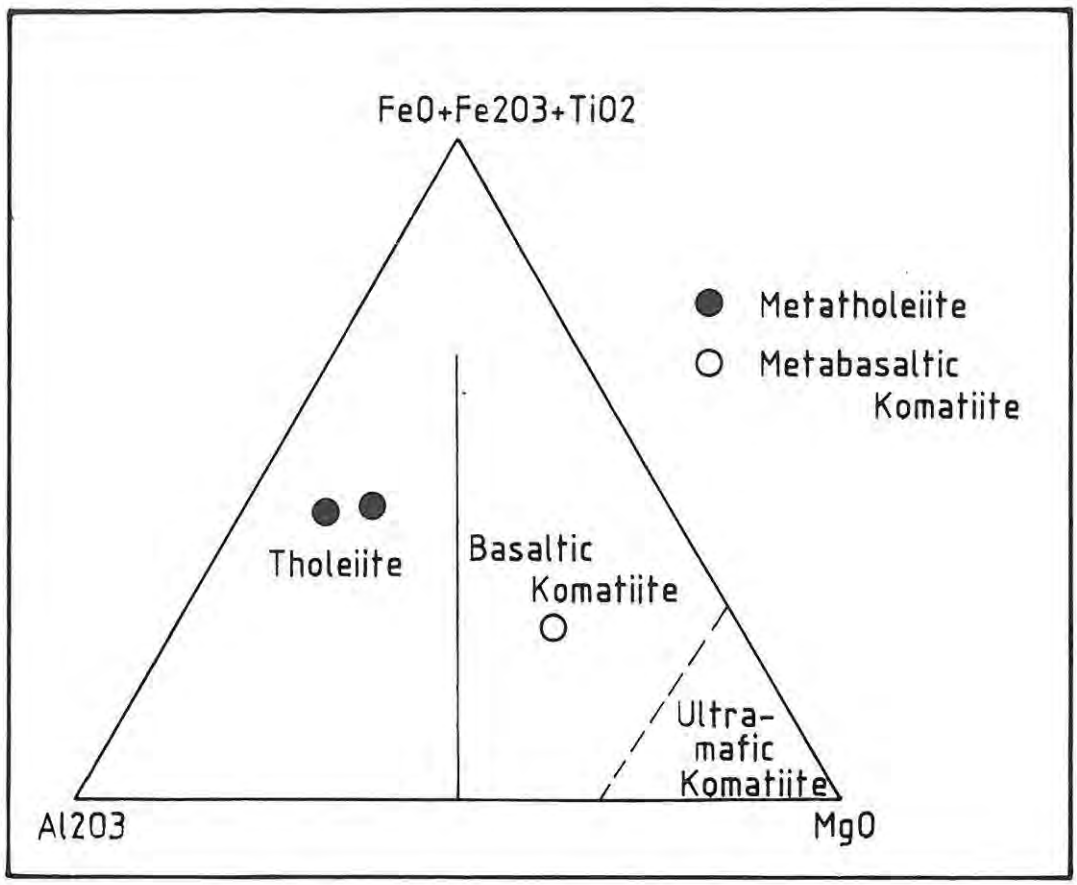

Figure. 3.3 Plot of Al_2O_3:FeO+Fe_2O_3+TiO_2:MgO for the lavas of the greenstone sequence showing the distinction between tholeiitic and komatiitic types. (Field boundaries after Jensen, 1976).

Both Archaean tholeiites and basaltic komatiites may be further subdivided into a number of groups - the former according to major and trace element contents and the latter according to REE distributions (see Condie, 1981). According to Nisbet and Walker (1982), the eruption of Komatiitic lavas was probably the Archaean earth's principal means of dissipating excess heat. Subsequently erupted lavas of tholeiitic composition were probably produced by the high-level fractionation of komatiitic magmas leading to the generally observed stratigraphic sequence - komatiite followed by tholeiite.

The fine- to medium-grained, highly fractured lavas of the MGGR (Figs. 3.4 and 3.5) appear pale blue when fresh and reddish to yellowish orange when weathered. Flattened, up to 1 cm diameter,

Table 3.1 Comparison of tholeiitic and komatiitic lavas in the MGGR. The final column provides criteria used by Brooks and Hart (1974) to define komatiites (see text). Nesbitt and Sun (1976) questioned Brooks and Hart's (1974) usage of $CaO/Al_2O_3>1$ as a komatiite parameter on the grounds that the ratio would be affected by metamorphism and hence be an unreliable indicator. In addition, Condie (1981) pointed out that most Archaean high-Mg ultramafic and mafic lavas have CaO/Al_2O_3 ratios of less than 1.

	THOLEIITE	KOMATIITE	Komatiite Criteria
MgO (%)	4.46	19.88	>9.0
K_2O (%)	0.98	0.05	<0.9
TiO_2 (%)	1.44	0.25	<0.9
CaO/Al_2O_3	0.64 (n=2)	0.72 (n=1)	>1.0
Actinolite-Tremolite + Chlorite (%)	88.48	94.88	
Clinozoisite (%)	7.64	0.58	
Albite (%)	25.32	3.60	
Quartz (%)	5.48 (n=2)	0.04 (n=1)	
Normative Quartz (%)	3.97 (n=3)	0.00 (n=2)	

quartz, chlorite and/or clinozoisite-filled amygdales are occasionally preserved. The lavas are generally well foliated, the foliation being particularly apparent in the more weathered outcrops. Although pillow structures were not observed in the study area, they are known to occur in related lavas some 2.5 km to the northeast (Matthews, pers. comm., 1990). A subaqueous origin for the lavas is therfore inferred. Their intimate association with recrystallized chert supports this contention (see section 3.1.3). As pillows are known to survive fairly high degrees of deformation and metamorphism however, their absence suggests that the lavas in the study area were originally massive and probably formed during the subaqueous eruption of large volumes of hot magmas of low viscosity. A similar origin is attributed to massive lavas in the Rouyn-Noranda area of the Atibiti greenstone belt (Dimroth *et al.*, 1978)

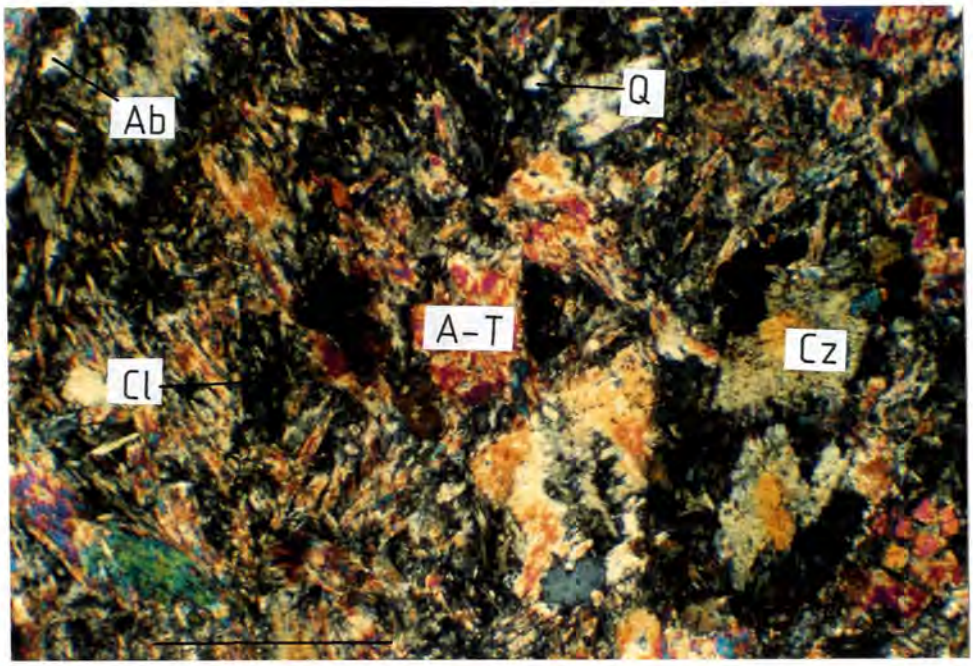

Figure 3.4 Photomicrograph of tholeiitic metalava from locality 52 (polars crossed) - refer to Fig. 3.1. Quartz (Q), Actinolite-Tremolite (A-T), Mg-rich Chlorite (Cl), Albite (Ab) and Clinozoisite (Cz) are indicated. Actinolite-tremolite, plagioclase and quartz predominate, imparting a (grano)nematoblastic texture. In non-sheared varieties such as above, amphibole crystals are randomly oriented within a two dimensional plane indicating $\sigma_1>\sigma_2=\sigma_3$. In sheared varieties however, amphibole crystals define a mineral lineation parallel to σ_1 indicating $\sigma_1>\sigma_2>\sigma_3$. Note replacement of actinolite-tremolite by chlorite around crystal margins. Plagioclase crystals display pervasive sausuritization. Grain-size varies up to 1.04 mm. Scale bar 0.5 mm.

3.1.2 Serpentinite, Serpentine-Talc Rocks and Talc Schist

Serpentinites (greater than 95% serpentine), serpentine-talc rocks (5% to 95% talc) and talc schists (greater than 95% talc) make up about 20% of the greenstone sequence (Figs. 3.1 and 3.2). They invariably occur together, the last two representing sheared products of the first. The original igneous mineralogy of the serpentinites has not been preserved although thin-section studies suggest that they were originally coarse-grained, olivine-rich cumulates (for example - magnetite dust mantles original olivine grains producing a mesh texture; magnetite-filled, sinuous alteration cracks typical of olivine crystals are present - Fig. 3.6). The serpentinites lie (apparently)

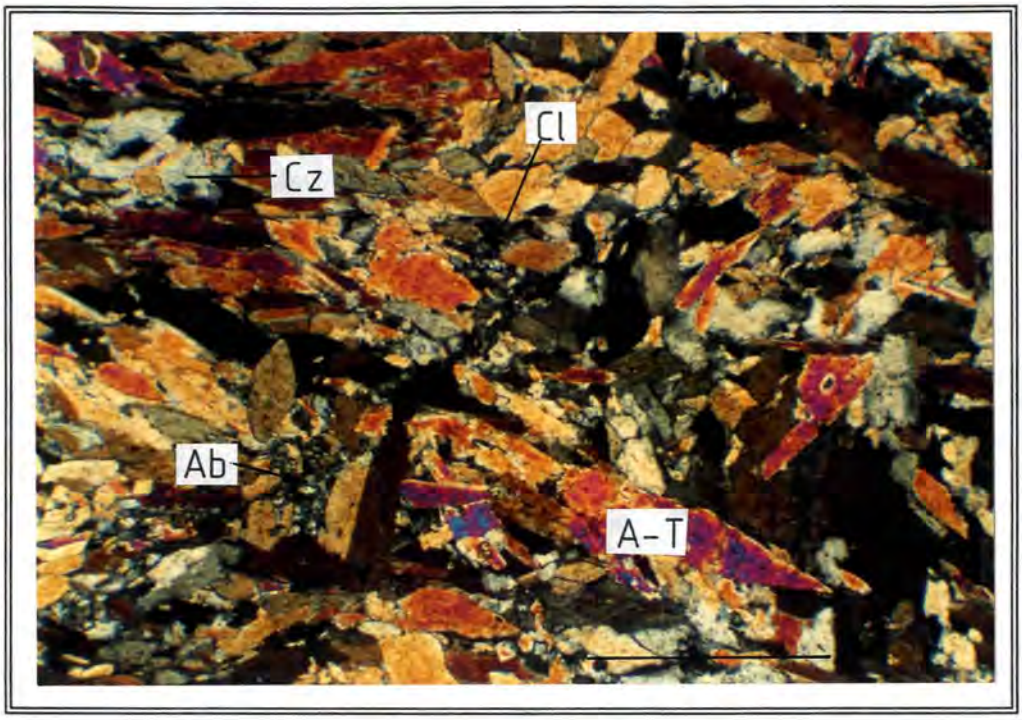

Figure 3.5 Photomicrograph of basaltic komatiite from locality 96 (polars crossed). Actinolite-Tremolite (A-T), Albite (Ab), clinozoisite (Cz) and Mg-rich chlorite (Cl) are indicated. Actinolite-tremolite predominates almost to the total exclusion of the other constituents. The rock displays a nematoblastic texture. Note replacement of actinolite-tremolite by chlorite around crystal margins. Orientation of actinolite-tremolite crystals as described for tholeiites (see Fig. 3.4). Grain-size is relatively uniform up to 0.73 mm. Scale bar 0.5 mm.

conformably within metalavas and metasediments and are intrusive in origin. It is however uncertain whether the sill-like bodies, which vary from 10 m to greater than 400 m in thickness, were intruded as peridotites or serpentinites although the latter is considered more likely. The thicker sills represent multiple intrusions. Some of the serpentinite and serpentinite-talc rocks display weak fabics whereas others appear massive. This is considered a function of talc content rather than an indication of the relative age of intrusion (all are pretectonic).

The serpentinites have been extensively altered to impure talc schists during shearing - talc contents vary between 57.0% and 73.8%, serpentine between 2.2% and 11.2% and magnetite between 0.2 and 37.6%. In addition, some of the schists contain considerable amounts of Mg-rich chlorite (up to 36.8%) (Fig.

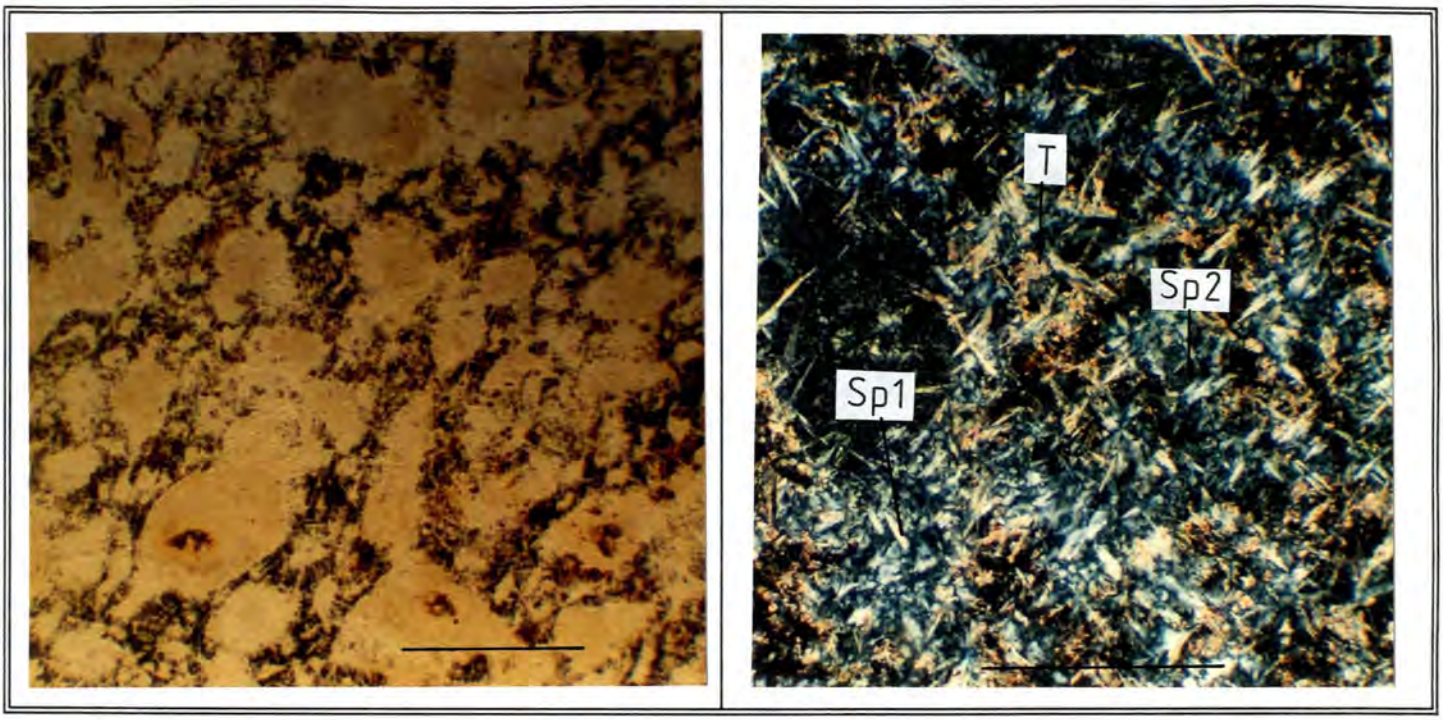

Figure 3.6 Photomicrograph of serpentine-talc rock from locality 61. a) Plane polarized light, showing serpentinized olivine grains outlined with fine magnetite giving mesh texture. Scale bar 1mm b) View under crossed polars showing two varieties of serpentine - a lighter coloured variety (Sp1) and a dark, somewhat finer grained variety (Sp2). Talc (T) indicated. Scale bar 0.5 mm.

3.7). Major element analyses of talc schist and serpentinite at locality 67 (Appendix 1) indicate that the principal chemical changes which took place during shearing involved the introduction of Si and the removal of Mg.

On the Dundee Sheet 2830 (1:250 000), the serpentinites, serpentinite-talc rocks and the talc schists are correlated with the Hlagothi Complex (refer to section 2). Peridotites from the type area northeast of Nkandla have been altered to tremolite, chlorite, talc and serpentine (Groenewald, 1984). In terms of major element compositions however, the serpentinites from the study area differ markedly to the ultramafic rocks of the Hlagothi Complex (Table 3.2). Furthermore, structural considerations (see section 3.4) suggest that the serpentinites were intruded early in the history of the greenstone belt prior to the onset of deformation, thus predating the Hlagothi Complex.

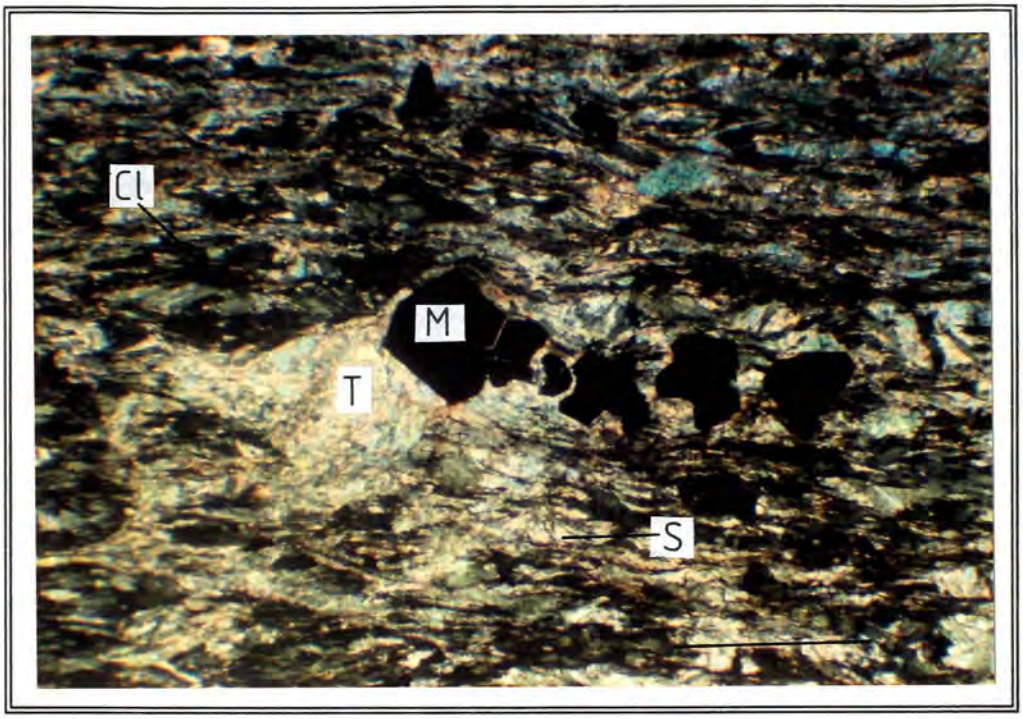

Figure 3.7 Photomicrograph of talc-chlorite schist from locality 67 (polars crossed). Talc (T), Mg-rich chlorite (Cl), serpentinite (S) and magnetite are indicated. The rock displays a nematoblastic texture. Note the euhedral, pretectonic, magnetite grains (shown by the foliation wrapping around broken crystals and the development of pressure shadows). Scale bar 1 mm.

Hunter and Wilson (1988) interpreted the irregularly shaped serpentinite intrusions in the Nondweni supracrustal suite as the final subvolcanic products of Nondweni magmatism.

Table 3.2 Comparison between average peridotite from the Hlagothi Complex (after Groenewald, 1988) and serpentinite from the MGGR with regard to selected major element compositions. The differences between the two rock types are readily apparent.

	Hlagothi Complex Peridotite	MGGR Serpentinite
Al_2O_3	6.67%	0.82%
$FeO_{(T)}$	11.30%	5.57%
MgO	26.77%	45.14%
CaO	5.57%	0.00

3.1.3 **Pyroclastic and Sedimentary Rocks**

Pyroclastic and sedimentary rocks account for about 6% of the greenstone sequence (Figs. 3.1 and 3.2). Pyroclastic material crops out at localities 75, 76 and 77. A minor calc-silicate unit of probable sedimentary origin crops out in the vicinity of locality 83. In addition, a number of thin quartzite horizons occur throughout the greenstone sequence.

A thin (less than 10 m in thickness) tuffaceous unit of dacitic composition crops out at locality 77 (Fig. 3.8). Tightly folded, quartz-muscovite rocks lie immediately to the south (Fig. 3.9). The latter contain abundant white mica. Lowe and Knauth (1977) have shown that many impure chert units which **overlie** thin felsic tuffs in the Barberton Mountain Land formed during the devitrification, recrystallization and silicification of volcanic ash. The presence of abundant phyllosilicate minerals was considered a product of recrystallization. The silica-rich fluids were probably derived from the interaction of convecting seawater and oceanic crust (Paris et al., 1985). The fluids silicified lava, sediments and pyroclastic rocks upon re-entering the near surface environment. The micaceous, quartz-rich unit in the study area is therefore interpreted as the recrystallized and highly silicified product of fine-grained, vitric, pyroclastic material **overlying** the dacitic tuffs. Younging directions in this particular section of the river traverse are therefore to the south. Silicified volcanic ash deposits are an important component of the Nondweni Group in the type area (Hunter and Wilson, 1988; refer to section 2).

A number of thin, intercalated, banded quartzite units are also present. These lack phyllosilicate minerals, display centimeter-scale banding, and are interpreted as the product of recrystallized, chemically precipitated chert. Annealing textures are common. The banded quartzites crop out at various localities throughout the greenstone sequence (Fig. 3.10). The close spatial association between chert layers and pyroclastic material suggests that the latter were deposited subaqueously, although subsequent redistribution by sedimentary processes cannot be ruled out. The quartzitic units were deposited under volcanically

quiescent conditions.

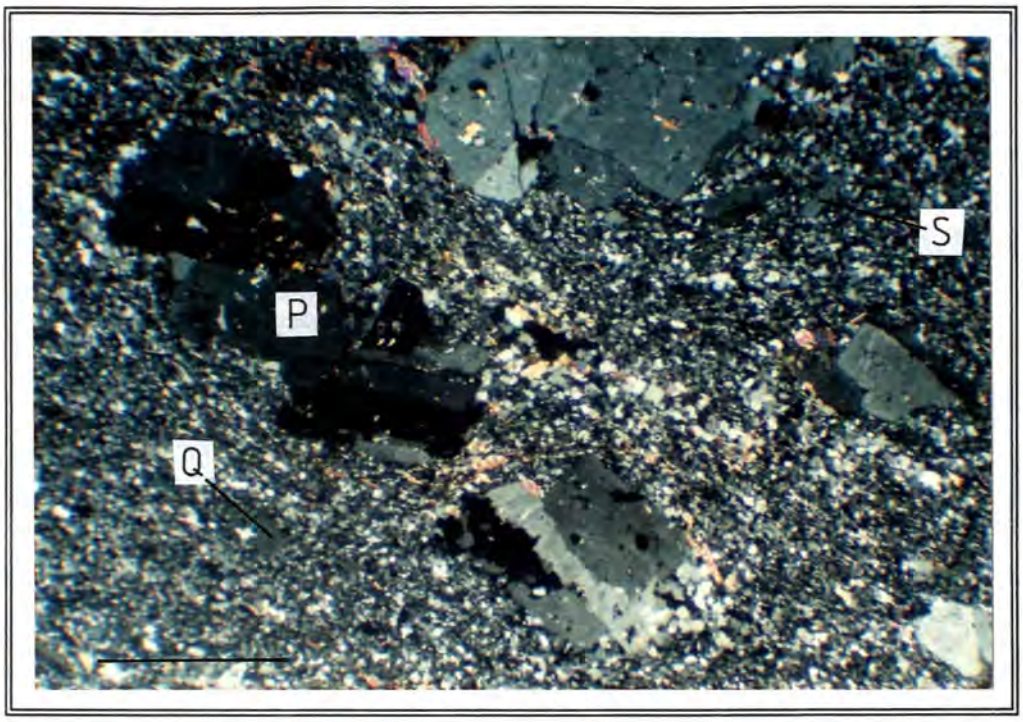

Figure 3.8 Photomicrograph of dacitic tuff from locality 77 (polars crossed). Phenocrysts mainly twinned or untwinned plagioclase (P) with a composition of ± An_{26}, with minor sanidine (S) and quartz (Q). The groundmass is a fine-grained mixture of quartz, feldspar and white mica - derived in part from the devitrification and recrystallization of the original (presumably glassy) matrix. Note the fractured and broken nature of the phenocrysts, zoned plagioclase and silicification - with silica replacing feldspars and forming quartz veinlets. Muscovite/sericite minerals impart a weak foliation to the rock which probably mimics previous bedding surfaces. In addition, feldspar crystals are oriented such that the c-axes define a lineation lying within the plane of foliation. Scale bar 1 mm.

A narrow band of clinozoisite-quartz-actinolite-tremolite-bearing rocks (± epidote ± albite) crop out in the vicinity of locality 83 (Fig. 3.11). Based on mineral content, the chemical composition of these rocks is (in decreasing order of abundance) SiO_2, CaO, Al_2O_3, FeO and MgO with minor Na_2O and K_2O. It is suggested that the calc-silicates were derived from marls or impure, carbonaceous cherts metamorphosed under greenshist facies conditions.

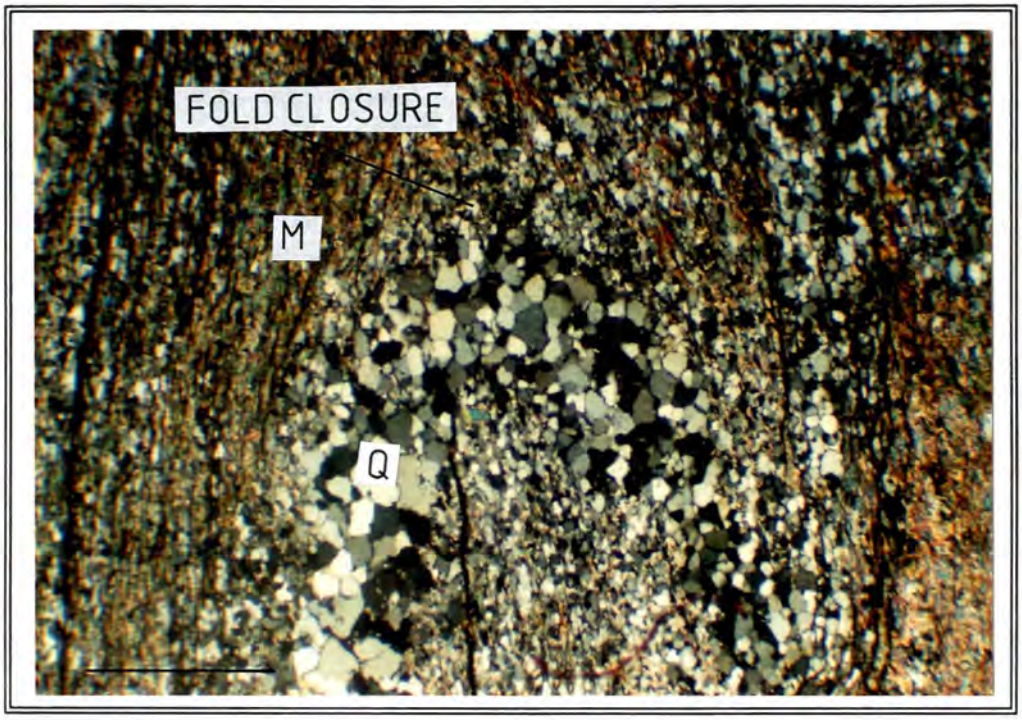

Figure 3.9 Photomicrograph of tightly folded, micaceous, quartz-rich rock from locality 75 (polars crossed). Note the alternating quartz-rich and muscovite-rich layers (Q=quartz, M=muscovite) - a function of the compositional differences within the original tuffs. Note also the axial planar cleavage as defined by muscovite grains. A fold closure is indicated. The rock shows evidence of recrystallization - for example: triple junctions, unstrained quartz crystals, elongate quartz grains constrained by contemporaneously growing mica crystals. See text for further explanation. Scale bar 1 mm.

Figure 3.10 Photograph of slightly dislodged, banded quartzite boulder east of locality 86 (taken from **above**). Note the conjugate fault set - a function of the north-south compressional regime (see section 3.4).

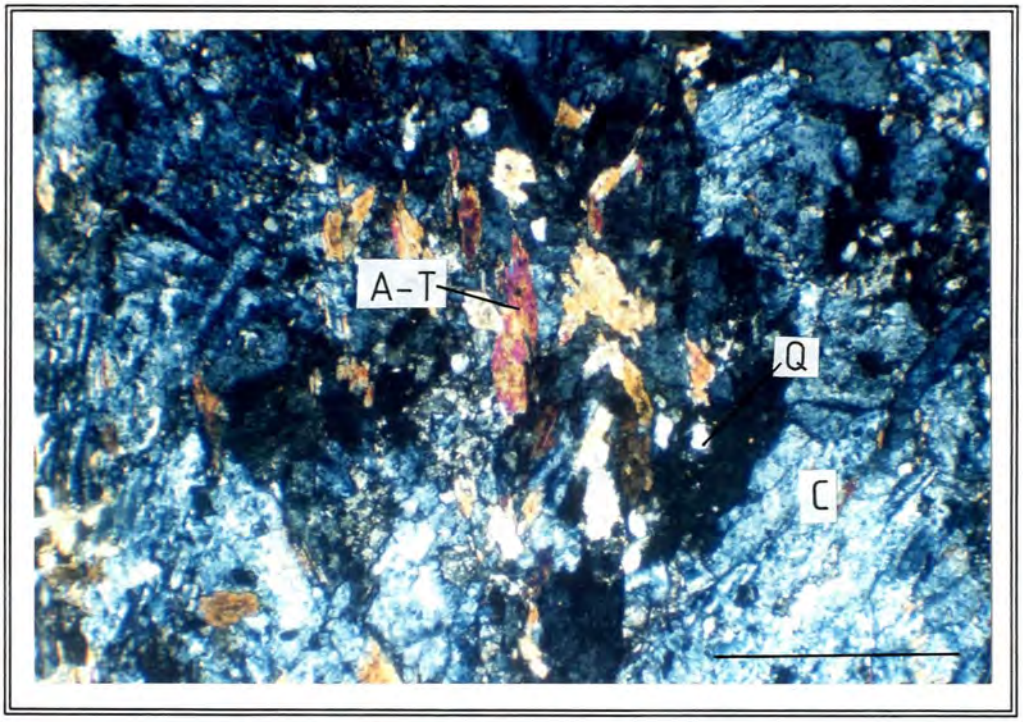

Figure 3.11 Photomicrograph of calc-silicate rock from locality 83 (polars crossed). Clinozoisite (C), quartz (Q) and actinolite-tremolite (A-T) indicated. Clinozoisite is the dominant mineral phase (accounting for greater than 50% of the rock). Note the poikilitic textures exhibited by the amphibole crystals. Scale bar 0.5 mm.

3.2 Granitoid Intrusives

3.2.1 Trondhjemitic Gneiss

Syntectonic, prominently foliated, high alumina, trondhjemitic gneisses crop out to the north of the greenstone sequence (Fig. 3.1; Table 3.3; Fig. 3.12). The presence of a number of related trondhjemite dykes in metalavas just to the south of the contact attests to their intrusive origin. On a Streckeisen diagram the rocks plot well within the tonalite field (Fig. 3.13). Robb et al. (1986) pointed out that syntectonic trondhjemitic and tonalitic gneisses represent the earliest granitoid component of most Archaean granite-greenstone terranes. The prominent fabric displayed by the trondhjemites in the study area suggests that they are the earliest granitoid intrusives in the MGGR.

Table 3.3 Quantitative, major element distinctions between trondhjemite and tonalite after Barker (1979) - as compared with trondhjemite from locality 107.

TRONDHJEMITE CRITERIA	TONALITE CRITERIA	TRONDHJEMITE FROM LOCALITY 107
SiO_2 > 68%	SiO_2 < 68%	SiO_2 = 73.63
Fe_2O_3 + MgO < 3.4%	Fe_2O_3 + MgO > 3.4%	Fe_2O_3 + MgO = 0.98
CaO 1.5 - 3.0%	CaO > 3.0%	CaO = 2.91
Na_2O typically 4.0 - 5.5%		Na_2O = 4.85%
K_2O typically < 2.0%		K_2O = 0.83%
High alumina trondhjemites have > 15% Al_2O_3 at 70% SiO_2		14.97% Al_2O_3 at 73.63% SiO_2 = high alumina trondhjemite

Granitoid intrusives in the Barberton area have been categorized into three "magmatic cycles" based on geochemical, geochronological and field characteristics (Anhaeusser and Robb, 1981). The first cycle lasting from ≈3.5 Ga to ≈3.2 Ga involved the intrusion of Na-rich, leucocratic trondhjemites and tonalites together with a complex series of bimodal gneisses and migmatites. The second cycle commenced approximately 3.2 Ga ago with the widespread intrusion of large, multi-component,

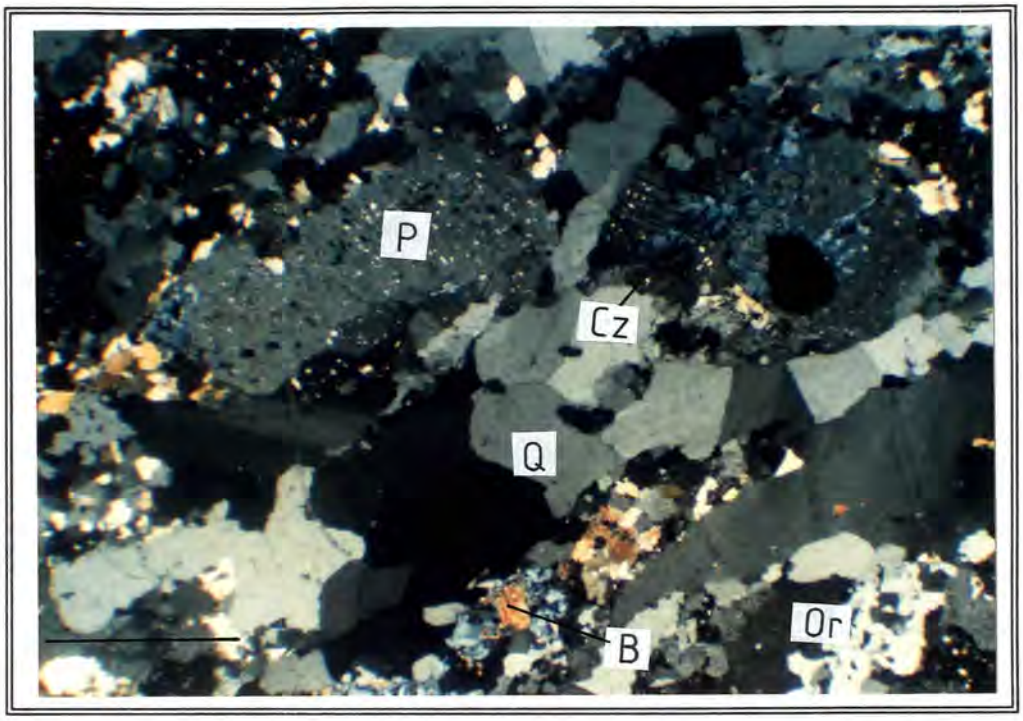

Figure 3.12 Photomicrograph of trondhjemitic gneiss from locality 107 (polars crossed). Sodic plagioclase (P) of composition An_{25}, quartz (Q), biotite (B), micropegmatitic orthoclase (Or) and biotite (B) are indicated. A relict, hypidiomorphic-granular texture is evident. The rock has been partially silicified as evidenced by the marginal replacement of plagioclase crystals by quartz. Quartz grains are anhedral, exhibit undulose extinction and are elongated within the foliation planes. Partial recrystallization is evidenced by the presence of small, strain free quartz crystals developed along serrated quartz grain margins. Zoning within the plagioclase crystals is evidenced by the nature of the alteration - with clinozoisite (Cz) predominating in the more Ca-rich, central portions of the crystals and sericite along the more Na-rich margins. Biotite is yellowish in colour - a reflection of the low TiO_2 content of the rock (0.26%). A number of thin (± 0.25 mm in thickness) clinozoisite veins disect the rock. Scale bar 1 mm.

granodiorite-adamellite batholites. The third cycle beginning at about 2.9 Ga involved the intrusion of discrete, mainly K-rich granite and syenite plutons.

The three magmatic cycles are clearly distinguishable from each other on a plot of Rb versus Sr (see Robb and Anhaeusser, 1981, pg 8). The trondhjemitic and tonalitic gneisses of the first magmatic cycle are characterized by Rb/Sr ratios of ≈0.1. The trondhjemites of the MGGR have Rb/Sr ratios of 0.12 and plot

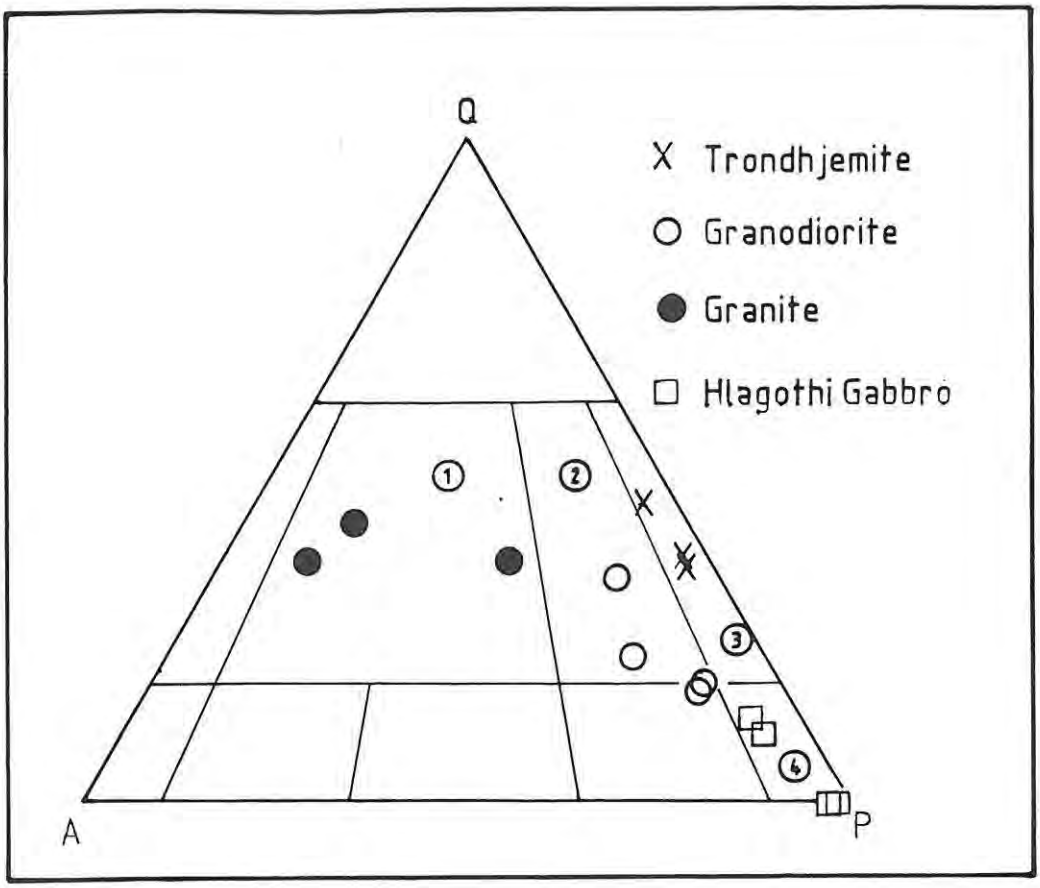

Figure 3.13 Streckeisen diagram showing the distribution of the three granitoid intrusives. Also plotted are rocks considered to be part of the Hlagothi Igneous Complex. Fields (1) = Granite, (2) = Granodiorite, (3) = Tonalite/trondhjemite and (4) = Gabbro {An>50}.

close to the field defined by first magmatic cycle tonalites and trondhjemites (and well away from the fields defined by the second and third magmatic cycles) on the Rb verses Sr diagram. It is therefore postulated that the trondhjemites in the study area may have been generated during the first magmatic cycle and, if so, would be somewhat older than the Mvunyana granodiorite, currently considered by Matthews et al. (1989; refer to section 2) to be the oldest granitoid component south of Swaziland. Alternatively, the trondhjemites might form part of the Anhalt Granitoid Suite, a group of predominantly tonalitic and trondhjemitic gneisses which crop out in the vicinity of Piet Retief and PaulPietersburg in northern Natal and the southeastern Transvaal (Hunter, 1990; in press [b]). If so, they would be similar in age to the Mvunyana granodiorite.

Literature on the genesis of Archaean tonalitic and trondhjemitic gneisses is abundant. They are generally considered to be orthogneisses, derived by partial melting of mafic precursors (for example - Robb et al., 1986). Martin (1987) on the other hand, envisaged a multi-stage process involving both partial melting and fractional crystalization. Partial melting within the upper mantle produced a tholeiitic crust which was itself partially remelted giving rise to a magma of granodioritic composition. Fractional crystallization of the magma gave rise to tonalitic and trondhjemitic melts. According to Maalφe (1982) high alumina trondhjemites were generated from a fractionating, tonalitic magma.

3.2.2 **Granodioritic Gneiss**

Weakly foliated, inhomogeneous, granodioritic gneisses crop out to the south of the greenstone sequence (Figs. 3.1, 3.13 and 3.14). The presence of numerous mafic xenoliths indicates an intrusive origin. The **weak**, steep southerly dipping fabric displayed by the granodiorites (Fig. 3.15) suggests that they post-date the trondhjemitic gneisses and are late-tectonic in nature. Chemical and mineralogical differences between the gneisses are marked (refer to Appendix I and Table 3.4) suggesting that a genetic relationship between the two is unlikely.

3.2.3 **Granite**

A number of leucocratic, K-rich granitic dykes lying either within the plane of foliation or at a shallow angle to it, have intruded the granodioritic gneisses in the south of the study area (Figs. 3.1, 3.13 and 3.16). The dykes are up to 15 m in thickness and dip steeply to the south at about 70°. Dyke margins are extremely irregular (Fig. 3.17). Grain size increases towards the center of the intrusives. The granites are unfoliated and are therefore considered to be post-tectonic. The dykes are probably offshoots from a granitic pluton which is not exposed in the study area.

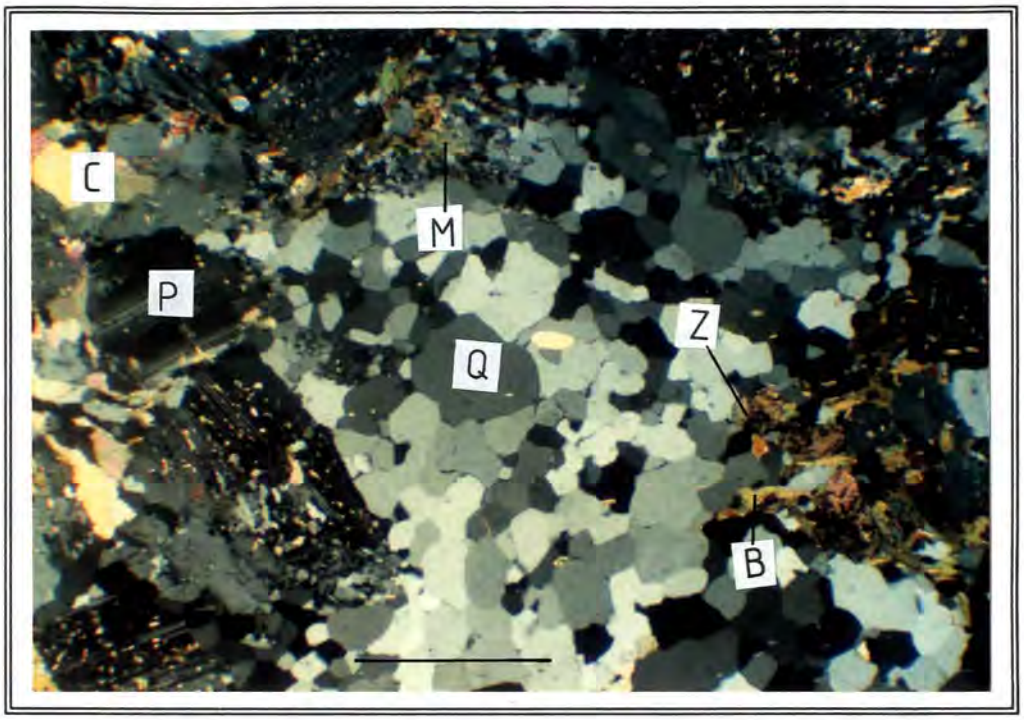

Figure 3.14 Photomicrograph of granodioritic gneiss from locality 24. Antiperthitic plagioclase of composition An_{17} (P), quartz (Q), biotite (B), zircon (Z), muscovite (M) and calcite (C) are indicated. The granodiorite shows evidence of silicification with quartz replacing plagioclase. In addition, recrystallization of the quartz has occurred as evidenced by triple junctions as well as the fact that the crystals themselves are completely unstrained. Plagioclase is partially altered to zoisite, epidote, sericite and, in places, calcite. Secondary calcite (C), which accounts for 2.4% of the rock, also occurs as thin cross-cutting veinlets. Biotite is dark brown - a function of the high TiO_2 content of the rock. The biotite has been completely replaced by poikilitic hornblende adjacent to post-tectonic granite dykes. The rock displays a relict hypidiomorphic-granular texture. Scale bar 1 mm.

Table 3.4 Average mineral compositions of granodiorite and trondhjemite from the MGGR. In both cases n = 4.

	Granodiorite	Trondhjemite
Quartz	17.3%	35.0%
Plagioclase	47.2%	53.4%
K-Feldspar	10.2%	3.1%
Biott/Hbl/ Opaque/Acc	23.9%	7.9%

Figure 3.15 Photograph of partially oriented mafic xenoliths in granodiorite from locality 27 attests to the weakly developed fabric displayed by the gneisses. The orientation of the foliation, which runs obliquely across the photograph (from top right to bottom left), is indicated by the orientation of the xenoliths.

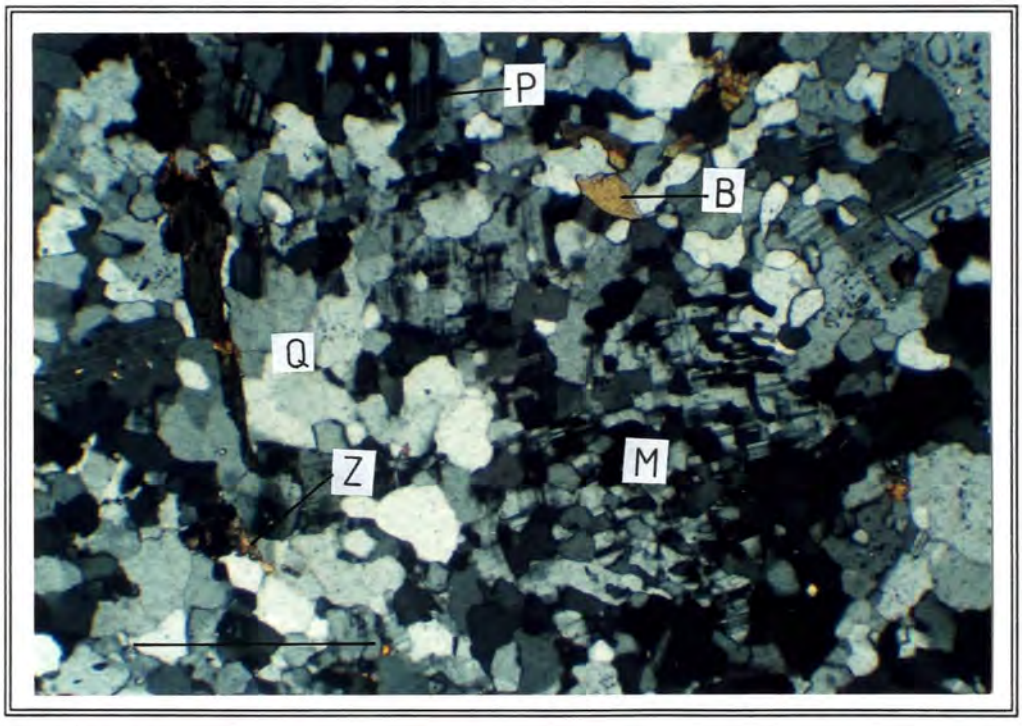

Figure 3.16 Photomicrograph of potassic granite from locality 34. Perthitic microcline with vermicular quartz intergrowths (M), quartz (Q), plagioclase of composition An_{12} (P), biotite (B) and zircon (Z)

indicated. The xenomorphic-granular texture is ascribed to silicification which has resulted in the partial replacement of feldspars along crystal margins. Green biotite, opaques and zircon make up about 3% of the rock. Zircon often mantles opaque minerals - probably a result of the expulsion of Zr from the lattice of opaque minerals during crystallization. The highly perthitic, micropegmatitic nature of the K-feldpar suggests that the original composition of the melt lay very near to the eutectic. Scale bar 0.5 mm.

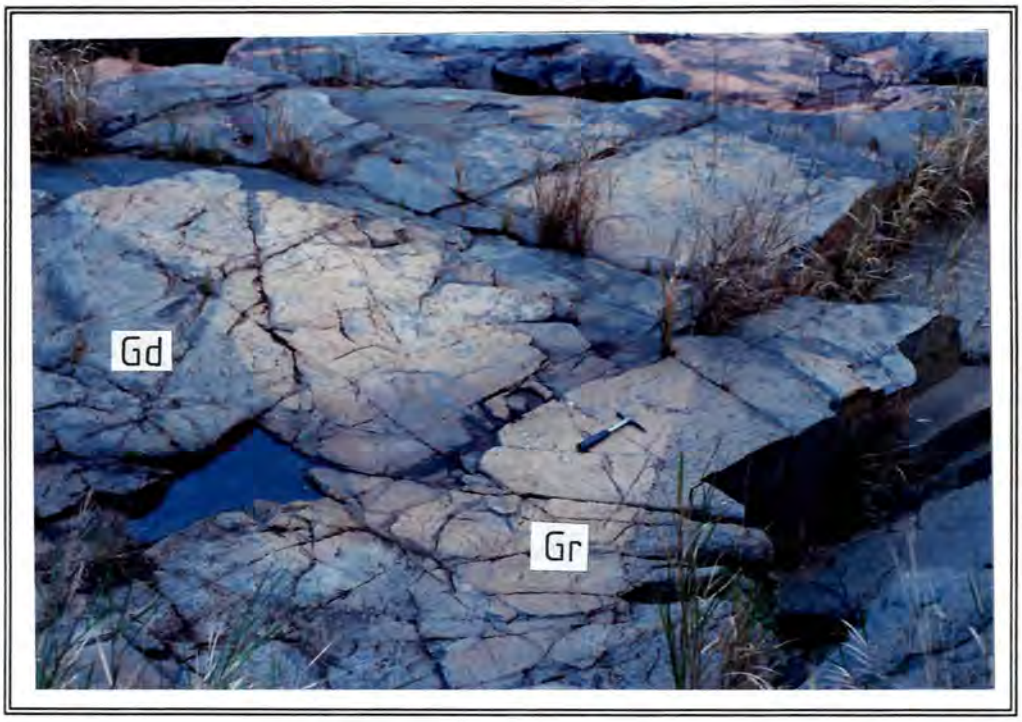

Figure 3.17 Photograph highlighting the irregular nature of granitic dyke/granodioritic gneiss contact at locality 34. Granite = Gr and granodiorite = Gd.

3.3 Later Intrusives

3.3.1 Metagabbro

A 750 m thick, composite, sill-like metagabbro intrudes the granodioritic gneisses near the southern margin of the study area (Fig. 3.1). Thin-section studies point to the presence of two distinct rock types namely, a centrally emplaced, relatively unaltered olivine gabbro surrounded by a more voluminous, silicified, uralitized gabbro (Table 3.5; Figs. 3.18 and 3.19).

Table 3.5 Modal compositions of the two metagabbroic intrusions. Accessory and secondary phases excluded.

	Olivine Gabbro (n = 1)	Uralitized Gabbro (n = 2)
Quartz	-	7.5%
Plagioclase	57.4%	49.5%
K-Feldspar	1.4%	3.3%
Olivine	9.4%	-
Augite	20.6%	-
Hypersthene	8.8%	-
Uralite	-	29.4%
Biotite	-	6.4%

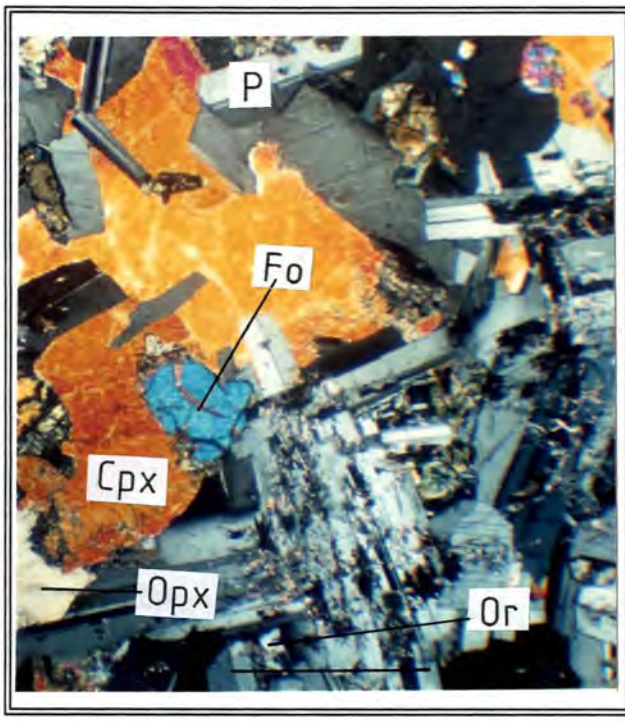

Figure 3.18 Photomicrograph of olivine gabbro cumulate from locality 41 (polars crossed). Olivine of composition Fo_{∞} (Fo), hypersthene (Opx), augite (Cpx), plagioclase of composition An_{53} (P) and antiperthitic orthoclase (Or) indicated. Note the sub-ophitic texture. Alteration is highly selective - some olivines are entirely unaltered whereas others are completely altered to a mixture of serpentine and talc. Pyroxenes show

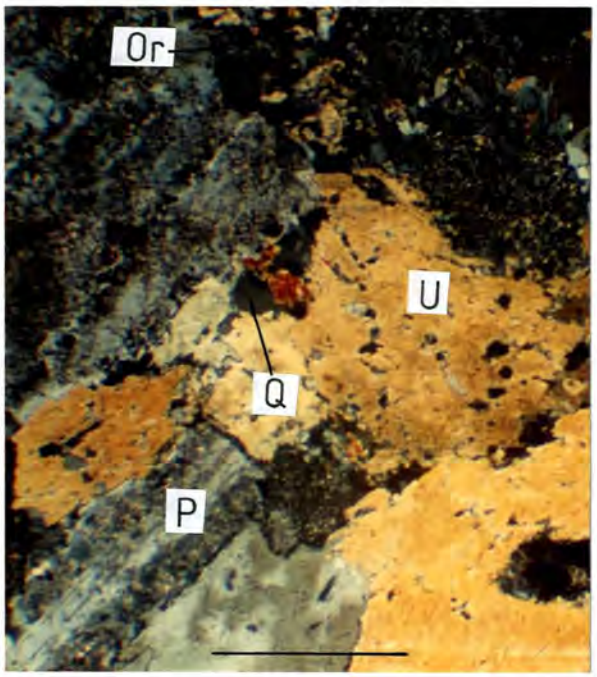

Figure 3.19 Photomicrograph of **uralitized** gabbro from locality 40 (polars crossed). Plagioclase of composition An_{51} (P), uralite (U), quartz (Q) and orthoclase (Or) indicated. Poikilitic pyroxene has been mimetically replaced by amphibole (uralite). The rock displays a sub-ophitic texture - that is cumulus plagioclase with interstitial amphibole, quartz and K-feldspar. Plagioclase is altering to

minimal alteration to amphibole (uralite), chlorite and calcite. Plagioclase is being altered to sericite. Scale bar 1 mm.

a mixture of clinozoisite and sericite. Some recrystallization of the quartz component has occurred. Scale bar 1 mm.

On the Dundee Sheet 2830 (1:250 000) the metagabbros are correlated with the Hlagothi Complex. This is considered correct since:

a) major element compositions of gabbros from the Hlagothi Complex (see Groenewald, 1988) are similar to those of the metagabbro from the MGGR.

b) with the exception of the subordinate olivine gabbro, gabbros from both areas are characterized by the **pervasive and mimetic replacement of pyroxene to amphibole.**

c) metagabbros from the MGGR do not display a fabric (in spite of the fact that they contain up to 36.0% hornblende) and are therefore probably post-tectonic with respect to the deformation of the MGGR. Gabbros from the Hlagothi Complex are similarly characterized by a lack of fabric development.

A 30 to 40 m thick, unfoliated, extensively uralitized, pyroxenite dyke cropping out in the vicinity of locality 101 (Fig. 3.1) is probably also of Hlagothi age.

3.3.2 Karoo Dolerite

Two dolerite dykes of probable Karoo age crop out in the Nyani River (Fig. 3.1). In addition, a thin dolerite sill, intrusive into sandstones of the Natal Group, caps the greenstone sequence on the farm Koningsberg, north of the Vira Au Mine.

3.4 Structure and Metamorphism

Deformation and metamorphism in the MGGR are intimately related. The initial sequence of events involved the closure of the basin in which the greenstone sequence accumulated, **accompanied** by the intrusion of syn and late-tectonic granitoids. The first two phases of deformation are viewed as a progressive phenomenon rather than as two **unrelated** events. Work on the Nondweni greenstones in the type area pointed to two main deformational

events (Versfeld *et al.*, 1988; Matthews *et al.*, 1989). The first involved tectonic flattening which produced thrust sheets and associated large and small-scale isoclinal folds. The second involved the formation of large-scale, upright, westward-plunging folds which developed as accomodation structures during the emplacement of the Mvunyana granodiorite.

Paucity of outcrop in the study area precludes a **detailed** structural analysis. Field data together with thin-section studies however, point to the following sequence of events:

D_1M_1: North-south compression associated with basin closure resulted in the tilting and folding of, and thrusting within, the greenstone sequence. **Concomitant** with basin closure was the intrusion of syntectonic trondhjemitic magmas. The dominant fabric (S_1), which developed as an axial-planar cleavage, strikes east-west and dips steeply to the south (Fig 3.1). The gneissosity displayed by the trondhjemites parallels the schistosity of the adjacent metalavas attesting to the early nature of the former. The steep dip of the foliation implies tectonic flattening in a subhorizontal direction. Small-scale, isoclinal folding related to the D_1 event was observed in silicified pyroclastic material at locality 75 (Fig. 3.20).

Silicification must therefore have occurred prior to deformation. Silica veins and breccias were produced in response to the infusion of silica-rich fluids (refer to section 3.1.3) during this period (Fig. 3.21).

The effects of D_1 on the volcanic and ultramafic intrusive rocks is less clear. The foliation varies from penetrative to nonpenetrative and is, in places, absent. Folding was not observed although this is ascribed both to poor outcrop, and to the absence of layering (which could be used to identify folding) in the originally massive mafic and ultramafic rocks. In all of the quartzite units in the study area, the banding (a relict sedimentary feature) invariably parallels the foliation in the adjacent schistose rocks suggesting that S_1 is oriented parallel to S_0 - that is S_1 mimics the original sedimentary bedding and volcanic layering. This implies that, at the very least, the

mafic and ultramafic rocks were steeply tilted (and probably folded) during the D_1 event.

Figure 3.20 Inclined, isoclinal F_1 folds in altered pyroclastic material at locality 75. The photograph was taken looking east. Fig. 3.9 is a photomicrograph of the same rock. The original fabric (S_o) is indicated by quartz-rich (white) and quartz-poor (light reddish orange) bands. The folds plunge at 10° on 117. S_1, an axial planar cleavage defined by the alignment of white mica grains, dips to the south at 61°. Note the parasitic "S" folds indicating **northward** vergence as well as the sheared-out limbs of the folds - the displacement being of the order of a few milimeters.

s-c Fabrics indicative of shearing were observed at locality 75 (Fig. 3.22). The brittle-ductile shearing (see Ramsay and Graham, 1970) postdated the folding (as observed by the sheared out limbs of the folds) and probably occurred during the final stages of the D_1 event. Similarly oriented s-c fabrics were observed in sheared metalavas at locality 64 (Fig. 3.23). Talcification of serpentinite is considered to have occurred, to varying extents, in response to D_1 shearing. In the vicinity of localities 51 and 71 almost complete talcification has occurred. In other localities, such as locality 61 for example, talcification has occurred along fracture surfaces only (Fig. 3.24).

Figure 3.21 Photograph of hydraulic, quartz infilled breccia in a metalava xenolith from locality 34. The quartz veins do not extend into the host granodiorite indicating that the brecciation predates the intrusion of the granodiorites, probably occurring *in situ* on the seafloor.

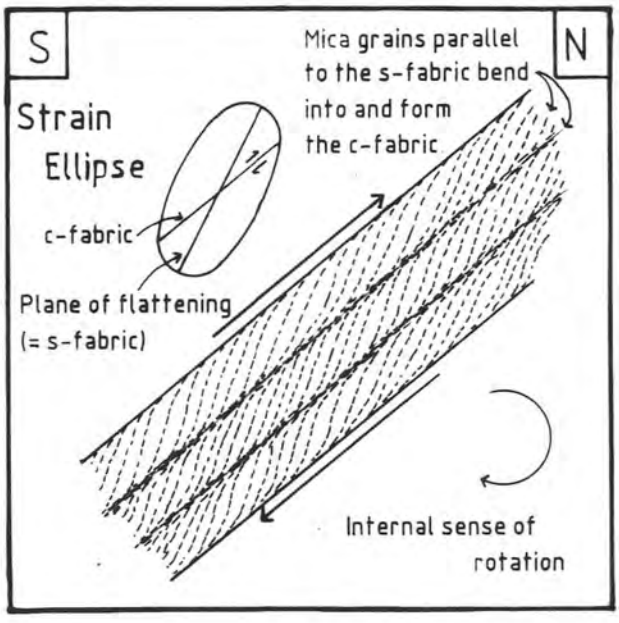

Figure 3.22 Idealized diagram showing s-c band structures in altered tuff at locality 75. The "c" shears dip to the south at around 40° and define the orientation of the shear zone. The dominant fabric, the s-fabric, develops parallel to the plane of flattening (see strain ellipse) and therefore represents a slightly rotated S_i fabric (rotation

being clockwise - looking west). The oblique relationship of the s-c band structures gives a clear indication as to the sense of displacement.

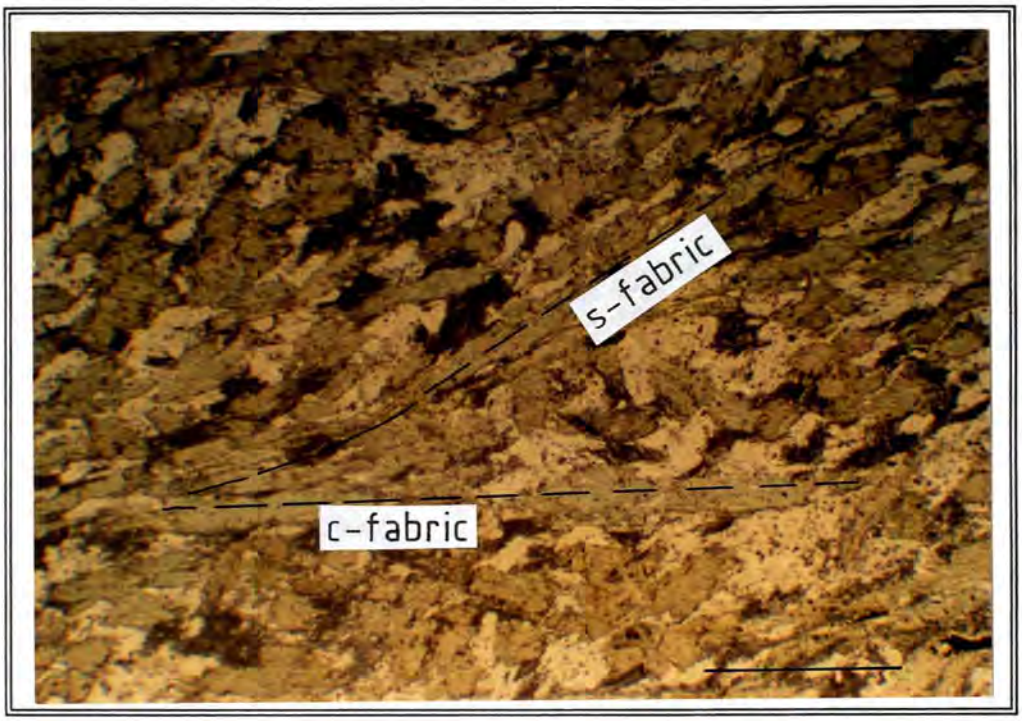

Figure 3.23 Photomicrograph showing s-c band structures in actinolite-tremolite schist from locality 64 (plane polarized light). The s-fabric, defined principally by amphibole grains, can clearly be seen bending into the c-fabric - the latter being defined mainly by elongate, polycrystalline, partly recrystallized, quartz ribbons. s-c Relationships indicate that the shear zone dips to the south at around 84°. The sense of displacement is shown. The brown mineral is highly altered feldspar. Scale bar 1 mm

The exact onset of metamorphism is difficult to determine, although it probably commenced prior to the D_1 event and involved initially seafloor metasomatism under the influence of convecting seawater. Seawater-dominated alteration of ocean floor metabasalts has been documented in modern ocean ridges, both in the axial parts as well as in the ridge flanks (Seyfried and Mottl, 1982; Erzinger, 1989). The effects are dependant on crustal depth - with water temperatures increasing and water/rock ratios and pH values decreasing downwards. Metamorphism continued through into D_1, reaching lower greenschist facies away from the intruding trondhjemitic gneisses and amphibolite facies adjacent to the gneisses. The former is exemplified by the mineral

Figure 3.24 Photograph showing talc developed along fracture surfaces within otherwise massive serpentinite (locality 61). The fractures acted as conduits for hydrous fluids which reacted with serpentine to produce talc. The talc crystals are oriented perpendicularly to fracture margins.

assemblage - actinolite-tremolite + (Mg-rich) chlorite + clinozoisite + plagioclase (albite) ± quartz ± epidote - displayed by the metalavas. Green hornblende replaces actinolite-tremolite and chlorite in metalavas adjacent to trondhjemitic sills, near the northern margin of the study area. Calcite veinlets present in serpentinite at locality 67 are ascribed to early seafloor metasomatism.

D_2M_2: The north-south compressive regime persisted during the intrusion of the late tectonic granodioritic gneisses. The margins of the granodiorite pluton are sheared, suggesting that it was emplaced in a semisolid state. Thin-section studies of the tectonized marginal zone show silicified, fractured and broken feldspar crystals set in a somewhat finer grained groundmass of Mg-rich chlorite, recrystallized quartz and clinozoisite. Biotite has been completely replaced by chlorite - a function of fluid ingress during shearing. Elsewhere, S_1 fabrics have been folded about east-west trending axes. For example, a small F_2 synform with the fold axis plunging at 75° on 277 was observed in talc

schists at locality 63. In addition, the schists were crenulated, with the crenulation lineation plunging at 60° on 286. F_2 folding was also observed in a metalava xenolith in granodiorite at locality 28 (Fig. 3.25). Close, westerly plunging folds in the vicinity of localities 81 and 82 are also ascribed to the D_2 event.

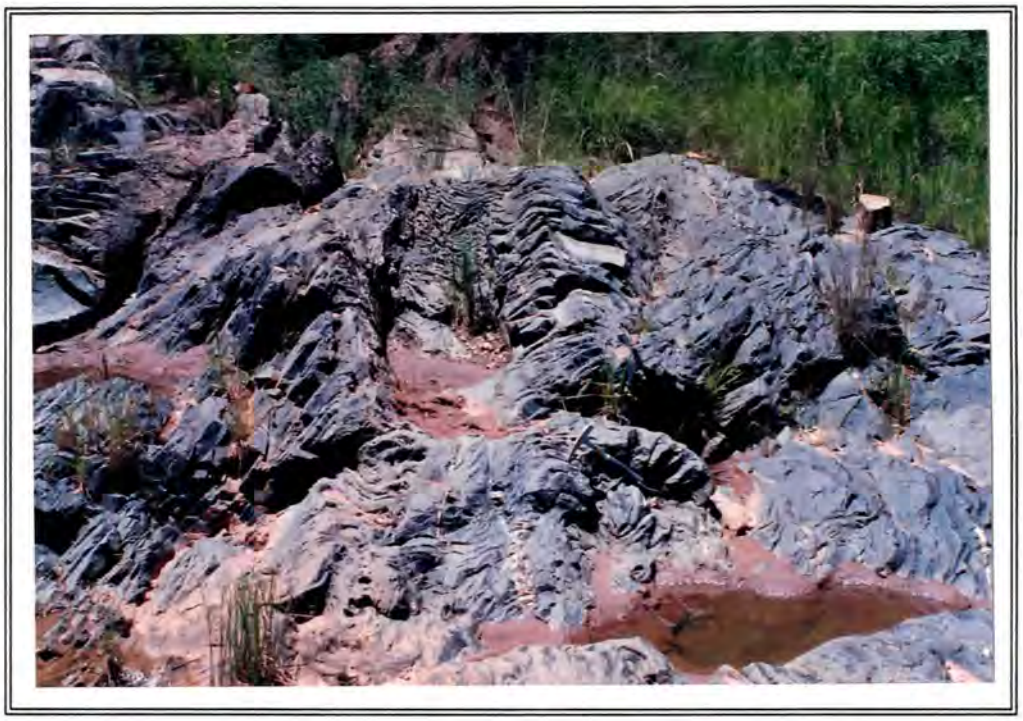

Figure 3.25 Photograph showing upright plunging, F_2 folds in metalava xenolith at locality 28. S_1 is clearly visible. The fold axis plunges at 35° on 115. The xenolith was folded during the emplacement of the partially solidified granodiorite.

Large-scale, brittle-ductile shearing was associted with the D_2 event. The Koningsberg Shear', an east-west trending, southerly dipping deformation zone cuts across the entire study area, disappearing under the Natal Group, both to the east and west of the study area. The shear zone, which varies from greater than 150 m to less than 40 m in thickness, is significantly enriched in Au, and will be discussed in detail in section 4.

Finally, a "Z" fold observed in banded quartzite at locality 92 suggests that right lateral shear stresses were operative at least on a local scale during part of the D_2 event (Fig. 3.26).

' **Name suggested by writer**

Figure 3.26 Photograph of "Z" fold in banded quartzite at locality 92. The sense of displacement is indicated. The coin is a twenty cent piece.

D_3M_3: Deformation associated with the intrusion of the post-tectonic Hlagothi Complex is confined to the southern parts of the study area. Two post-tectonic granite dykes which crop out to the south of the Complex (localities 31, 34 and 37), have been sheared out by vertical to steep northerly dipping, brittle-ductile shear zones (Fig. 3.1). Elongated, "smeared-out" biotite grains within sheared granite at locality 31 define a prominant mineral lineation with a mean plunge of 53° on 090 (Fig. 3.27). Such stretching fabrics develop parallel to the X-axis of the finite strain ellipsoid (Ramsay and Huber, 1987) and can therefore be used to determine the general sense of movement across a shear zone. In this case the displacement is oblique slip (Figs. 3.28 and 3.29).

Intense silicification accompanied the shearing event with the result that, towards the center of the shear zones, the granite has been altered to an almost pure quartz-muscovite rock containing 73.2% quartz and 20.9% muscovite respectively. Alteration decreases towards the margins of the shear zones. Minute (0.02 mm in diameter), euhedral garnet (probably almandine) crystals were also observed - the increase in

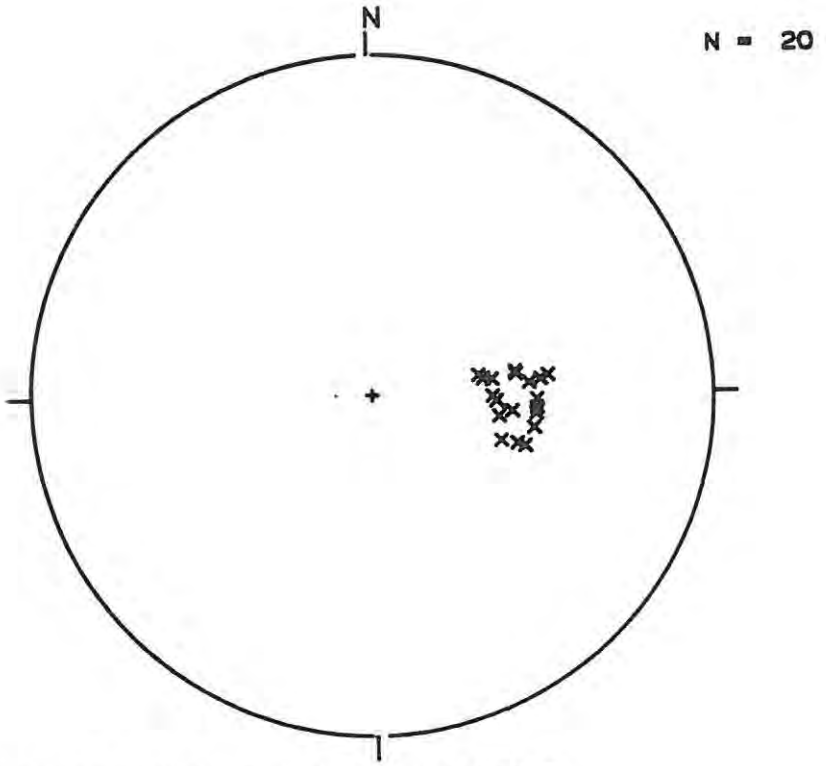

Figure 3.27 Stereographic plot of mineral lineations in sheared granite at locality 31.

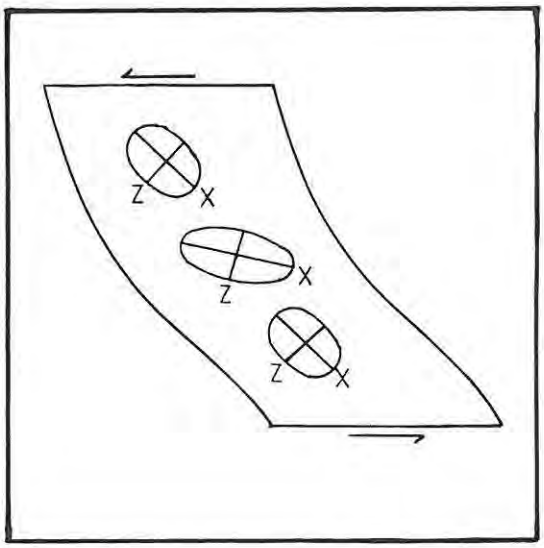

Figure 3.28 Diagram showing the orientation and shape of finite strain ellipsoids across a ductile shear zone undergoing deformation by way of heterogeneous simple shear. The mineral lineation develops parallel to the X-axis, thus defining the sense of movement across the shear zone.

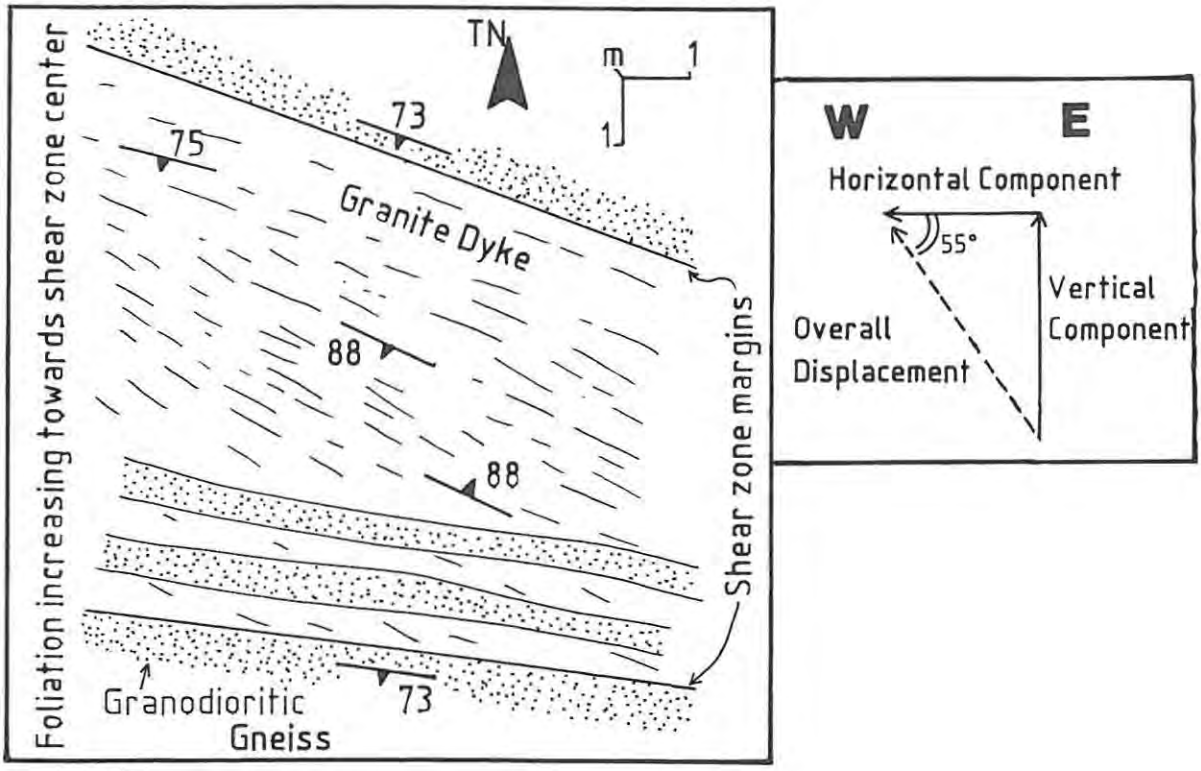

Figure 3.29 Plan view of D_3 shear zone at locality 31. The foliation (s-fabric) lies in the XY plane of the finite strain ellipsoid (that is the plane of flattening) and has been rotated in the center of the shear such that it dips steeply to the to the north. The tendency of s-fabrics to bend towards subparallelism with shear zone margins in the central part of shear zones (Hodgson, 1985), suggests that the D_3 shear is either vertical or steep northerly dipping. The overall sense of **movement** as defined by the mineral lineation, has been resolved into a horizontal and vertical component (inset).

metamorphic grade being directly attributable to D_3 shearing. The granodioritic gneiss along the northern margin of the Hlagothi Complex (locality 45) is similarly sheared. Again the alteration pattern is one of intense silicification with quartz making up 90.4% and fuchsite 5.0% of the rock in the center of the shear zone. Towards the margins of the shear zone, poikiloblastic fuchsite accounts for 53.0% and quartz 16.4% of the rock with clinozoisite (30.0%) and opaques making up the remainder. Analysis of a sample from locality 45 revealed significant enrichment with respect to both SiO_2 (89.09%) and Cr (2490 ppm). The Cr was probably leached out of the adjacent metagabbros and concentrated in the shear zone, resulting in the formation of fuchsite rather than muscovite.

D_4M_4: The final stage of deformation recognizable in the study area is marked by the presence of north and northeast striking, near vertical, normal faults, of possibly more than one age (Fig. 3.30). One such fault 150 m south of the Harewood working was sampled for Au and Ag. The results were however poor, with values of only 6 and 200 ppb respectively being obtained. Retrogressive effects accompanying the imposition of a tensional regime involved the chloritization of actinolite-tremolite and the partial replacement of hornblende by biotite in granodiorite adjacent to granite dykes.

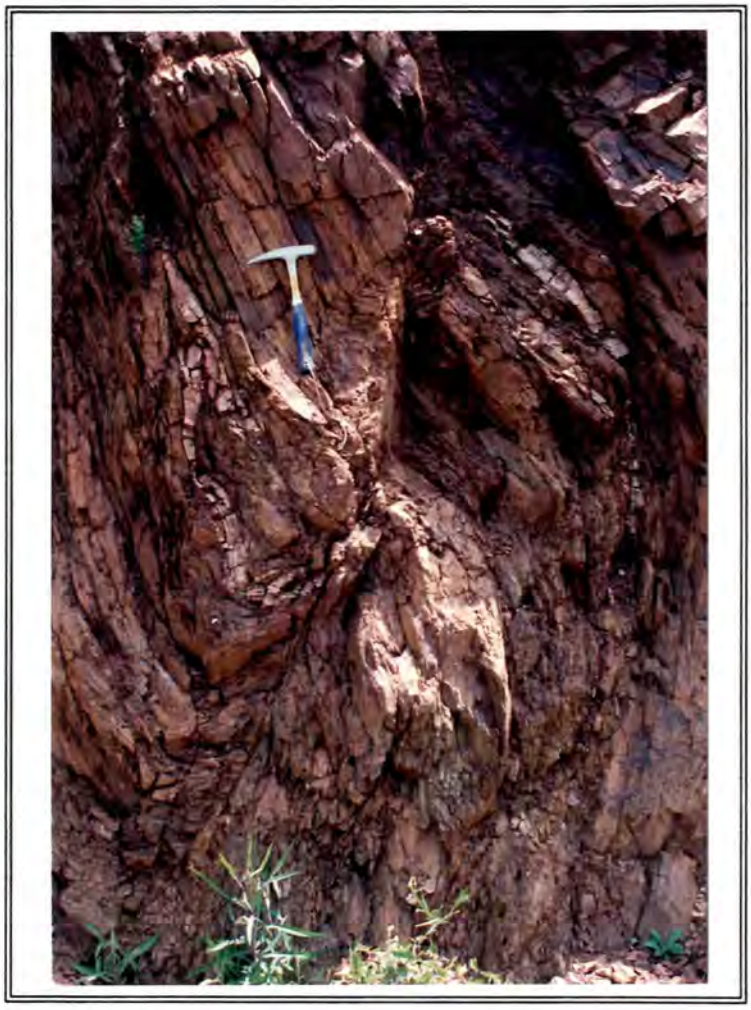

Figure 3.30 Photograph showing normal faulting associated with D_4 deformation in weathered granodioritic gneiss at locality 19. The fabric bends into the fault plane (oriented at 010/80 W) indicating the sense of displacement. The throw is approximately 1 m.

The four phases of deformation and associated metamorphism are summarized in Table 3.6.

Table 3.6 Deformational, metamorphic and intrusive history of the MGGR.

	Structure	Metamorphism	Granitoids	Mineralization
D_4	Tensional conditions, normal faulting, probably of more than one age	Retrogressive: chloritization of actinolite, replacement of hornblende by biotite		None
D_3	Minor shearing adjacent to Hlagothi gabbro	Upper greenschist, localized growth of garnet	Granite Dykes?	None
D_2	Continued north-south compression, folding of F_1 about east-west trending axes, major brittle-ductile shearing	Local amphibolite facies adjacent to D_2 intrusive	Granodiorite	Auriferous quartz reefs in the west trending, 40-150 m wide Koningsberg shear zone
D^1	North-south compression associated with basin closure: folding (with the development of a steep southerly dipping, axial-planar cleavage, minor shearing	Lower greenschist facies up to amphibolite facies adjacent to D_1 intrusive	Trondhjemite	Unmineralized quartz veins and breccias

3.5 Archaean Crustal Evolution

Theories concerning tectonic regimes operative during the Archaean can be categorized into "fixist" and "mobilist" - the former involving processes acting in place, such as rifting and diapirism, and the latter involving principally horizontal plate movements, **supplemented** by rifting and diapirism. An understanding of crustal processes operative during the Archaean has important implications for mineral exploration.

Whereas a general examination of the numerous models put forward to account for greenstone belt evolution (see Condie, 1981 and Pirajno and Jacob, 1984) is outside the scope of this thesis, two radically opposing models which have been applied to greenstone belt evolution in the Kaapvaal craton, will be briefly examined. The first involves predominantly vertical tectonics and the latter predominantly horizontal tectonics.

Anhaeusser (1983), the principal proponent of vertical tectonic models, attributed the deformation in the Barberton Mountain Land

to a process involving the downsagging of volcano-sedimentary greenstone sequences (owing to gravitational instability), and the concomitant intrusion of solid, granitic diapirs. The diapirs, derived from partial melting of the supracrustal root zones, were forced up owing to the gravitational imbalance induced by the pile of denser greenstones. This necessarily implied downsagging to some considerable depth, a feature not supported by geophysical evidence. For example, seismic profiling across a number of South African greenstone belts (Barberton, Murchison, Pietersburg and Giyani) by de Beer and Stettler (1986) showed that they were shallow features, rarely exceeding 5 km in depth. Kröner (1985), in a study of greenstone belts in Canada and Australia, questioned the predominance of vertical tectonics during the Archaean. Kröner pointed out that the derivation of the Archaean tonalite-trondhjemite-granodiorite suite from anatexis of downsagging mafic greenstone volcanics was incompatible with REE and isotopic systematics.

Models involving essentially horizontal deformation can be subdivided into proto-plate tectonic models and rifting tectonic models (Pirajno and Jacob, 1984), although the two simply represent the end-members of a continuous spectrum of tectonic environments. Condie and Hunter (1976) for example, envisaged a rifting tectonic model based on an ascending mantle plume for the evolution of the Barberton greenstone belt. Franey (1987) on the other hand, regarded the Pietersberg greenstone belt as an ophiolite suite, obducted onto continental crust during the closure of an ocean basin. The presence of at least five D_2 thrusts were sited as evidence for this. The greenstone sequence was deemed to have accumulated in a narrow, back-arc marginal sea, under conditions similar to those proposed by Tarney et al. (1976).

The consistently steep southerly dipping S_1 fabric displayed by all the rocks of the MGGR points to the predominance of horizontal rather than vertical tectonic processes operating during the evolution of the belt. The geochemistry of the tholeiites is similar to that of modern oceanic crust produced at mid-ocean ridges (see Condie, 1976) suggesting that the metalavas probably originated in an oceanic environment (Fig. 3.31). The

greenstone sequence is considered to have accumulated in response to limited back-arc spreading. Cessation of spreading followed by basin closure and the intrusion of syntectonic trondhjemites produced the observed compressional structures. Hence, the model proposed by Tarney et al. (1976) involving the evolution of an Archaean greenstone belt in a back-arc tectonic setting seems to best apply to the MGGR. The writer sees no need to invoke a unique Archaean tectonic model to explain the tectonic history of the MGGR.

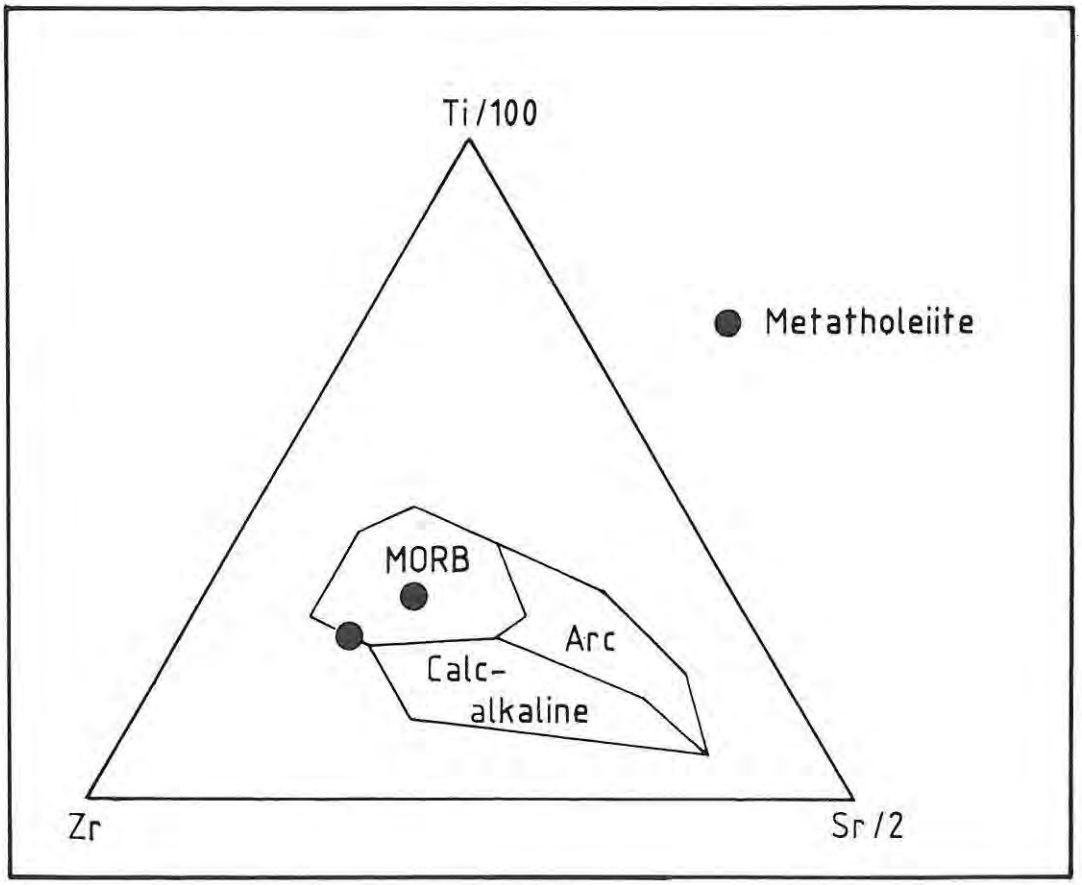

Figure 3.31 Ti-Zr-Sr plot of metatholeiites from the MGGR. The elements chosen are relatively immobile and hence their concentration in the Archaean tholeiites should have varied little over time. The fields for modern mid-ocean ridge (MORB), arc and calc-alkaline tholeiites are from Pearce and Cann (1973). The tholeiites (from localities 52 and 84) plot within of the MORB field.

4. GOLD DEPOSITS

As previously stated, Au mineralization is associated with the east-west trending, D_2 Koningsberg shear zone. Two old Au workings and one old Au prospect occur within the study area.

4.1 Harewood Gold Working

The old working is situated in highly altered trondhjemite near the eastern margin of the study area (Fig. 3.1). Outcrop is extremely limited and invariably highly weathered, the best exposures being in road cuttings and old trenches. The working, which is confined to an area of 120 x 120 m, is evidenced by the presence of numerous collapsed adits, infilled shafts, trenches and small spoil heaps (Fig. 4.1). All but one of the adits collapsed prior to the turn of the last century. The only open adit extends no more than 10 m into the hillside and does not intersect reef. One 40 m deep shaft remains free of rubble. The underground workings have in all probability collapsed.

Figure 4.1 Photograph of an old prospecting trench at the Harewood working.

According to the Commissioner of Mines reports for the year 1894 (Garrard, 1895), the Au occurred in two parallel, east-west striking, quartz reefs situated about 27 m apart. The steep southerly dipping reefs, known as the "N° 3 Leader" and "Main Reef", were believed to be encased conformably in the enclosing schists. The mineralization was not considered to be related to shearing and no mention was made of the extensive wall rock alteration. The quartz reefs varied from 0.1 to 0.6 m in thickness. The Au was distributed in easterly plunging shoots, each shoot being about 25 m in width and separated by about 30 m of low grade reef. Pertinent data deduced from the old records relating to grade, tonnages and mining depths are summarized in Table 4.1.

Table 4.1 Production data from the Harewood and Vira workings and the Times prospect. Information from Du Toit (1931) and the Commissioner of Mines (Natal) Reports for the years 1894 - 1909.

	Harewood Mine	Vira Mine	Times Prospect
Max Mining Depth (m)	80	± 40	± 35
Total Tons Mined	709	1222	926
Gold Produced (kg)	12.931	9.314	0.933
Average Grade (g/t)	18.24	7.63	1.01
Alluvial Gold (kg produced)	Insignificant	13.175	Not Applicable

Mapping by the writer revealed that the auriferous quartz reefs occur in quartz-sericite schists, in a zone of intense shearing (Fig. 4.2). To the north of the roughly 140 m wide, brittle-ductile shear zone, the schists pass into unsheared trondhjemitic gneiss. The southern margin of the shear zone is marked by a narrow band of talc schist which passes into unsheared serpentinite further south. The quartz-sericite and talc schists represent sheared and altered trondhjemite and serpentinite respectively. The shear zone cross-cuts the early S_1 fabric, the shearing therefore post-dating the D_1 event. The shearing is also unrelated to the intrusion of the Hlagothi Complex (D_3) which

crops out some distance to the southwest. It is concluded that the Koningsberg shear zone formed during the intrusion of the far more extensive, late-tectonic, granodioritic gneisses and is therefore D_2 in age.

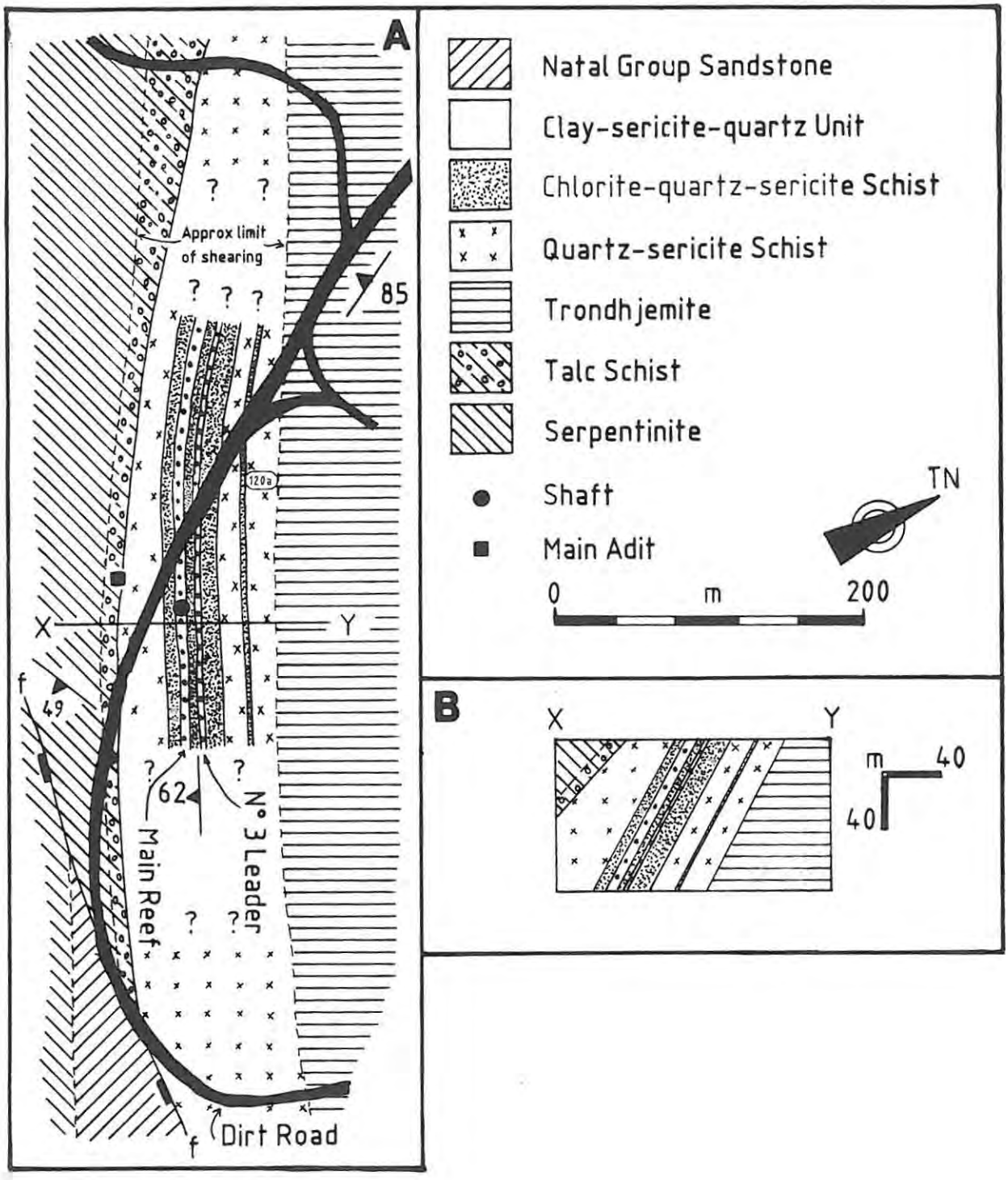

Figure 4.2 Geological plan (a) and section (b) of the Harewood Au working and surrounding area. Lack of exposure prevented detailed mapping.

The onset of shearing was marked by the ingress of large volumes of silica-bearing, hydrothermal fluids. These resulted in the pervasive to semi-pervasive alteration of trondhjemitic gneisses within the shear zone to quartz-sericite schist (Fig. 4.3). In addition, first generation, foliation-parallel quartz veins developed in response to cleavage-parallel fissuring. The highly boudinaged, inequigranular, coarse-grained veins vary from a few millimeters to 15 cm in thickness and consist of quartz, with occasional Fe-oxide coatings on fracture surfaces. Elongated, recrystallized quartz grains define a prominant, subvertically oriented, mineral lineation and indicate a subvertical sense of shear movement (Figs. 4.4 and 4.5). The boudins define a lineation plunging at between 50° and 60° to the east. The first generation quartz veins are **unmineralized**.

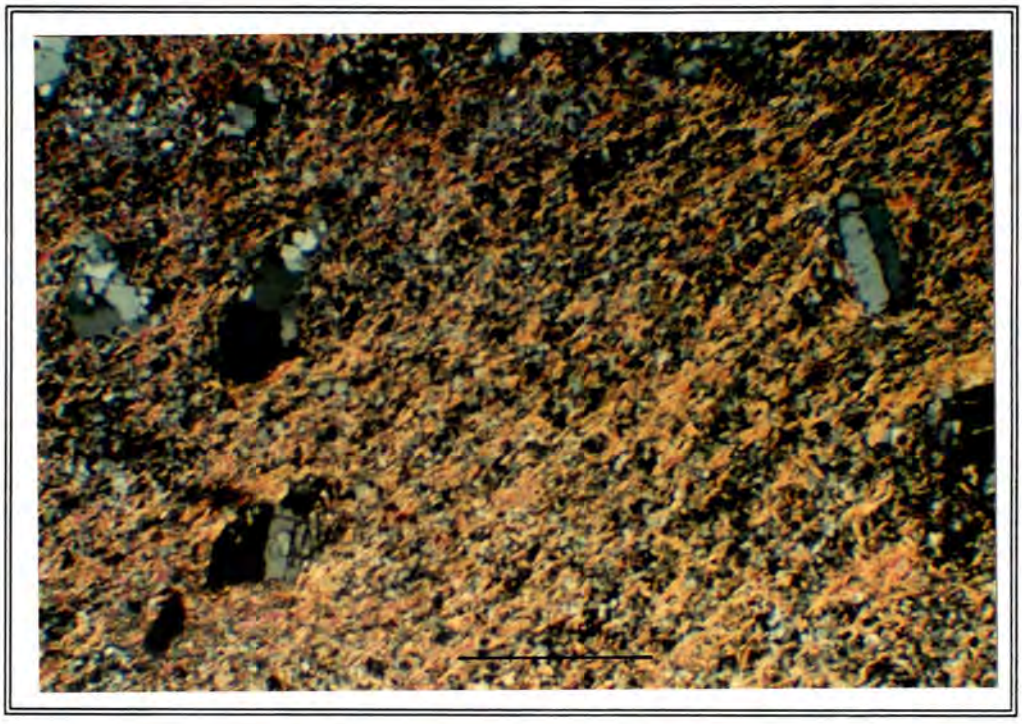

Figure 4.3 Photomicrograph of quartz-sericite-plagioclase schist from the Harewood Au working (polars crossed). The semi-pervasive nature of the alteration is evidenced by the presence of highly fractured, relict plagioclase crystals in the process of being replaced by quartz and sericite. Recrystallized quartz grains are elongate, the shape being controlled by the surrounding mica grains. The rock displays a blastomylonitic texture. Scale bar 1 mm.

Figure 4.4 Photograph of a first generation vein quartz from the Harewood Au working. The elongated quartz grains give rise to a stretching fabric parallel to the X-axis of the finite strain ellipsoid. Note the characterisitic white colour.

Towards the center of the shear zone, the schists dip to the south at between 62° and 69°. As previously stated, s-fabrics tend to be rotated into subparallelism with with the shear zone margins in the central part of the zone. The Koningsberg shear in the vicinity of the Harewood Au working is therefore envisaged as a steep southerly dipping (at around 65°) deformation zone.

A second generation of steep southerly dipping quartz veins cross-cuts the first at a shallow angle. These were observed at two localities only, that is where the Main Reef intersects a timber road and in an old trench to the north of the N° 3 Leader (Fig. 4.6). The second generation veins differ markedly to the first - particularly with respect to mineralogy and texture. They comprise predominantly medium-grained, equigranular quartz grains, with lesser tourmaline (variety schorl), specularite and sericite (Figs. 4.7a and b). Pyrrhotite, sphalerite and **native Au** (grading up to 5.6 ppm) occur in trace ammounts. The tourmaline crystals lie within the XY plane of the finite strain ellipsoid (that is the plane of flattening) and thus define a crude

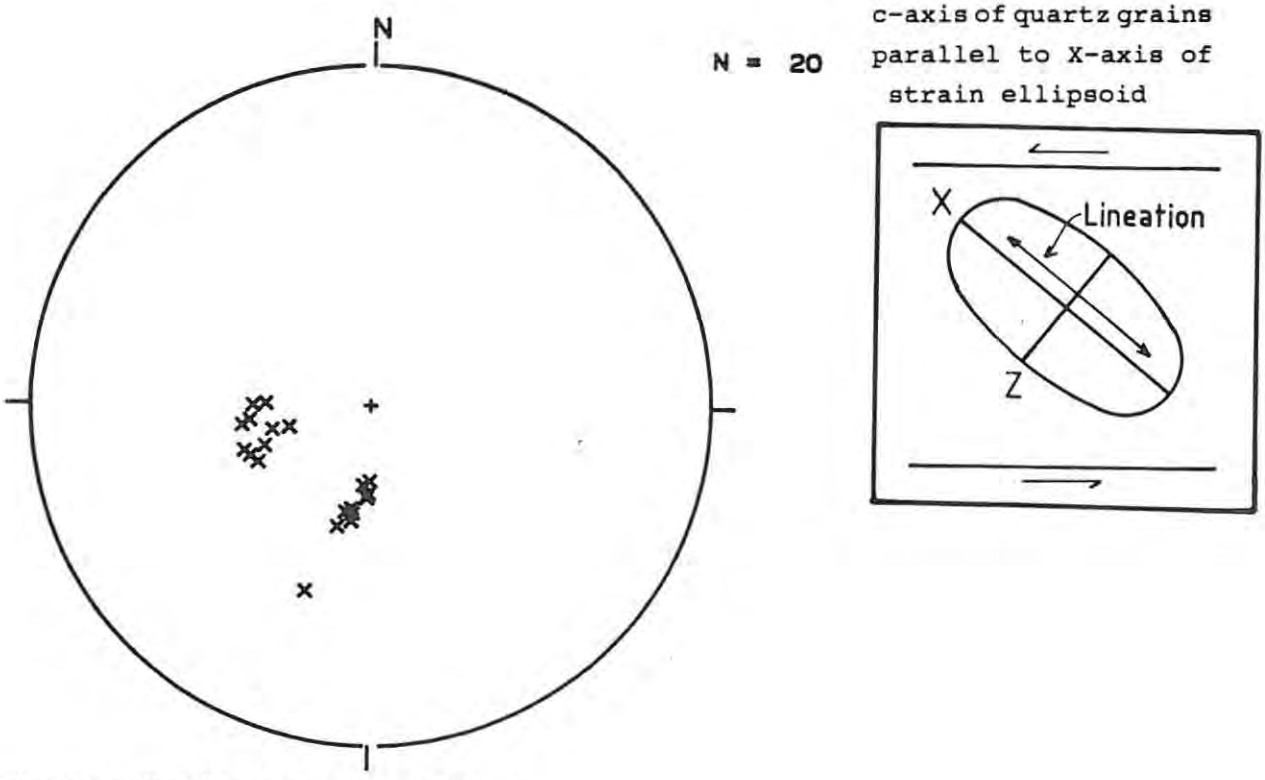

Figure 4.5 Stereographic plot of quartz grain lineations in first generation vein quartz from the Harewood Au working. Inset shows the relationship between the orientation of the principal axes of the finite strain ellipsoid, the stretching lineation and the sense of displacement across a shear zone. The lineations cluster about two points (averaging 69 on 191 and 64 on 254) which might indicate the presence of s and c band fabrics respectively. The sense of displacement is to the north.

"foliation" parallel to the s-fabric in the adjacent schists. Had the second generation quartz veins been deposited at the height of the shearing event, the enclosed tourmaline crystals would have been oriented parallel to the X axis of the strain ellipsoid. The auriferous quartz veins are therefore interpreted as being deposited under compressive conditions towards the end of the shearing event, **after displacement across the shear had ceased**.

In an ideal situation, five differently-oriented fracture sets, first identified experimently by Riedel in 1929, form during shearing (Fig. 4.8). The first two, referred to as *low angle*

Figure 4.6 Photograph of an old trench at the Harewood Au working looking west (locality 120a - refer to figure 4.2) showing highly boudinaged, first generation, foliation-parallel quartz veins being cross-cut by a steep southerly dipping, second generation, Au-bearing quartz vein. Note how the vein bends into the s-fabric near the center of the photograph.

Riedel and *high angle Riedel shears*, form at about 15° and 75° to the shear zone margins and are orientated such that the acute angle points in the direction of displacement (Hodgson, 1989). With continued deformation, a second set of fractures termed *P Shears* develops. These are inclined at about 15° to the shear zone margins but are oriented in the opposite direction to the Riedel shears. *C shears* occupy the central parts of, and develop parallel to, the shear zone. Extensional fractures (T in Fig. 4.8) form in the YZ plane of the finite strain ellipsoid at any instant of strain. Shear veins which form at an angle to the shear zone margins are **invariably oriented parallel to "P" shears** (Hodgson, 1989) and are, in addition, useful indicators as to the sense of displacement across the shear zone. Furthermore, they tend to occur in *en echelon* sets, with the sense of stepping corresponding to the sense of movement across the zone containing them.

Figure 4.7a Photograph of tourmaline-bearing, auriferous, saccharoidal vein quartz from the Harewood Au working. Note the equigranular nature of the quartz grains and the characteristic pale greyish colour - a function of the tourmaline (plus specularite) content.

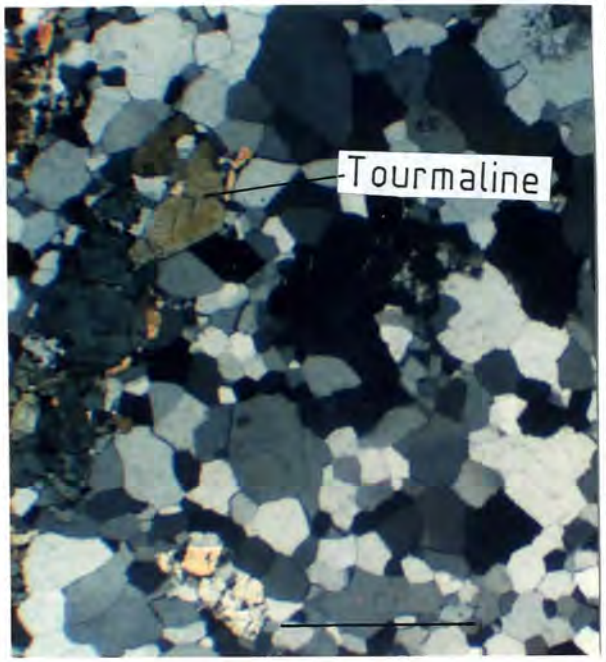

Figure 4.7b Photomicrograph of the same rock (polars crossed). The larger quartz grains are highly strained with curved to serrated margins indicative of incipient recrystallization. Recrystallization of the remaining quartz fraction has given rise to euhedral to subhedral quartz grains resulting in a mosaic texture. Scale bar 1 mm.

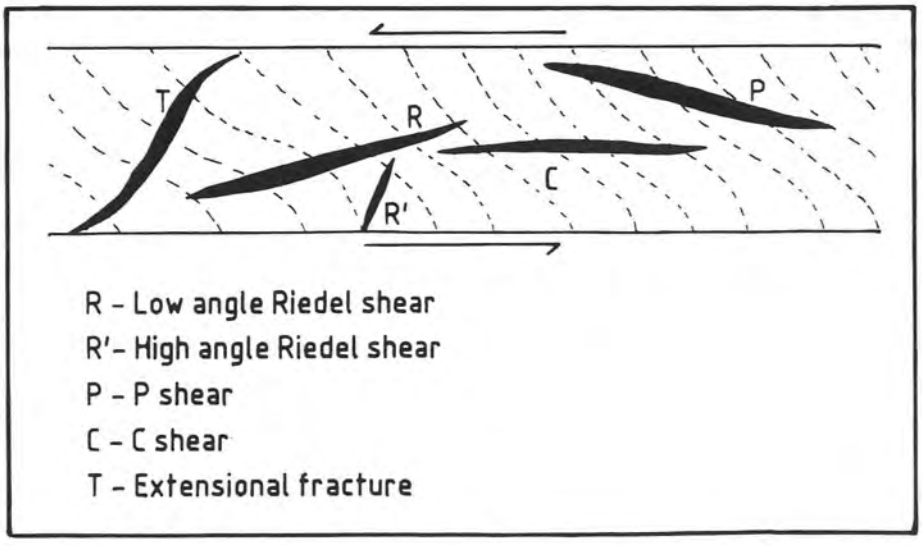

Figure 4.8 Diagram showing the orientation of fracture sets in a brittle-ductile shear zone (modified after Roberts, 1987). Note that the sense of displacement is in the opposite direction to the acute angle formed by the intersection of the *P* shear with the shear zone boundary.

The ± 1 m wide, Main Reef ore zone (Fig. 4.2) consists of a number of quartz veins and stringers up to 12 cm in thickness. The auriferous veins dip to the south at between 72° and 82° - that is about 7° to 17° steeper than the shear zone itself - and are therefore classified as **oblique shear veins** (Fig. 4.9). They therefore probably occur in an *en echelon* array, a feature not recognized by the original miners.

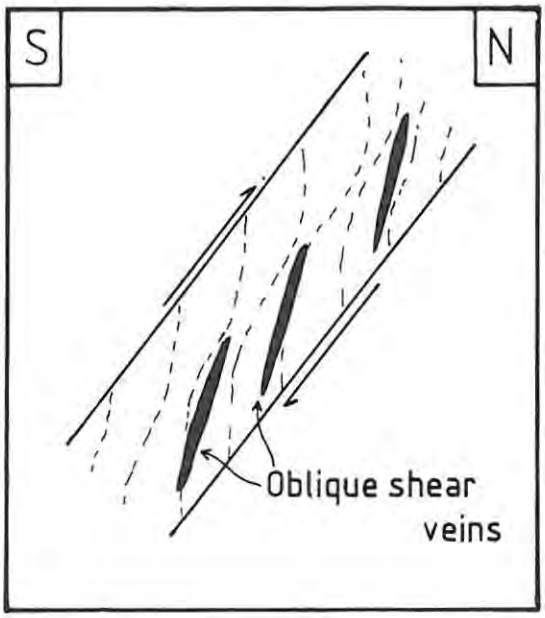

Figure 4.9 Diagram depicting oblique shear veins in a reverse shear zone (modified after Hodgson 1989). The shear zone in the diagram is oriented similarly to the Harewood shear zone in order to elucidate the geometric relationships between the s-fabric observed at the Harewood Au working and the second generation, Au-bearing quartz veins.

4.1.1 Alteration-Mineralization

In quartz vein-hosted Au deposits of this nature, mineralization and wall rock alteration are intimately related, with Au precipitating largely in response to fluid/wall rock interaction (Hodgson, 1985). The nature of the alteration depends on the nature of the original wall rock, the characteristics of the mineralizing fluid and the temperatures and pressures at which fluid/wall rock interaction took place. The most important alteration process involves hydrolysis, in which anhydrous silicates like the feldspars are converted to hydrolyzed silicates such as the micas and clays. The process also buffers the pH of the mineralizing solutions, significantly affecting the chemical properties of the fluids. For example, the alteration of

feldspar to sericite consumes H^+, increasing the pH of the mineralizing fluids thereby decreasing the solubility of Au-bearing thio-complexes. Clearly then, ore minerals can be deposited directly in response to the hydrolysis of feldspars.

As previously stated, early, hydrothermal activity associated with the D_2 shearing event altered the trondhjemitic gneisses across the entire width of the shear zone (with the exception of the central portion) to a quartz-sericite-(plagioclase) assemblage. Towards the center of the shear zone near the N° 3 Leader and Main Reefs, the quartz-sericite alteration assemblage passes into a quartz-chlorite-sericite assemblage (Fig. 4.2). Adjacent to the reefs, the quartz-chlorite-sericite assemblage passes into a clay (kaolinite)-sericite-quartz-(chlorite) assemblage (Fig. 4.10). Hence, three distinct wall rock alteration facies are recognized, namely an outer zone of sericitic alteration, a central zone of chloritic alteration and an inner zone of argillic alteration (Fig. 4.11). It is unclear whether the alteration occurred during discrete phases of fluid ingress or is simply an expression of the degree of fluid/wall rock interaction over a sustained period of hydrothermal activity. The uniform loss or gain (relative to unaltered trondhjemite) of certain components across the **entire** Harewood shear **irrespective of the alteration zone**, supports the latter contention. For example, Na_2O and CaO concentrations decrease uniformly by factors of 34 and 53 respectively while K_2O, Fe_2O_3 and FeO concentrations increase by factors of around 5, 2 and 2 respectively, across the shear zone (Fig. 4.11). Boyle (1979), in an appraisal of epigenetic Au deposits generally, related the associated wall rock alteration facies to the degree of interaction between the ore-forming solutions and the adjacent rocks, rather than to fluids of differing compositions introduced at differing periods.

The highly deformed, non-Au-bearing, first generation quartz veins must have formed early during the deformation event. The small increase in the overall silica content of the quartz-sericite schists near the margins of the shear relative to unaltered trondhjemite (Fig. 4.11), suggests that the early veins formed mainly in response to the **diffusion** of SiO_2 through a

Figure 4.10 Photograph looking east showing showing weathered clay-sericite-quartz rock inbetween the N° 3 Leader and Main Reefs at the Harewood deposit. Quartz reef float is evident along the left-hand margins of the photograph.

static intergranular fluid from the **immediate** host rocks to suitable vein sites, rather than to the voluminous introduction of SiO_2 from an extraneous source.

It is concluded that the zonally-related nature of the alteration is an expression of the progressively increasing intensity of the fluid/wall rock interaction as the Au-bearing quartz reefs are approached. The fact that the first and second generation quartz veins were deposited during the early and late stages of the D_2 shearing respectively (see preceeding argument) suggests that fluid/wall rock interaction operated over a protracted period of time - that is throughout the shearing event.

The wall rock alteration at the Harewood working resulted from the progressive breakdown of the silicate phases and the introduction of certain elements, notably K. The dominant chemical process involved hydrogen ion metasomatism, the H^+ ions being derived from the ascending hydrothermal solutions (Hodgson, 1985). Another important wall rock alteration process which is considered by most authors to be invariably associated with

Archaean lode Au deposits (for example - Phillips, 1984; Kerrich, 1986; Barley and Groves, 1987) - namely carbonatization - is absent. According to these authors, carbonatization is most intense **nearest** the vein systems. CO_2, which is derived from the ascending hydrothermal fluids, reacts with bivalent metal cations in the wall rocks (that is Fe, Mg, Ca and Mn) to form carbonate minerals, particularly ankerite. Chloritization, considered by Gélinas *et al.* (1982) to result from the substitution of MgO (specifically) and FeO (to a much lesser extent) for CaO in the original ferromagnesian minerals, is the typical peripheral alteration facies in Archaean lode Au deposits. According to Roberts (1987), the typical alteration sequence in felsic host rocks (which is similar in mafic, ultramafic and intermediate host rocks) consists of an outer zone of chloritization (chlorite-carbonate-sericite), a central zone of sericitization (carbonate-sericite) and an inner zone of carbonitization (carbonate-albite) The wall rock alteration facies associated with the Harewood Au lodes is therefore **atypical**, particularly with respect to the absence of carbonate alteration **of any kind**. The mineralizing fluids were thus H_2O-bearing but not CO_2-bearing.

The chemical changes evident in the wall rock alteration zone are depicted in Fig. 4.11. The chemical variations cannot be ascribed to differing wall rock lithologies since the original wall rocks were comprised of homogeneous trondhjemite. The mineralogical changes were therefore **not** isochemical in nature.

The dominant reactions considered to have given rise to the peripheral zone of sericitic alteration involved first potassium metasomatism followed by hydrogen ion metasomatism. Potassium metasomatism affected the entire alteration zone. The reactions can be written as follows (Guilbert and Park, 1986):

1) $\underset{\text{plagioclase}}{(Na,Ca)AlSi_3O_8} + K^+ \rightarrow \underset{\text{K-feldspar}}{KAlSi_3O_8} + Na^+ + Ca^{2+}$

2) $\underset{\text{K-feldspar}}{3KAlSi_3O_8} + K^+(aq) + 2H^+(aq) \rightarrow \underset{\text{sericite}}{KAl_3Si_3O_{10}(OH)_2} + 6SiO_2 + 3Na^+(aq)$

The breakdown of plagioclase would have liberated Ca and Na, both

of which appear to have been almost completely flushed from the system. K was introduced into the system in significant quantities although a small portion must have been derived from the breakdown of biotite. The silica liberated by the reaction probably gave rise to the first generation quartz veinlets.

Mg and Fe were introduced into the system from the breakdown of biotite and also from the mineralizating solutions, leading to the formation of chlorite. MgO concentrations in the wall rocks increase significantly in the vicinity of the chlorite alteration facies. Again a two-phase alteration process is envisaged involving initially potassium metasomatism followed by magnesium (and lesser iron) metasomatism. The first corresponds to reaction (1) above. The latter may be written as follows (Guilbert and Park, 1986):

$$3)\ \underset{\text{K-feldspar}}{KAlSi_3O_8} + 6.5Mg^{2+} + 10H_2O \rightarrow \underset{\text{chlorite}}{Mg_{6.5}(Si,Al)O_{10}(OH)_8} + K^+ + 12H^+$$

Chlorite typically breaks down to form albite, particularly immediately adjacent to the zone of mineralization (Hodgson, 1895). The depletion of Na and enrichment of K at the Harewood deposit however, favoured the formation of sericite instead. Further hydrolysis stripped K from the sericite leading to the formation of kaolinite, the reaction being written:

$$4)\ 2\underset{\text{sericite}}{KAl_3Si_3O_{10}(OH)_2} + 2H^+ + 3H_2O \rightarrow 3\underset{\text{kaolinite}}{Al_2Si_2O_5(OH)_4} + 2K^+$$

Silicification increases towards the center of the shear zone. The process simply involved the precipitation of silica (derived from both the hydrothermal fluids and from wall rock reactions) in available pore spaces and in dilatant fractures, **ultimately** leading to the formation of the mineralized quartz reefs.

Based on the nature of the wall rock alteration together with the mineralogy of the auriferous quartz reefs (see above), the mineralizing fluids must have been H_2O-bearing, rich in K, Mg, Fe, and Au, but depleted in CO_2. S enrichment does not occur indicating that the fluids had low S contents. Auriferous vein quartz in the same D_2 shear in mafic rocks to the west does not

Wall Rock Alteration Zones

Unaltered	Sericitic	Chloritic	Argillic	Reef

Mineralogical Changes

Quartz		Quartz added		Quartz +
Orthoclase	Sericite	Sericite (chlorite)	Sericite/clay	Sulphides
Plagioclase	(K-feldspar) Sericite	Sericite (chlorite)		Tourm. &
Biotite	Chlorite	Chlorite	Chlorite	Haematite

Relative Chemical Changes

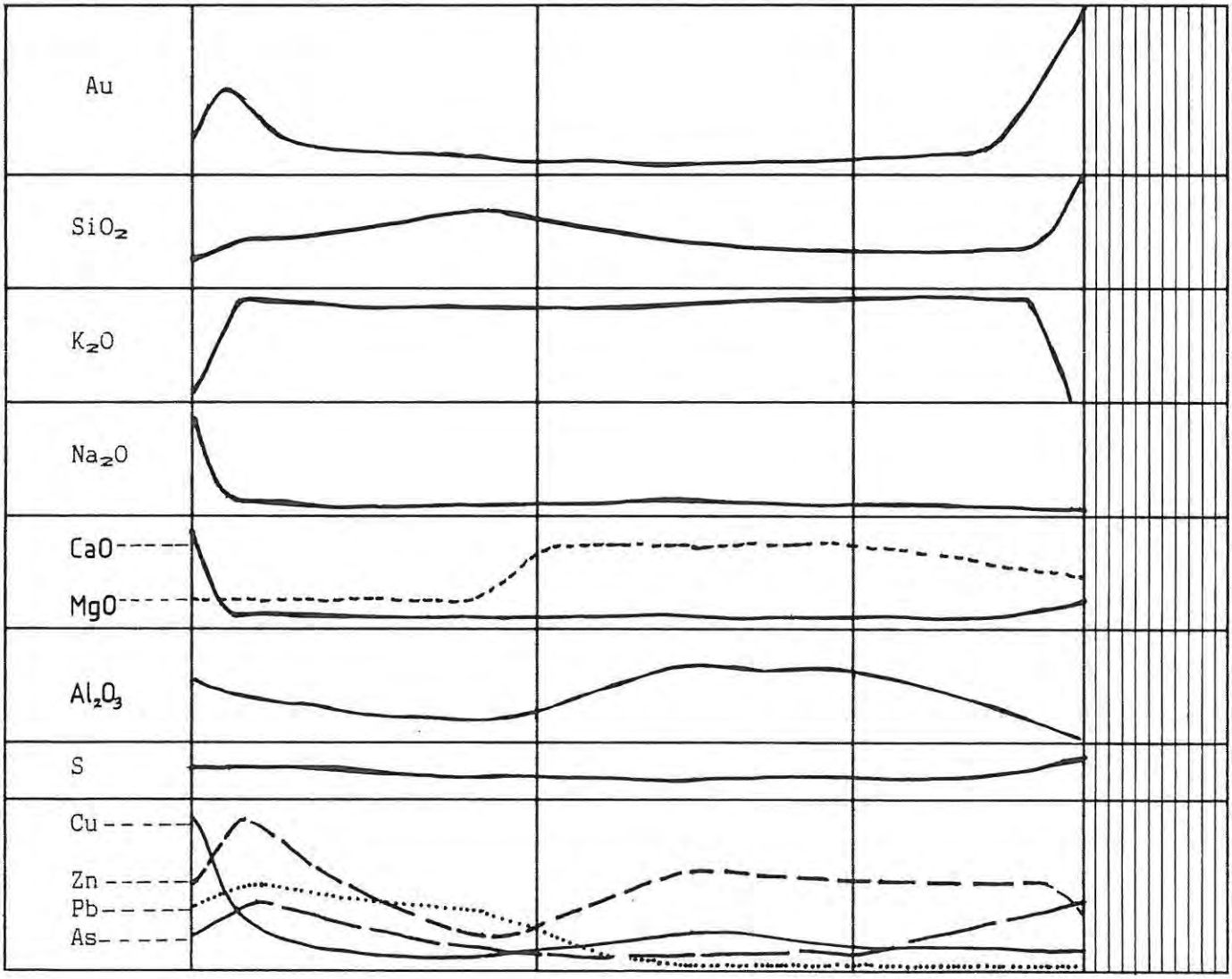

Figure 4.11 Diagrammatic summary of wall rock alteration around the Harewood Au lodes. Owing to deep weathering and extremely poor outcrop, sampling sites were extremely restricted. Hence samples could not be taken at predetermined distances away from the quartz reef as desired,

but rather where outcrop permitted. For the sake of clarity, the "reef zone" includes both the N° 3 Leader and Main Reefs. See text for detailed discussion.

Note:

a) K has been flushed from the wall rocks immediately adjacent to the fluid channelways.

b) The depletion of Al adjacent to the quartz reefs and the corresponding increase away from the mineralized zone. The migration of Al probably took place in conjunction with the depletion of K in wall rocks near the reefs, since the latter, when present, tends to fix Al, in the form of sericite (Hodgson, 1985).

c) The increasing Au contents as the reef is approached as well as the zone of Au enrichment at locality 120a (refer to Fig. 4.2), which corresponds broadly to a zone of weak chloritic alteration. The Au is essentially confined to the quartz reefs with only minor amounts being disseminated in the wall rocks.

carry tourmaline, suggesting that the mineralizing fluids did not contain B. Instead, tourmaline in the Harewood reefs probably owes its origin to B leached from the adjacent wall rocks.

Polished-section studies of the mineralized, oblique shear veins reveal anhedral, granular masses of pyrrhotite and sphalerite. Two generations of pyrrhotite are present, the second of which has partially replaced both the first generation pyrrhotite and the sphalerite (Figs. 4.12a and b). The Zn (in the sphalerite) was probably derived from the wall rocks adjacent to the reefs, thus explaining the observed Zn depletion in these rocks. Pyrite is not present - a function of the low Fe to S ratios. Haematite occurs as fracture and grain coatings. Au occurs as minute, anhedral grains (average 9 μm diameter; largest grain observed 20 μm) along quartz crystal margins, particularly within "brecciated" portions of the quartz reefs - the brecciation being caused by high fluid pressures during the **final stages of auriferous quartz reef deposition** (Fig. 4.13). The Au is free milling. However, experiments would need to be carried out in order to determine the degree of comminution necessary to liberate the Au. With respect to the oblique shear veins only, the textural evidence points to the following paragenetic sequence:

Quartz (I) + tourmaline + sericite
↓
Haematite
↓
Pyrrhotite (I)
↓
Sphalerite
↓
Pyrrhotite (II)
↓
Quartz (II) + Gold

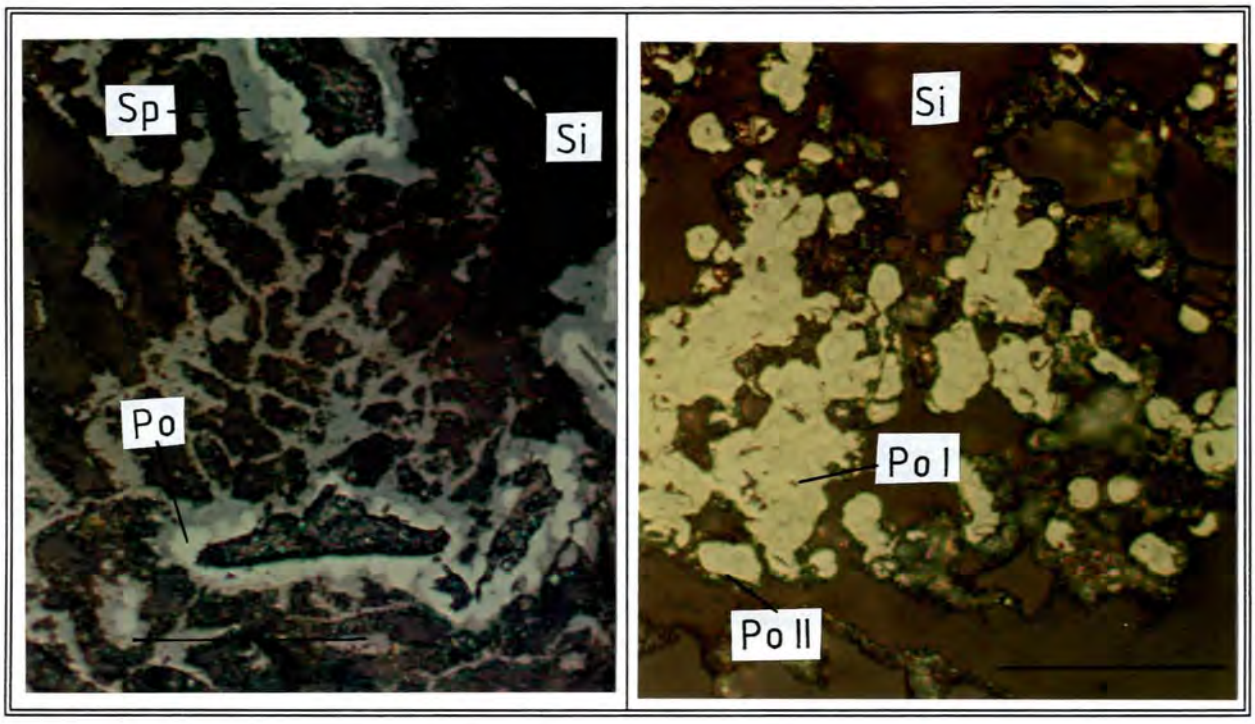

Figure 4.12a Photomicrograph showing irregular sphalerite mass (Sp) being replaced by pyrrhotite (Po) and silica (Si). The darker patches represent pits in the surface of the polished-section. Note the classic caries texture. Scale bar 50 μm.

Figure 4.12b Photomicrograph showing overgrowths of later pyrrhotite (Po II) on early, partially replaced pyrrhotite (Po I) giving cockade texture. Pyrrhotite (II) is being replaced by silica (Si). Scale bar 50 μm.

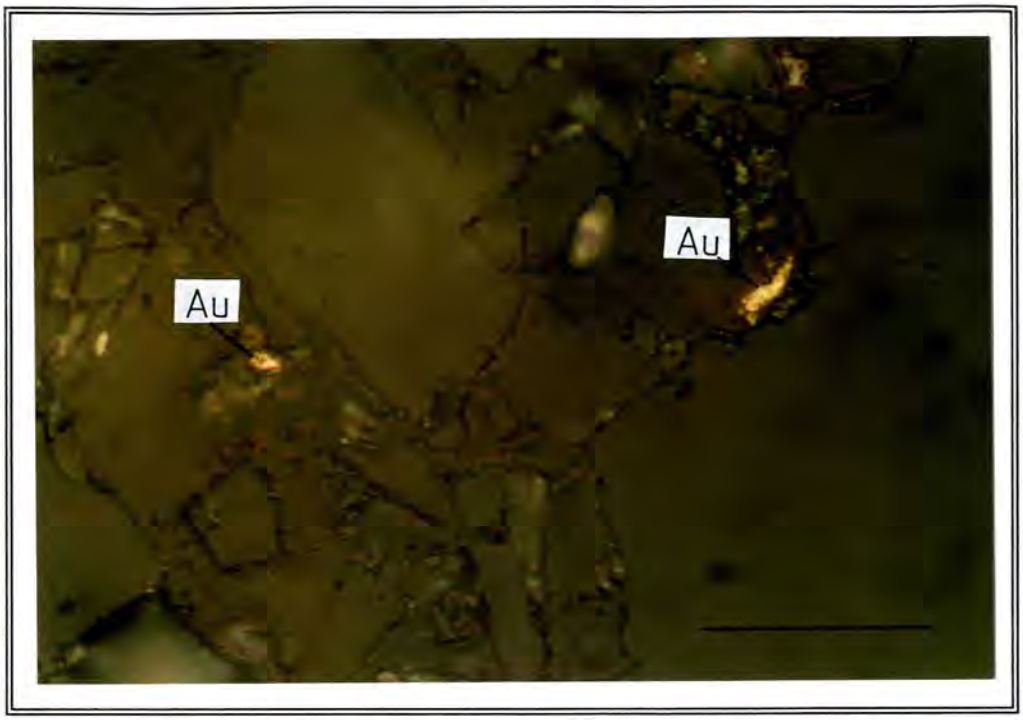

Figure 4.13 Photomicrograph showing Au grains along quartz crystal margins in highly fractured (brecciated) portion of the reef. Scale Bar 50 μm.

4.2 Vira Gold Working

The Vira working is situated in the Koningsberg shear zone about 1 km west of the Harewood deposit (Fig. 3.1). A number of collapsed adits as well as the main open-cast working are still evident (Fig. 4.14). According to Gray (1910), the Au was disseminated in chlorite and talc schists and in thin quartz stringers which followed the east-west trending foliation planes. Production data are summarized in Table 4.1. Of note is the significant quantity of alluvial Au which was extracted from the banks of the Harewood River below the working. Work commenced in 1909 and proceeded intermittently until 1928 (Du Toit, 1931). The Vira deposit is similar in many ways to the Harewood and will thus be described only briefly.

The working occurs in metalavas just below the contact of the Natal Group with the greenstone sequence (Fig. 4.15). The lavas have been altered to a chlorite-quartz assemblage across almost the entire width of the shear zone. The central portion however comprises a 3 m thick, sericite-quartz-clay-chlorite unit which

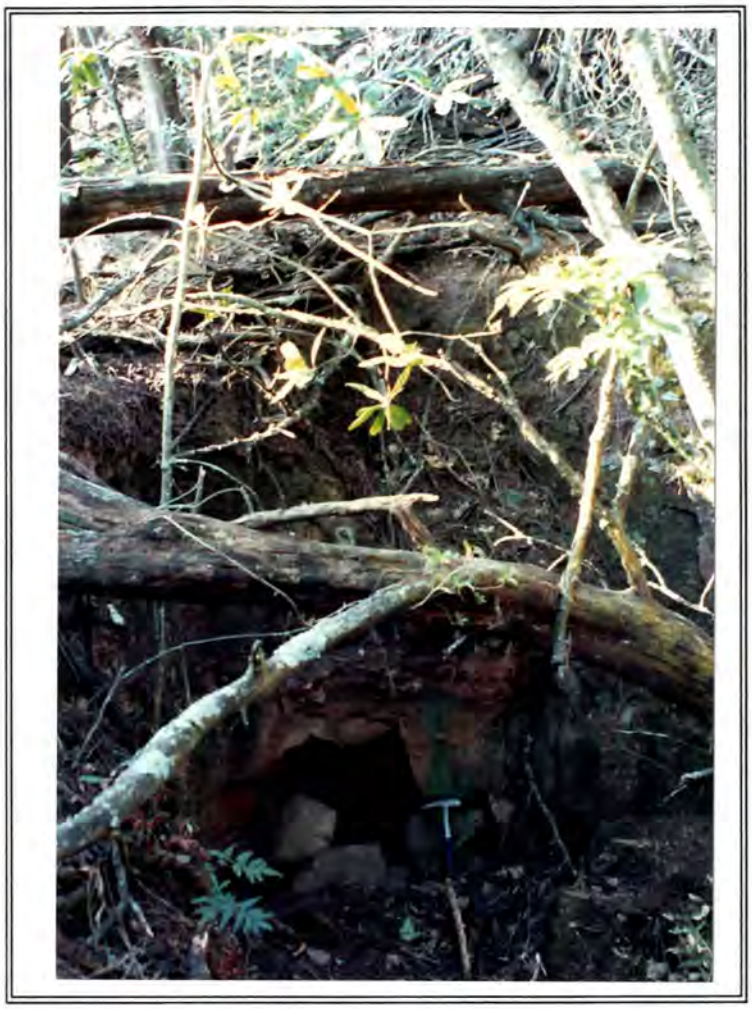

Figure 4.14 Photograph of a partially open adit entrance at the Vira working. The adit was driven along the contact between the overlying Natal Group and chlorite schists of the greenstone sequence.

is overlain by a 1 m thick, sericite-quartz-(chlorite-talc) schist layer. The greenstone sequence has been displaced by atleast three post-Natal Group, normal faults, the southern-most of which can be traced eastwards past the Harewood working (refer to Fig. 3.1). Unaltered and unmineralized serpentinites, similar to those observed at the Harewood working, crop out to the south of the Vira working.

An early generation of highly boudinaged, **unmineralized**, foliation-parallel quartz veins are present across the entire width of the shear zone. These veins are comparable to those described from the Harewood working and probably originated in a similar manner - that is mainly by the diffusion of SiO_2 through a static intergranular fluid from the adjacent rocks to suitable

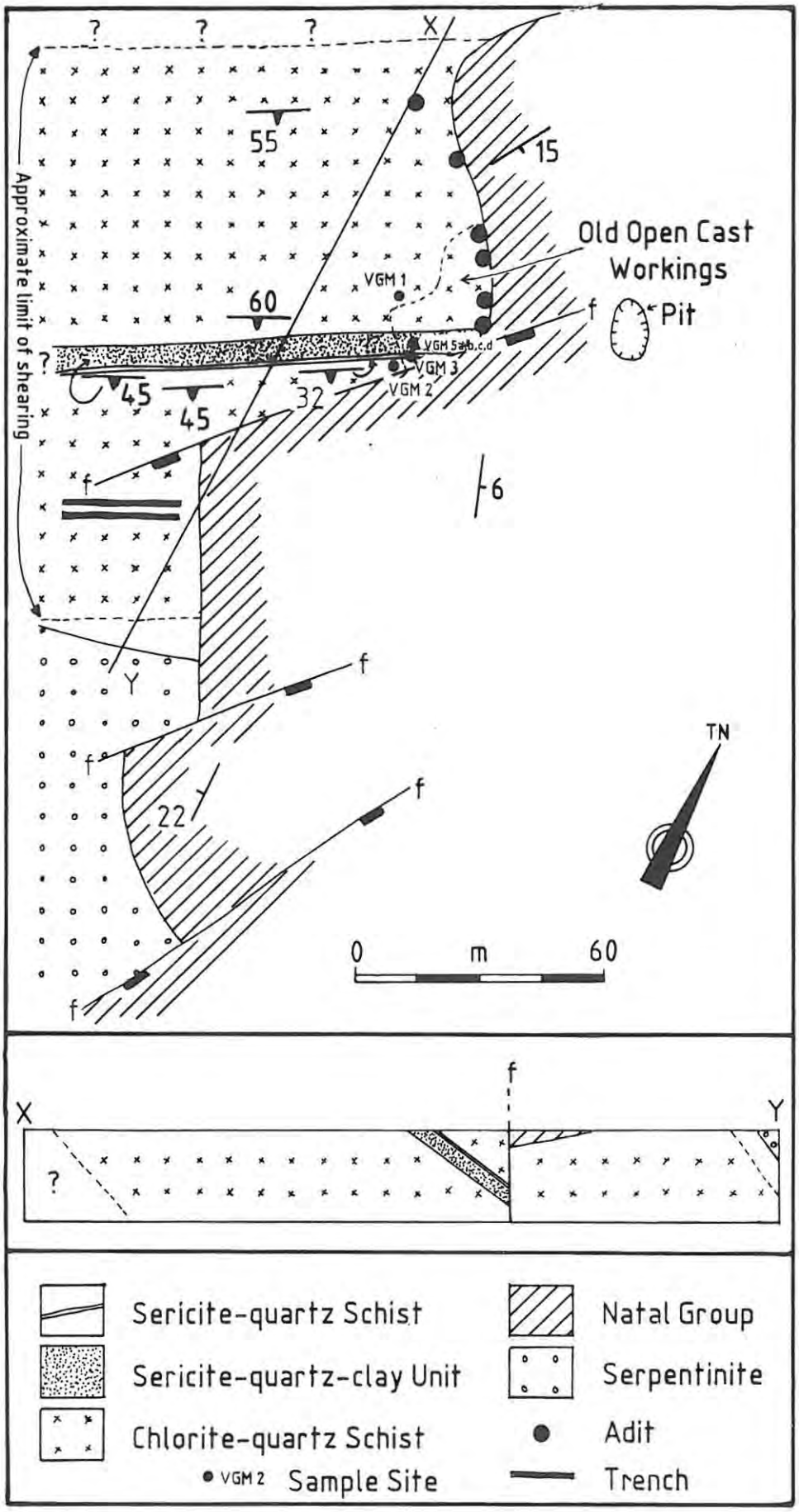

Figure 4.15 Geological plan (a) and section (b) of the Vira Au working and surrounding area. Lack of exposure prevented detailed mapping.

vein sites during the initial stages of shearing. Elevated SiO_2 concentrations across the shear zone however indicate that some Si was introduced during the ingress of the large volumes of hydrothermal fluids necessary for the alteration and mineralization.

In contrast to the Harewood deposit however, is the apparent absence of thick, Au-bearing quartz reefs. Detailed sampling was therefore carried out across the central portions of the shear zone (in the vicinity of the old working) in order to define the orebody and to obtain a clear understanding of the nature of the mineralization. In general, Au grades were found to increase towards the centrally situated clay-rich layer, the highest grades being associated with the layer itself (Fig. 4.16). This accords with work done on the Harewood deposit which pointed to a relationship between Au deposition and argillic alteration.

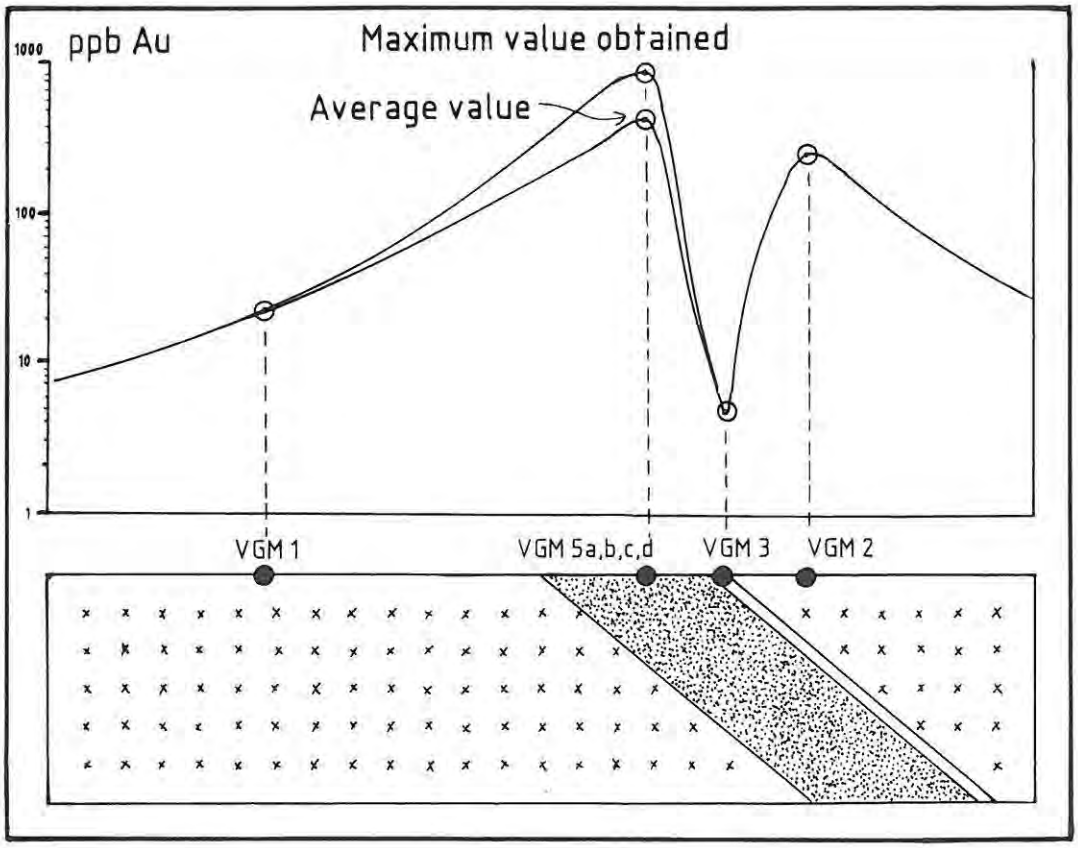

Figure 4.16 Profile showing Au values across the central parts of the shear zone at the Vira Au deposit. Rock types as for Fig. 4.15. The sample sites are shown on Fig. 4.15. The sericite-quartz-clay-chlorite unit in the center of the shear zone is highly enriched in Au and thus clearly constitutes the "orebody". Note the absence of mineralization in the overlying sericite-quartz-chlorite-talc schist.

Numerous, ferruginous, millimeter thick, discontinuous quartz veinlets (Fig. 4.17) and a lesser number of rotated, quartz infilled, extension fractures are present in the clay-rich layer. The former cross-cut the latter and were thus deposited later. The veinlets also cross-cut the fabric at a steeper, albeit variable, angle, in a similar manner to the Au-bearing veins at the Harewood deposit. The rotated extension fractures provided a clear indication as to the sense of displacement across the shear zone (Fig. 4.18). Goethite was patchily distributed throughout the layer - a weathering product of haematite and/or Fe sulphides. Gossanous textures were observed in a few places, and are ascribed to the **weathering out of Fe sulphides**. Haematite coatings on fracture and foliation surfaces are common.

The results of detailed sampling across the clay-rich layer (Table 4.2) indicate a close association between Au content and the goethite-rich portions (Fig. 4.19), cross-cutting quartz veinlets and quartz infilled extension fractures. The gossanous material however showed no Au enrichment. The fact that Au values were enhanced in the goethite-rich portions but depleted in the gossanous material suggests that the Au was intimately associated with Fe sulphides. The Au-Fe sulphide association would almost certainly manifest itself at depth, below the near-surface, oxidized zone. Au grades could thus be expected to improve significantly in the unweathered, sulphide-bearing material. The presence of Au in both the quartz infilled extension fractures as well as in the later cross-cutting veinlets suggests either that Au was deposited over an extended period of time, or that there were a number of pulses of Au mineralization. Work on the Harewood deposit revealed that the Au was deposited after displacement across the shear had ceased. The presence of Au in rotated extension fractures at the Vira deposit therefore points to an earlier, less significant phase of Au deposition, **prior to the cessation of movement across the shear zone**.

Figure 4.17 Close-up photograph of ferruginous, cross-cutting, quartz veinlet in the sericite-quartz-clay-chlorite layer in the center of the shear zone. Note the boudinaged, foliation-parallel veinlet similar to those found at the Harewood deposit. Scale bar 5 cm.

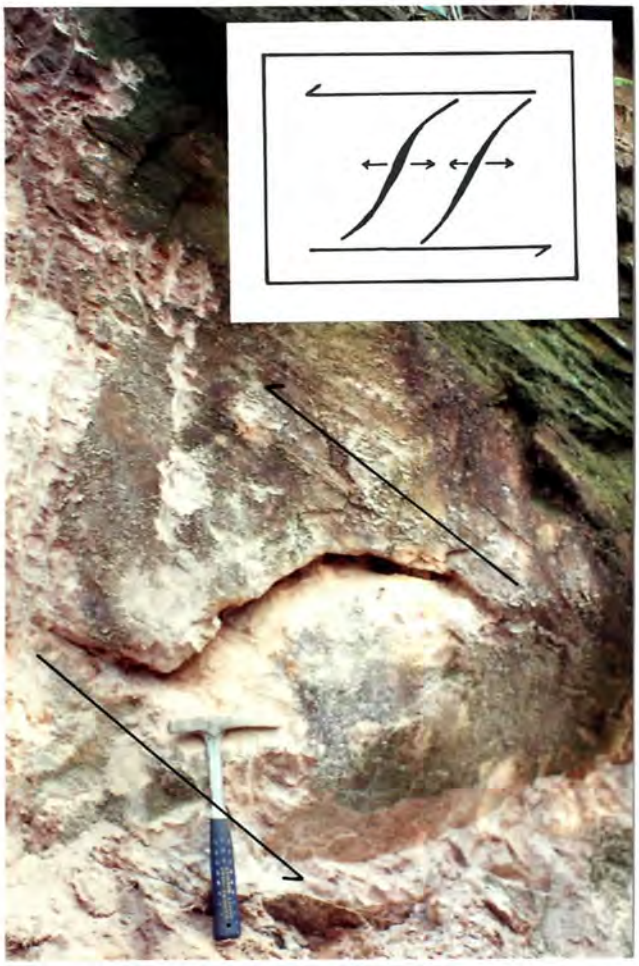

Figure 4.18 Photograph of a rotated, extension fracture in the sericite-quartz-clay-chlorite layer (the quartz infilling was removed for sampling purposes). The sense of displacement across the shear zone is indicated. Note the thin, foliation-parallel, highly boudinaged quartz veinlets. They are similar to the first generation quartz veins described from the Harewood deposit (see text).

Inset - Schematic illustration showing the development of extension fractures in a shear zone undergoing deformation by way of simple shear strain. The fractures rotate, and consequently dilate, in response to movement across the shear zone.

Table 4.2 Distribution of Au in the sericite-quartz-clay-chlorite layer in the center of the shear zone.

Sample	Au Content (ppb)
Fe-rich portions	917
Cross-cutting quartz veinlets	695
Quartz from extension fracture	257
Gossanous Material	25

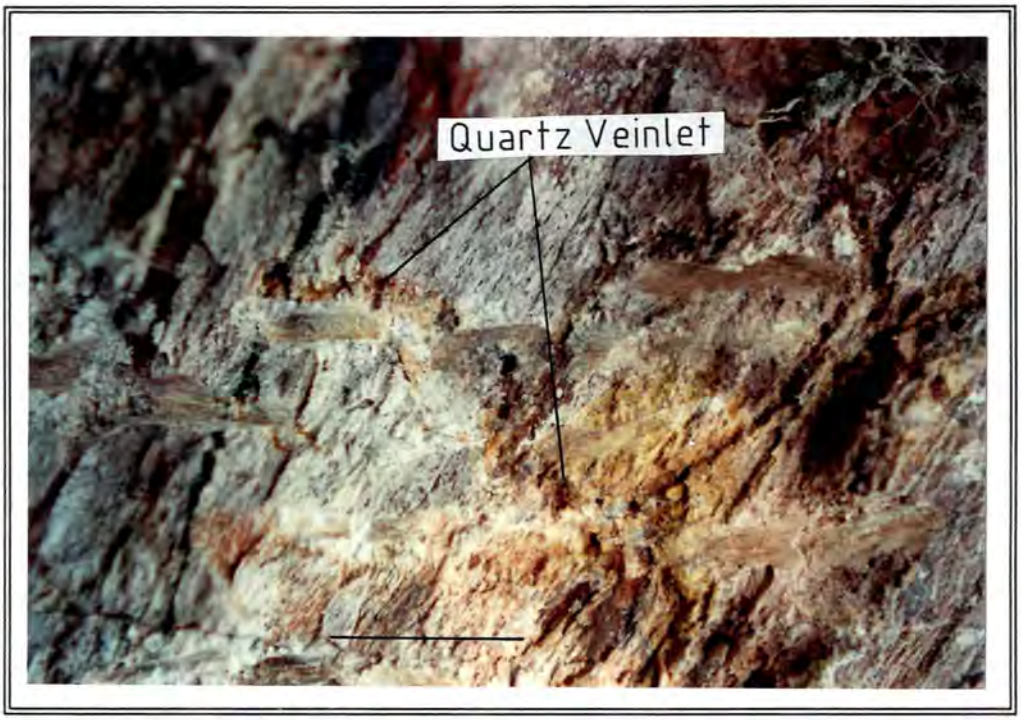

Figure 4.19 Close-up photograph of the sericite-quartz-clay-chlorite layer showing Au-bearing, goethite-rich (ochre) material. Note the cross-cutting, ferruginous, quartz veinlets which also exhibit enhanced Au contents. The white material consists of sericite and clay. Scale bar 5 cm.

4.2.1 Alteration-Mineralization

The original rock types in the vicinity of the Vira working were largely mafic lavas, the exact nature of which is uncertain owing to the paucity of outcrop on either side of the shear zone. Nevertheless major and trace element analyses clearly show that similar chemical changes occurred in sheared rocks at both the Harewood and Vira deposits. These included progressive increases in K, Zn and As and decreases in Na, Ca, Cu and Sr, towards the

orebody. The Au-bearing, sericite-quartz-clay-chlorite unit was **extremely** weathered and thus not analysed for major and trace element compositions. Chemical changes which occurred within the orebody are thus unknown, although they are certain to reflect changes in the adjacent rocks.

The wall rock alteration at the Vira working is broadly similar to that observed at the Harewood working. The rocks have been altered across almost the entire width of the shear zone to a chlorite-quartz-(sericite) assemblage (Fig. 4.20). Sericitization becomes increasingly important towards the orebody. This is particularly apparent in the sericite-quartz-(chlorite-talc) layer which overlies the orebody. These rocks grade into unaltered talc-magnetite schists to the west of the working (Fig. 4.15). Seritization is not as pervasive in the chlorite-quartz schists underlying the orebody. This is ascribed to the chemistry of the original rocks (mafic lavas), and not to differences in the nature of the alteration in the hanging wall and footwall. The orebody itself has been altered to sericite-quartz-clay-chlorite assemblage (Fig. 4.21). Therefore three wall rock alteration facies are recognized, namely an inner zone of argillic alteration, a surrounding zone of sericitic alteration and a peripheral zone of chloritic alteration (Fig. 4.15).

Although similar wall rock alteration facies are present at both the Harewood and Vira workings, the extent to which each is developed differs markedly. This is ascribed simply to the different mineralogy of the host rocks rather than to differences in the mineralizing fluids. Chloritic alteration dominates at the Vira deposit (Fig. 4.15) owing to the mafic nature of the original lavas. The chlorite formed by the substitution of MgO (mainly) and FeO for CaO in ferromagnesian minerals (actinolite) under conditions of increasing hydration. Magnesium metasomatism may also have been an important alteration process in converting plagioclase to Mg-rich chlorite - for example:

5) $(Na,Ca)AlSi_3O_8 + 6.5Mg^{2+} + 10H_2O \rightarrow Mg_{6.5}(Si_3Al)O_{10}(OH)_8 + Na^+ + Ca^{2+} + 12H^+$
Plagioclase — Mg-chlorite

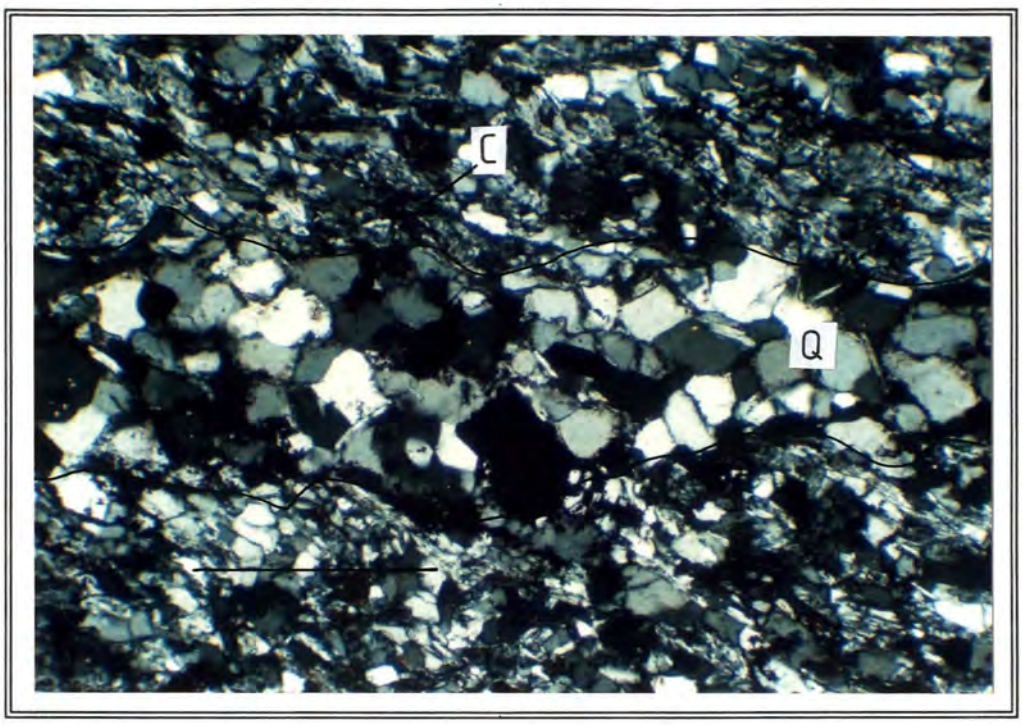

Figure 4.20 Photomicrograph of chlorite-quartz schist immediately to the north of the orebody (polars crossed). Mg-rich chlorite (C) and quartz (Q) indicated. Note the cross-cutting, undeformed, Au-bearing, quartz veinlet (outlined). Scale bar 0.5 mm.

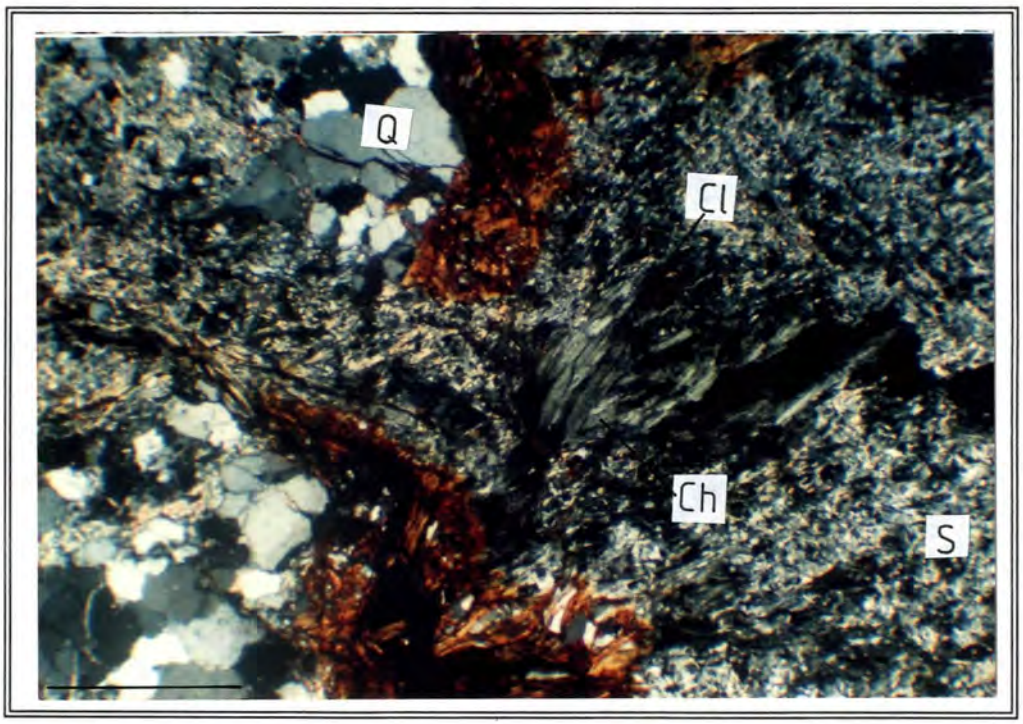

Figure 4.21 Photomicrograph of mineralized sericite-quartz-clay-chlorite rock in the center of the shear zone. Sericite (S), quartz (Q), clay (Cl) and Mg-rich chlorite (Ch) indicated. Note the haematite infilled fractures. Scale bar 1 mm.

Chloritization of wall rocks at the Harewood deposit was far less extensive owing to the lack of ferromagnesian minerals in the trondhjemites. Instead, sericitic alteration dominated - a feature ascribed to the high plagioclase content of the original rocks (refer to reactions 1 and 2; section 4.1.1). At the Vira deposit, sericitization (indicative of K^+ and H^+ metasomatism) was limited mainly to the orebody and the overlying sericite-quartz-(chlorite-talc) schists, due to the relatively low plagioclase content of the host rocks (and not to the absence of K^+-rich hydrothermal fluids). The hanging wall schists contain in excess of 80% sericite indicating that the original talc schists were highly susceptible to K^+ metasomatism - for example:

6) $\underset{\text{Talc}}{Mg_3Si_4O_{10}(OH)_2} + K^+ + Al^{3+} \rightarrow \underset{\text{Sericite}}{KAl_3Si_3O_{10}(OH)_2} + 3Mg^{2+} + Si^{4+}$

Al^{3+} was derived from the breakdown of plagioclase in the adjacent rocks. Argillization, the innermost zone of alteration in both the Harewood and Vira deposits, occurred as result of the hydroysis of sericite (refer to reaction 4; section 4.1.1). The close spatial relationship between Au mineralization and argillic alteration at both deposits suggests that Au may have been deposited largely in response to argillization.

The envisaged paragenetic sequence is similar to that described for the Harewood deposit - that is:

Sericite/chlorite/clay + quartz (I)
↓
Haematite
↓
Fe sulphides
↓
Quartz (II) + Fe(?) sulphides + Au

5. GENETIC MODEL FOR THE GOLD MINERALIZATION

The development of a genetic model with respect to the Harewood and Vira Au deposits necessitates an examination of the following aspects: the source of the Au and of the mineralizing fluids; the mechanism(s) of Au mobilization and transport; the site of deposition; the cause of deposition; the timing of the mineralization with respect to the evolution of the greenstone belt. Wall rock alteration is of fundamental importance not only in helping to elucidate the processes leading to Au deposition, but also as an exploration target.

5.1 Source of the Gold

The Au in the Harewood and Vira deposits must have been derived from the greenstone sequence and/or the syn and late-tectonic granitoid intrusives. None of the rock types in the study area was found to be particularly enriched with respect to Au (Table 5.1), making the identification of the actual source rocks difficult. However, as Keays (1984) pointed out, it is virtually impossible to ascertain the premetamorphic Au content of a rock, since Au is readily dissolved (during, for example, seawater metasomatism) and flushed from the system during the earliest stages of cleavage development. In MORB pillows, the glassy rims contain significantly higher Au concentrations than the pillow interiors, a feature ascribed by Keays and Scott (1976) to the dissolution and mobilization of Au (and S) from the pillow centers during reactions between seawater and the still hot lavas. This led Keays (1984) to suggest that Au not locked up in silicate and oxide phases and hence available for the ore-forming process, was leached from Archaean volcanic piles prior to regional metamorphism and deformation - that is prior to the formation of any Au deposits. Keays therefore emphasized the importance of some sort of trap which would retain the Au until the ore-forming environment had been created. Interflow sediments, particularly BIF, were considered to be ideal protore lithologies.

The idea of a sedimentary protore is not new (see for example -

Knight, 1953; Viljoen *et al.*, 1969, and Ridler 1973). BIF in Zimbabwean greenstone belts have long been considered an important source of Au (Foster, 1985). Ward (1987) noted the spatial association between the auriferous, sedimentary Zwartkoppie Formation in the Barberton Mountain Land and epigenetic Au deposits, and used the former for exploration purposes.

Table 5.1 Average crustal Au concentrations of selected rock types as compared to rocks from the MGGR. None of the rocks from the MGGR are particularly enriched with respect to Au. Average analyses referenced as follows: [1] -Kwong and Crocket, 1978; [2] - Boyle, 1979; [3] - Keays, 1984; [4] - Kerrich, 1986; [5] - Korobeynikov, 1988. The large differences in the values obtained for basic intrusive and extrusive rocks is ascribed to differences in sampling techniques as well as to the inhomogeneous nature of basic igneous rocks in greenstone belts around the world.

Rock Type	Average Au Conc. (ppb)	MGGR Analogues	
		Rock	Max Au Conc.
Ultrabasic Intrusive	11[2]	Serp/Talc Schist	23
Ultrabasic Extrusive (High-Mg Basalts/ Komatiites)	6-8[3] 0.5-2[4]	Basaltic Komatiite	< 5
Basic Intrusive	23[2] 1[1]	Hlagothi Gabbro	< 5
Basic Extrusive	17[2] 2[4] 4[5]	Tholeiite	16
Intermediate Intrusive	8[2]	Granodiorite	< 5
Acid intrusives	11[2]	Trondhjemite	13
	11[2] 2[4]	Granite	< 5
Chert	17[2]	Quartzite	7

Keays (1984), in an effort to pinpoint the original source rocks for Archaean epigenetic Au deposits throughout the world, examined Pd concentrations in Archaean greenstones. Although Au and Pd behave similarly during magmatic processes, Pd is virtually insoluable during fluid/wall rock interaction. The most Pd-rich igneous rocks, and hence the probable source rocks for the Au, were identified as high-Mg basalts and komatiites. The Pd (and Au) enrichment was ascribed to the high temperatures of

these magmas and their consequent late-stage saturation in S. Lower temperature magmas (for example intermediate and felsic magmas) become S-saturated at an early stage with the result that precious metals are scavenged by immiscible sulphides in the melts which remain at depth. Viljoen (1984) agreed with Keays, and considered komatiites in the greenstone belts of Southern Africa the most likely source rocks for the Au.

Another possible Au source may have been ultramafic intrusions, particularly those enriched in S, as suggested by Keays (op. cit.) for the Barberton Mountain Land. Serpentinitic intrusions would not have been affected by seawater alteration and subsequently would not have suffered Au loss prior to metamorphism and deformation.

Saager *et al.* (1982), Saager and Meyer (1984) and Meyer and Saager (1985) examined Au concentrations in various Archaean granite-greenstone terranes in Southern Africa. They identified two statistical populations, namely a background population with Au concentrations of around 1 ppb and an "excess value" population with Au concentrations of around 4ppb with respect to granitic rocks and 33 ppb with respect to volcanic rocks. 19% of the volcanic rocks and 6% of the granitic rocks fell within the excess value population. Au in rocks displaying background values was believed to be bound in silicate and oxide phases whereas Au in "excess value" rocks was considered to be associated with highly reactive sulphide phases. These authors ruled out granitoids as a principal Au source owing to lower concentrations of leachable Au (that is - sulphide-associated Au), instead favouring mafic and ultramafic rocks, as well as Au-bearing, Fe-rich chemical sediments (which contained an average of 150 ppb Au).

An enriched source rock might however not be a prerequisite for the formation of Au deposits. Assuming average Au concentrations of 6 ppm in vein quartz from the Harewood shear and 3 ppb in mafic and ultramafic volcanic host rocks, then concentration factors would need to be in the order of 2000. This rather large number is however within an order of magnitude of the concentration factors involved in the formation of numerous other

ore deposit types (Hodgson, 1985) (Table 5.2). Hodgson argued that, since enriched source rocks are not considered fundamental to the formation of other deposit types, anomalous concentrations of Au in source rocks may similarly have been unnecessary in the formation of Archaean lode Au deposits.

Table 5.2 Concentration factors for various deposit types (after Hodgson, 1985). ' donates value used to calculate concentration factors.

Metal	Average Au Conc. (ppm) Crust	Basalt	Granite	Deposit Type	Typical Grade	Concentration Factor
Au	0.003	0.003'	0.002	Lode	6 ppm	2000
		0.003'		M.S.D.	0.9 ppm	300
Cu	50	100'	12	M.S.D.	3.0 %	300
	50'			Porphyry	0.5 %	100
Zn	70	100'	50	M.S.D.	10.0 %	1000
Pb	12.5	3.5	20'	M.S.D.	2.0 %	1000
Mo	1.5	1.0	1.5'	Porphyry	0.2 %	700
W	1.2	0.8	1.5'	Skarn	1.0 %	7000

Clearly, the source of the Au in epigenetic Au deposits in granite-greenstone belts throughout the world remains equivocal. Current opinion though, generally favours a greenstone source.

5.2 Source of the Mineralizing Fluids

The formation of Archaean lode Au deposits requires the access of large quantities of fluids to source rocks, coupled with effective leaching for efficient Au extraction. The ore-forming fluids have, on the basis of fluid inclusion, isotope and wall rock alteration studies conducted in granite-greenstone terranes throughout the world (for example - Kerrich, 1984; Ho *et al.*, 1985; Hodgson, 1985; Kerrich, 1986; Ho, 1987), been found to be remarkably homogeneous. The fluids are characterized by low salinity (less than 2 wt% NaCl equivalent), near neutral pH (owing to fluid interaction with mafic-ultramafic rocks), Na/K $\approx$ 0.1, high CO_2 contents (12 to 30 mol%), $\delta^{18}O$ values of 6 to 10 °/$_{oo}$, δD values of -80 to +50 °/$_{oo}$, $\delta^{13}C$ values of 0 to -5 °/$_{oo}$ and $\delta^{34}S$ values of 5 to 8 °/$_{oo}$. Fluid densities are around 0.7-0.8 g/cm^3, temperatures vary between 270-480°C and pressures probably exceeded σ_1, the maximum principal stress.

Numerous hydrothermal fluid sources have been proposed. These include juvenile fluids formed by granulitization of the lower crust and/or degassing of the upper mantle (Colvine *et al.*, 1984), fluids of metamorphic origin (Phillips and Groves, 1983; Fyfe and Kerrich, 1984), magmatic hydrothermal fluids (Cameron and Hattori, 1987; Cameron, 1988) and re-circulated seawater (Hutchinson and Burlington, 1984).

The low salinity, low chloride and high carbonate content of the solutions rules out a seawater origin for the fluids. Geochemical and isotopic incompatibility between Archaean granulites and Archaean lode Au deposits (Kerrich, 1989) suggests that granulitization of the lower crust was not an important fluid source. Fluids derived from mantle degassing have been ruled out on the grounds that the crustal-scale shears necessary for tapping the fluids are seldomly mineralized (Perring *et al.*, 1987). However, this could be ascribed to the high temperatures associated with ductile shearing, together with the absence of any dilational features in crustal-scale shears (Eisenlohr *et al.*, 1989). In the case of the MGGR, the CO_2-poor nature of the mineralizing fluids suggests that the fluids were not derived by way of mantle degassing.

Magmatic (granitic) fluids have been proposed by Burrows *et al.* (1986), on the basis of geochemical evidence, to account for the genesis of certain Au deposits (namely the Hollinger and Mink Lake) in Ontario, Canada. δD and $\delta^{18}O$ values were found to be compatible with those of magmatic water while $\delta^{13}C$ values (of -3.3 ± 0.4 °/$_{oo}$) were compatible with a deep igneous carbon source but incompatible with derivation by way of metamorphic processes. Work by Cameron and Hattori (1987) and Cameron (1988) on some of tha largest Archaean Au deposits (for example - Hemlo and McIntyre in Ontario and Kalgoorlie in Australia), suggested that the mineralizing fluids were strongly oxidizing in nature. Sulphides showing depletion in ^{34}S from the mantle value of ≈0 °/$_{oo}$ and the presence of both sulphate minerals and haematite are considered evidence of this. Since metamorphic fluids, seawater and meteoric waters were mainly reduced in Archaean times, these authors concluded, in conjunction with field evidence, that the fluids responsible for the Au mineralizion were derived from

oxidized felsic magmas.

Evidence against magmatic fluids includes low salinity (Phillips and Groves, 1983), the absence, in western Australia, of spatial relationships between the large Au deposits and granitic rocks (Ho *et al.*, 1985) and the remarkable similarity in the nature of the ore-forming fluids in contrast to the great diversity of granitic rocks in Archaean terranes (Perring, 1988). Burnham (1979) has however shown that a small amount of CO_2 in aqueous fluids in equilibrium with a granitoid intrusive, would suppress the concentration of alkalis in the fluid, thus giving rise to fluids of low salinity. Furthermore, Au deposits in the Southern African greenstone belts commonly show a close spatial relationship with granitoid intrusives (Anhaeusser, 1976) pointing to a possible genetic connection between the two.

Many workers in Western Australia (for example - Phillips and Groves, 1983; Groves *et al.*, 1984), favour fluids of metamorphic origin based principally on the numerous similarities exhibited by the ore-forming fluids and fluids which occur in amphibolite facies metamorphic rocks. The model involves metamorphic dehydration and decarbonation of greenstone sequences at upper amphibolite-granulite facies (400-600°C) deep in the greenstone pile. The fluids accumulate along grain boundaries (given $P_{fluid} \geq P_{load}$), and react with the rocks, liberating both major and trace elements. The fluids are ultimately channelled upwards along crustal-scale shear zones. Kerrich (1986) and Groves and Phillips (1987) however, pointed out that stable isotope data and timing evidence from Archaean lode Au deposits throughout the world, was insufficient to distinguish accurately between fluids of magmatic and metamorphic origin. The source of the ore-forming fluids in Archaean epigenetic Au deposits thus remains equivocal.

The principal features of the fluid source models are summarized in Fig. 5.1.

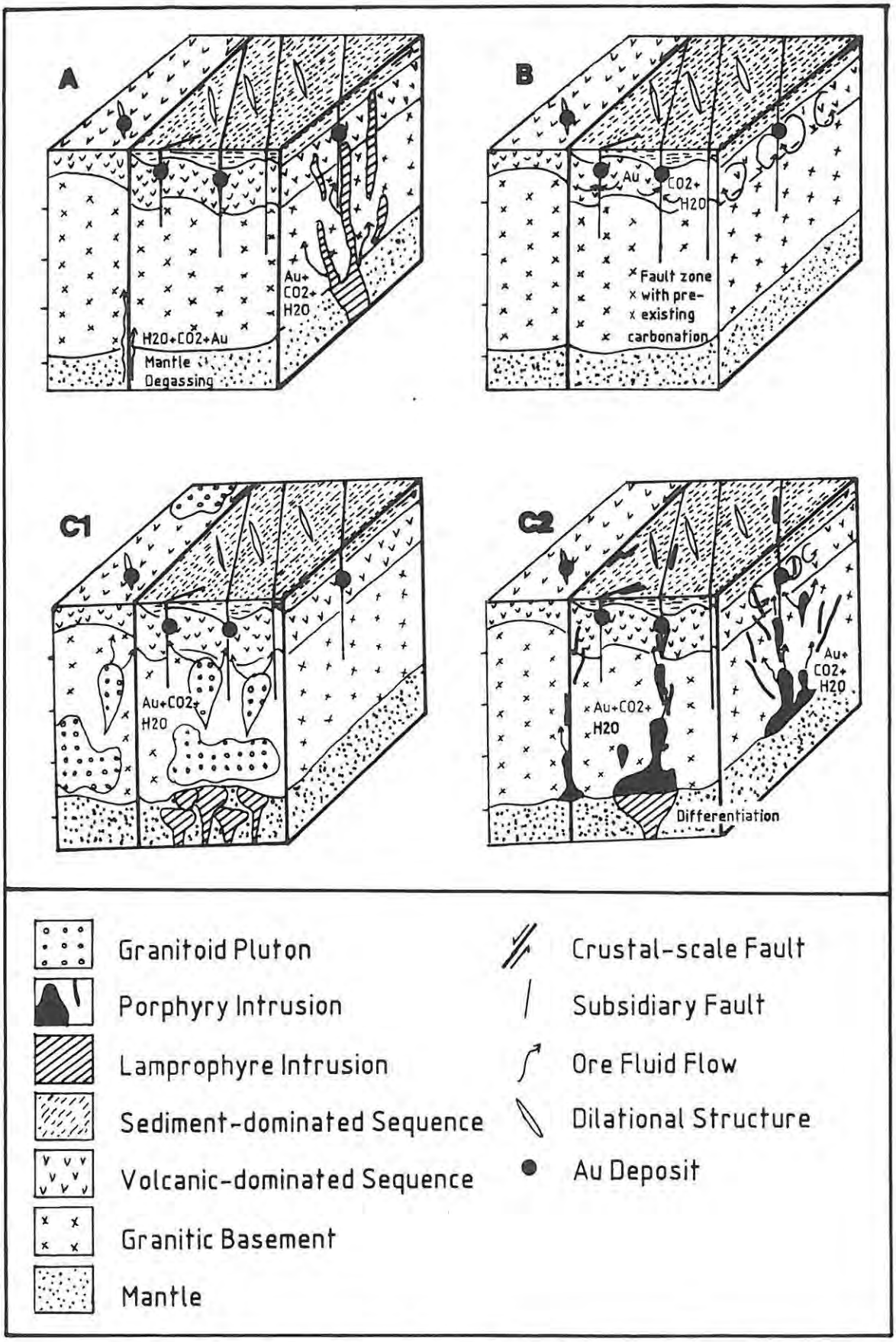

Figure 5.1 Schematic diagrams showing the main models for auriferous fluid (and ore-component) sources (modified after Perring *et al.*, 1987) **A** - Mantle degassing either by direct degassing or by delivery of mantle

fluids to upper crust by way of lamprophyric melts: **B** - Metamorphic model with fluids being derived from devolatilization of amphibolite facies greenstones: **C1** - Magmatic fluids derived from granitoids generated above a mantle plume and or above ponded lamprophyric magmas: **C2** - Magmatic fluids evolved from porphritic intrusions, the magmas being generated by differentiation of a lamprophyric magma and/or by partial melting at the base of the crust. Note that in both cases, the Au and the fluids are derived from a similar source. Perring *et al.* (1987) favour model **B** - that is the metamorphic model.

5.3 Mechanisms of Mobilization and Transport

Au must have been mobilized during each metamorphic event which affected Archaean granite-greenstone terranes. The four principal factors which control the theoretical solubility of Au are Eh, pH, temperature and sulphide concentration. Hodgson (1985) sites two possible transport mechanisms, namely diffusion through a static fluid and mass transport by a moving fluid. The former is precluded owing to mass balance problems together with the fact that it would take impossibly long periods of time for an ore deposit to form by diffusive lateral secretion processes alone.

During early, seafloor metasomatism, pillow lavas become porous owing to differential thermal contraction of minerals and glass (Keays, 1984). Fluids permeating through the rock react with Fe-sulphides which reside along grain boundaries, liberating S. The S would, under reducing conditions, react with and transport Au as a thio-complex (Glasson and Keays, 1978). The slightly alkaline to neutral pH of seawater would ensure the stability of this complex. Low grade Au concentrations may have formed during this syn-volcanic stage giving rise to enriched protore lithologies (for example - auriferous interflow sediments such as BIF).

A second and probably more significant phase of Au mobilization would have occurred during the recrystallization of potential source rocks during prograde metamorphism. Au solubility increases exponentially with temperature so that the extraction of Au from source rocks becomes highly efficient with increasing temperature (Fyfe and Kerrich, 1984; Kerrich, 1986). Therefore, significant Au enrichment would occur in metamorphic fluids

generated at sufficiently high temperatures (± 500°C) even if the host rocks contained only a few ppb Au. High temperatures necessitate a heat source which, in the case of the MGGR, can be ascribed to the intruding granodiorite pluton.

Au may also be partitioned from magmas into magmatic hydrothermal fluids during cooling. In addition, it may have been drived from host rock sequences and incorporated into magmatic fluids during magma intrusion. Finally, Au may be released to hydrothermal fluids during wall rock alteration although this appears the exception rather than the rule (Hodgson, 1985).

Au aquo-ions are extremely unstable (Phillips and Groves, 1983) and therefore complexing ligands are recquired to transport dissolved Au. According to Seward (1984), Au in hydrothermal fluids occurs principally in the +1 oxidation state (rather than in the +2 and +3 states) owing to the low oxidation potential of fluids deep in the earths crust. The large highly polarized Au^{+} ion can form stable complexes with a number of elements and compounds common to hydrothermal fluids - namely S, Cl, NH, and As. Also important are B, carbonyl (CO), cyanide (CN) and thiocyanide (SCN^{-}) complexes (Hutchinson and Burlington, 1984). Seward (1988) suggested that Au was transported either as $Au(HS)_2^{-}$ or $Au(CN)_2^{-}$ since the two species are the most stable inorganic complexes of Au^{+} known. The C necessary for the generation of the CN ion (as well as the CO and SCN^{-} ions) must have been derived principally from the breakdown of CO_2. As previously mentioned however, the fluids responsible for Au mineralization in the MGGR were not CO_2 bearing suggesting therefore that cyanide (and carbonyl and thiocyanide) complexes were not important transporting agents in these fluids.

Au is very insoluble in near neutral chloride solutions even at relatively high temperatures of 350°C (Seward, op. cit.). In addition, the $AuCl_2^{-}$ complex is roughly twenty orders of magnitude less stable than $Au(HS)_2^{-}$. Seward thus considered Cl complexing and transport of Au in the crust of neglible importance, favouring rather the transport of Au by way of thio-complexes. These complexes could form as a result of the reaction

(Brown, 1988):

$$7)\ Au^{+} + H_2S + HS^{-} \rightarrow Au(HS)_2^{-} + 0.5H_2$$

5.4 Site of deposition

As previously stated, Au mineralization within the MGGR lies within a D_2 shear zone. The siting of the mineralization within the shear zone is of fundamental importance. The known Au deposits are invariably located towards the center of the shear zone, in the zone of most intense shearing. In addition, and more importantly, is the fact that the deposits lie at the contact between two rock types. The mineralization is invariably hosted in the least competent rock type. For example, the Harewood working, situated in highly sheared trondhjemite, lies adjacent to unmineralized, weakly sheared serpentinite (Fig. 4.2). Similarly, the Vira working to the west is situated in highly sheared metalavas that lie adjacent to the same (in this case unsheared) serpentinite (Fig. 4.14). The Times prospect is situated in talc schist adjacent to sheared metalava. The dilational sites necessary for mineralization therefore appear to have formed principally in response to shear zone refraction (see section 5.7.1).

Depositional sites developed in response to dilation in the YZ plane of the finite strain ellipsoid are rare, despite the fact that the YZ plane is the only plane in which dilation should occur during deformation. As Hodgson (1985) pointed out, auriferous, extensional fracture arrays rarely constitute a major part of Archaean lode Au deposits.

An important factor to consider is the depth of deposition. Fluid inclusion and geobarometric studies suggests that most hydrothermal ores were deposited within the upper 3 km of the crust (Skinner, 1979). Hence, if the MGGR was extensively eroded prior to the deposition of the Natal Group, the depth extent of the Au mineralization might be limited. This problem could only be resolved by way of drilling.

5.5 Cause of deposition

Fluid inclusion studies in Archaean lode Au deposits in Western Australia (Ho *et al.*, 1985; Ho, 1987) suggested that the auriferous vein quartz was deposited over a temperature range of 200 to 400°C (although more typically between 250° and 350°C) at pressures of around 1 kb. According to Fyfe and Kerrich (1984) and Seward (1984), Au precipitated in response to changes in temperature, pressure, Eh, pH and decreasing activities of the complexing ligands. Also of possible importance were amorphous arsenic and antimony sulphide sols, which efficiently extract Au from aqueous solutions over a wide range of temperatures. Kerrich (1986) noted the coexistance of Au + haematite and Au + pyrrhotite + graphite mineral assemblages in Au deposits in Canada, and concluded that Au could precipitate under a wide range of Eh conditions.

The type of complexing ligand is the most important control in terms of Au precipitation (Seward, 1984). Au transported as a simple hydrosulphide complex (for example; $Au(HS)_2^-$) could precipitate in response to decreasing temperature as well as in response to any process which caused a decrease in the activity of reduced sulphur - for example boiling, fluid dilution, oxidation, and precipitation of metal sulphides. However boiling will only lead to significant Au precipitation after major changes in oxidation potential (H loss), reduced S activity (H_2S loss) and pH (CO_2 loss) have occurred (Seward, op. cit.). Au transported as a chloride complex (that is $AuCl_2^-$), would precipitate in response to decreasing temperature as well as to a decrease in chloride activity owing to dilution.

It is generally agreed that fluid/wall rock interaction - or more particularly sulphidation of Fe-rich wall rocks (that is rocks with high Fe/(Fe + Mg) ratios such as tholeiite, BIF or other Fe-rich sedimentary units) - was the principal factor responsible for the precipitation of Au (for example - Groves *et al.*, 1984; Foster, 1985; Neall, 1987). The formation of pyrite during the sulphidation of Fe-rich wall rocks, would have the effect of decreasing the fH_2S (as well as lowering the pH and fO_2) in the fluid leading to the breakdown of Au-sulphide complexes. Lowering

the total dissolved sulphur content would obviously not affect Au transported as $AuCl_2^-$.

Sulphidation of metatholeiites would involve the following reaction (Phillips and Groves, 1984):

8) $Fe_6Si_4O_{10}$ + $12H_2S$ + $3O_2$ → $6FeS_2$ + $4SiO_2$ + $16H_2O$
chlorite (S^{2-}) (S^{1-})

Note the breakdown of hydrogen sulphide under oxidizing conditions and the concomitant replacement of chlorite by pyrite. Clearly then, the oxidation of S would have the effect of destabilizing the HS^- ligand, leading to the formation of pyrite. The removal of S from solution in this manner provides a mechanism for the precipitation of Au transported as a reduced sulphur complex, for example (Phillips and Groves, 1983):

9) FeO(in silicate) + $HAu(HS)_2$ + $\frac{1}{4}O_2$ → Au↓ + FeS_2 + $1\frac{1}{2}H_2O$
(Au^+/S^{2-}) Reduced (S^{1-})

Hence, the destabilization of Au-bearing thio-complexes during Fe-related redox reactions results not only in the deposition of pyrite in response to the oxidation of S, but also in the reduction of Au^{1+} and its concomitant precipitation from the mineralizing fluids. Yet a further precipitation mechanism, proposed by Starling *et al.*, 1989, involves the adsorbtion of Au-bearing thio-complexes onto pyrite, followed by reduction-driven chemisorption reactions as follows:

10) $Au(HS)_2^-$ + e^- → Au + $2HS^-$
(Au^+) Reduced

A decrease in the ratio of reduced to oxidized sulphur leading to the destabilization of Au-bearing thio-complexes and the deposition of pyrite and Au can also be caused by pH **increases** (Hodgson, 1985). Such increases could be effected by the fixing of H^+ in clay minerals in wall rocks undergoing argillic alteration adjacent to auriferous quartz reefs, for example:

11) $2KAl_3Si_3O_{10}(OH)_2$ + $2H^+$ + $3H_2O$ → $3Al_2Si_2O_5(OH)_4$ + $2K^+$
sericite kaolinite

Also important in terms of Au deposition is the structural setting of the Au deposit. Shear zone-hosted Au deposits occur in dilational sites. Decreases in pressure and temperature as the fluids enter these more permeable sites could result in the precipitation of Au. In addition, such changes would cause a shift in fluid/wall rock equilibria such that wall rock alteration would occur (Hodgson, op. cit.).

Finally, Au deposition may also take place in response to phase separation during boiling.

5.6 Timing of Mineralization

It is generally agreed that Au mineralization in Archaean granite-greenstone terranes was deposited during, or shortly after, peak metamorphism (for example - Boyle, 1979; Groves *et al.*, 1984; Barley and Groves, 1987; Vearncombe *et al.*, 1988).

5.7 Models of Ore Genesis

Until about 25 years ago, magmatic theories of ore genesis dominated. Current opinion favours exhalative and metamorphogenic theories of ore genesis. **It must be noted however that the three models all overlap to a certain extent**

Magmatic hypotheses relate Archaean lode Au deposits directly to granitoid intrusives which, during pressure release and magma crystallization, released both Au and hydrothermal fluids into the system (refer to Fig. 5.1, C1 and 2). A magmatic origin has been ascribed, on the basis of geochemical evidence as well on the close spatial association between the mineralization and granitoid intrusives, to numerous Au deposits. Examples include the Hollinger Au deposit in northern Ontario (Burrows *et al.*, 1986), and the Kalgoorlie Au deposit in Western Australia (Cameron and Hattori, 1987). Foster (1985) proposed a model involving fluids from granitoid intrusives and Au from auriferous protore lithologies to account for Archaean lode Au deposits in Zimbabwe (Fig. 5.2).

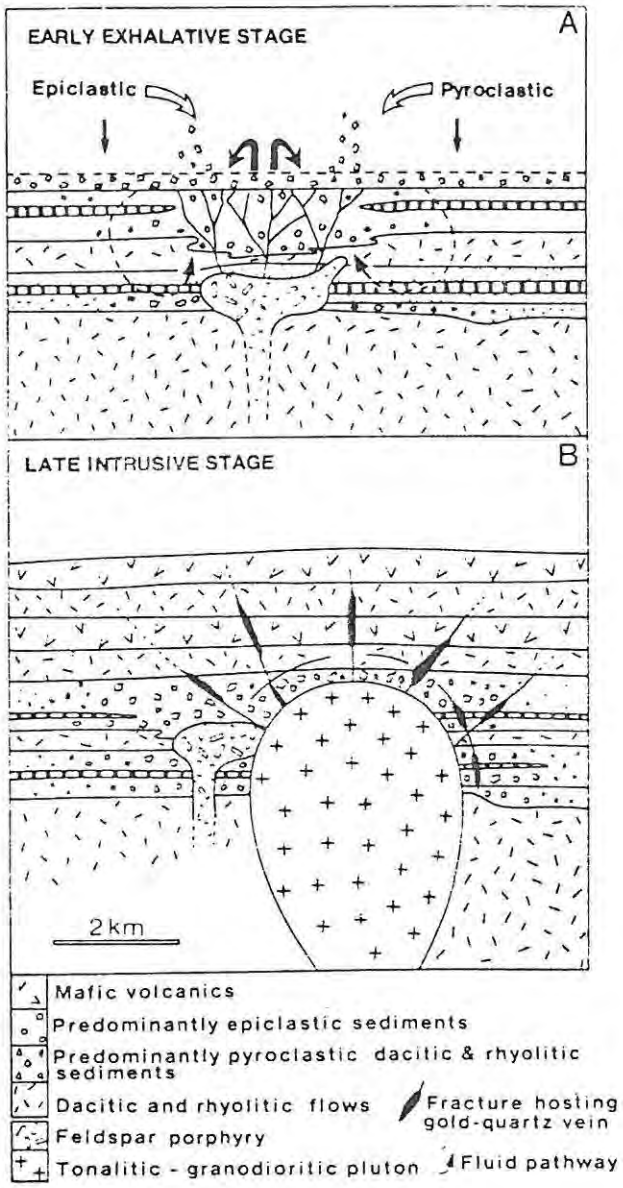

Figure 5.2 Illustration demonstrating the formation of Archaean epigenetic Au deposits in Zimbabwe (after Foster, 1985).
A - Convecting fluids (mainly seawater), heated by a high-level felsic stock, introduced Au, derived from ultramafic, mafic and felsic volcanics, into a zone of active clastic sedimentation.
B - Fluids from intruding calc-alkaline magmas remobilized the Au to form discordant vein-type deposits in the adjacent rocks.

Exhalative models of ore genesis involve the **syn-volcanic** deposition of Au from metamorphic fluids onto the seafloor thus forming protores. The Au was then subject to numerous phases of metamorphic remobilization commencing with diagenesis and

culminating in regional metamorphism (Hutchinson and Burlington, 1984; Fig. 5.3).

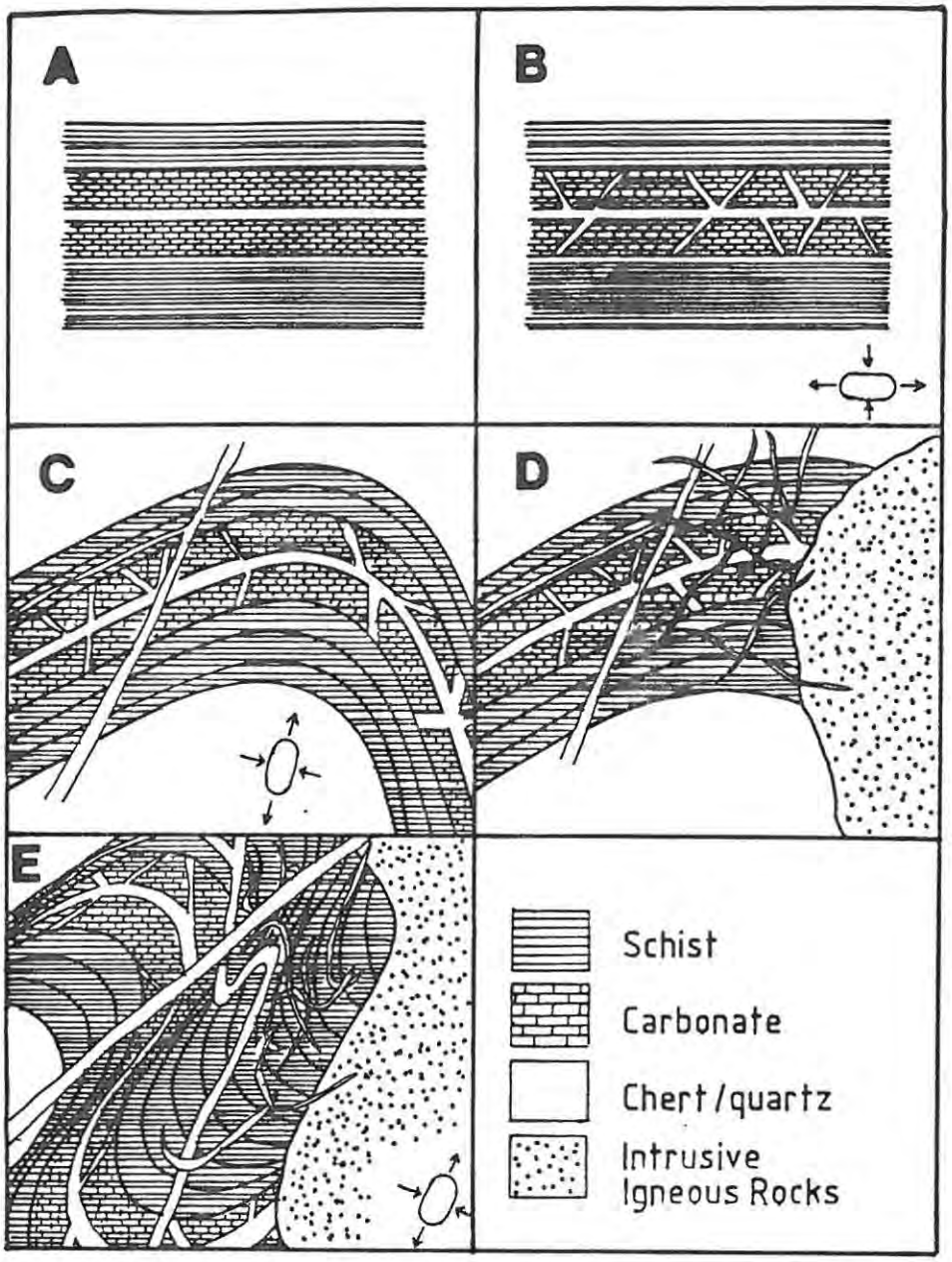

Figure 5.3 Diagrammatic illustration of the formation of Archaean lode Au deposits based on the exhalative hydrothermal model (redrawn from Hutchinson and Burlington, 1984).

A - Primary, seafloor exhalitive sedimentation with the concomitant deposition of Au from metamorphic fluids.

B - Burial, compaction and the generation of ladder veins in response to local-scale secretions from concordant cherty layers formed during diagenesis.

C - Synkinematic folding and the formation of Au-bearing, discordant veins in penetrative fractures, the silica again being derived from the cherty layers.

D - Granitoid intrusions which acted as heat engines, causing the

convective circulation of mineralizing fluids within the previously deposited auriferous strata, and resulting in the formation of discordant vein stockworks.

E - Deformation, metamorphism and further remobilization during late Archaean orogeny.

The metamorphogenic theory of ore genesis, first proposed by Boyle (1961), involves essentially the dissolution of Au derived from local host rocks into fluids generated during prograde metamorphism, followed by its transport and subsequent deposition in shear zones in response to decreasing pressure as well as to fluid/wall rock interaction (Fig. 5.4).

Groves and Phillips (1987) refined the theory considerably. Their so-called metamorphic-replacement model, considered applicable to Archaean lode Au deposits in Western Australia, commenced with the devolatilization of the lower portions of the greenstone pile, with melting inhibited owing to **high geothermal gradients at relatively low pressures** (Fig. 5.5). CO_2 may have been derived from the decarbonation of previously altered rocks, during mantle degassing along ductile, **crustal-scale** fault zones. The fluids, which evolved as a result of grain reactions extracted Au from the greenstone pile and were channelled upwards along brittle-ductile, **greenstone-scale** faults. Au was deposited in, or adjacent to, fault or shear zones under greenschist facies conditions in respose to decreasing temperature and to fluid/wall rock interaction. A further mineralization mechanism involves the replacement of Fe oxides in BIF by auriferous Fe sulphides. The principal features of the model are depicted in Fig. 5.6.

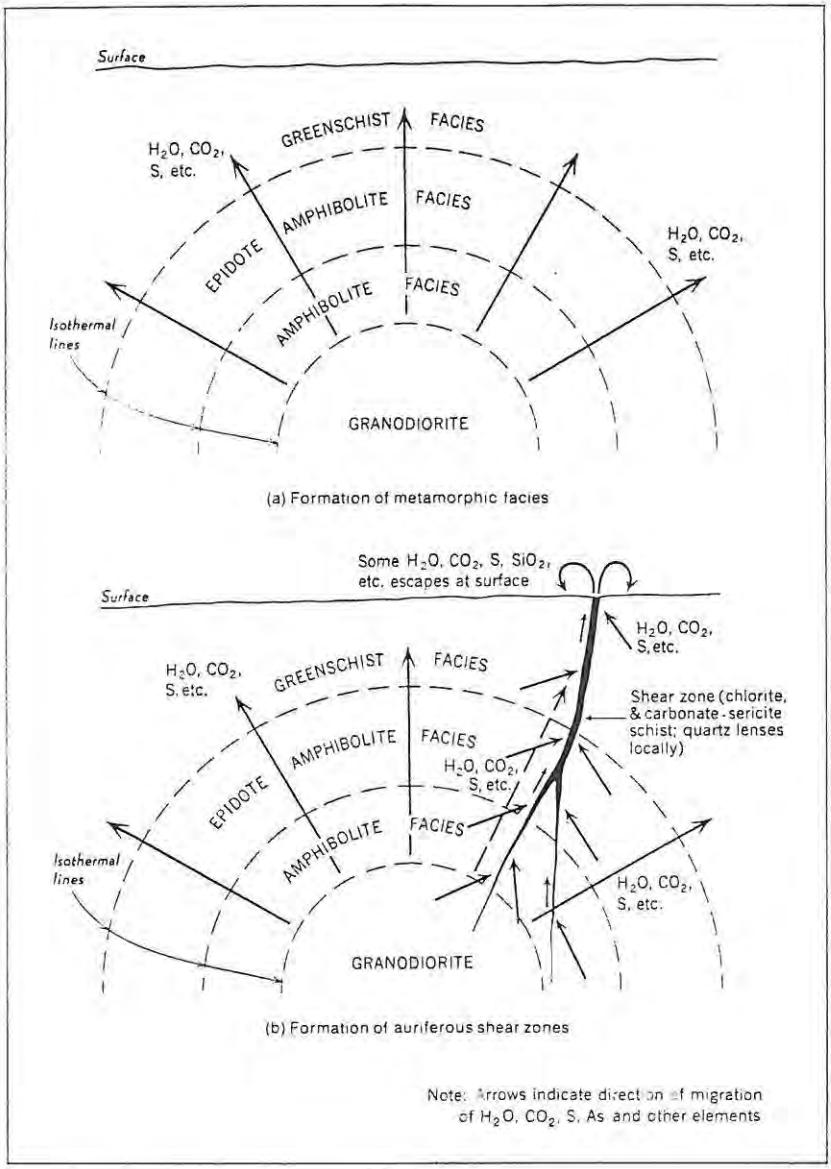

Figure 5.4 Schematic representation of Boyle's (1961) metamorphogenic theory of ore genesis.

A - Formation of metamorphic facies in response to an intruding granodiorite pluton.

B - Formation of mineralized shear zones with the fluids and the Au being derived mainly from the greenstone sequence.

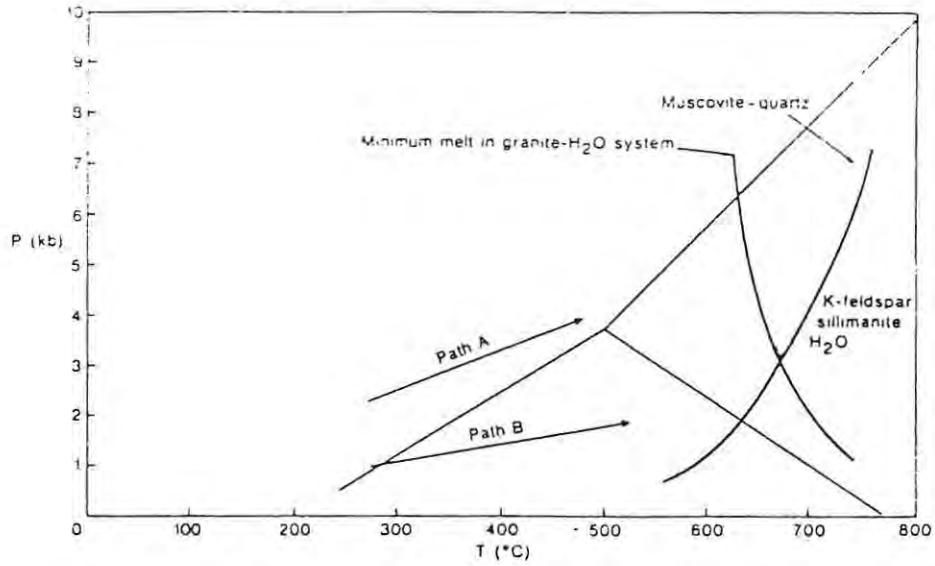

Figure 5.5 Diagram demonstrating the importance of high geothermal gradients at relatively low pressures in the generation of metamorphogenic mineralizing fluids (modified after Groves *et al.*, 1987). A rock undergoing pressure and temperature increases along path **A** leads to vapour absent melting. At lower pressures however (path **B**), dehydration at temperatures below the melting temperatures of the rocks, resulting in the generation of large volumes of Au transporting, metamorphic fluids.

A problem with the model is the fact that numerous Archaean lode Au deposits post-date peak metamorphism, suggesting that the mineralizion might not be related to metamorphic mineralizing fluids. In addition, Au-related alteration assemblages are often retrograde.

Finally, Bonnemaison and Marcoux (1990) proposed a three-stage model for the formation of shear zone-hosted, auriferous, quartz reefs. In the first stage, Au is considered to be fixed in the crystal lattice of Fe sulphides disseminated throughout the shear zone. The second stage involves the emplacement of vein quartz which acts as a "receptacle" for native Au released during the breakdown of the auriferous sulphides. The final stage involves the development of auriferous quartz or of quartz/carbonate stockworks during brittle shearing.

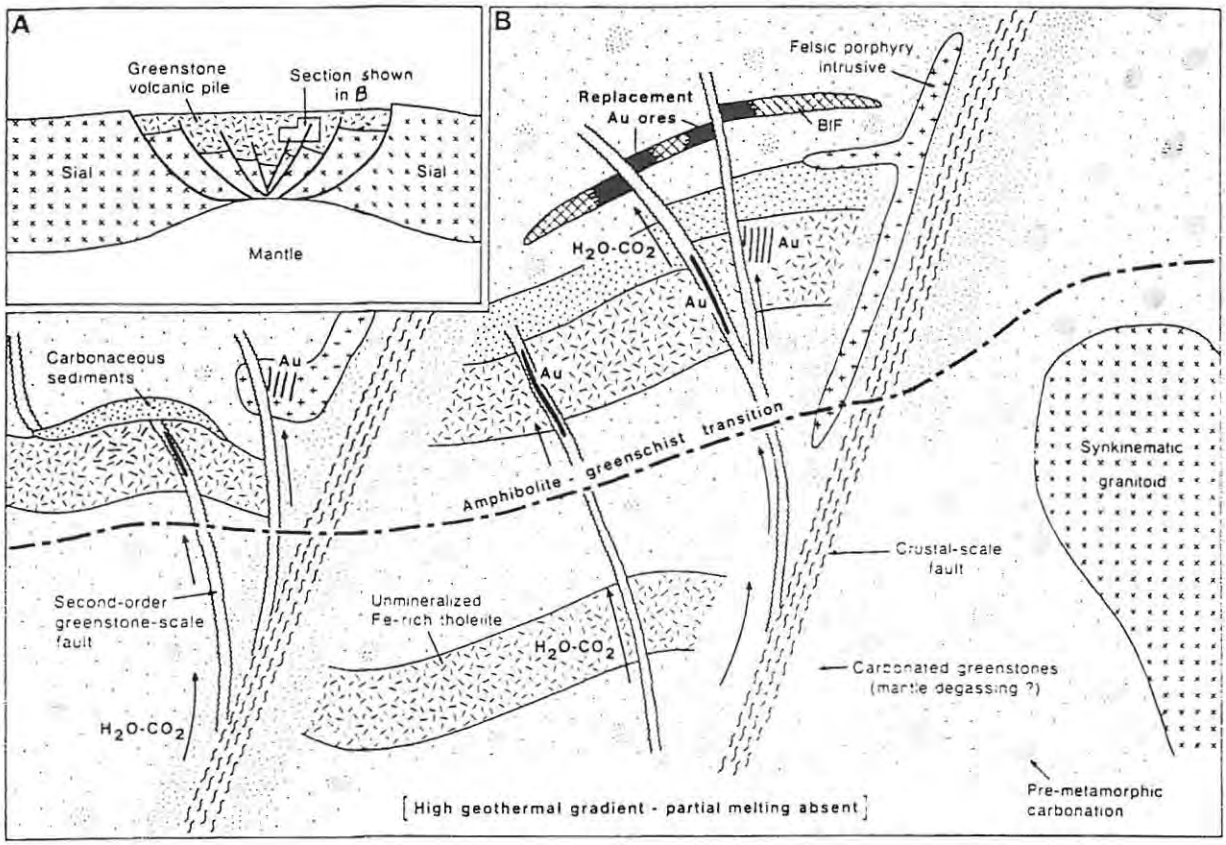

Figure. 5.6 Schematic representation of the metamorphic-replacement model for the generation of Archaean Au deposits (modified after Groves and Phillips, 1987). For the sake of completeness, replacement ores in BIF are indicated.

5.7.1 **Preferred Model for the Au deposits in the MGGR**

Site of Deposition: The mineralization is hosted in a D_2, greenstone-scale shear zone generated during the emplacement of a late-tectonic, granodioritic pluton. Economic concentrations of Au occur in dilational sites developed principally in response to **shear zone refraction** (Fig. 5.7). The auriferous quartz veins were deposited parallel to "P" shears, therefore forming oblique shear veins. Quartz-infilled extension fractures, although Au-bearing, were of limited importance. As previously mentioned, the deposits are situated towards the center of the shear zone, where shearing is most intense. These central portions must have been highly permeable, allowing for the ingress of the large volumes of hydrothermal fluids necessary for the formation of the Au deposits.

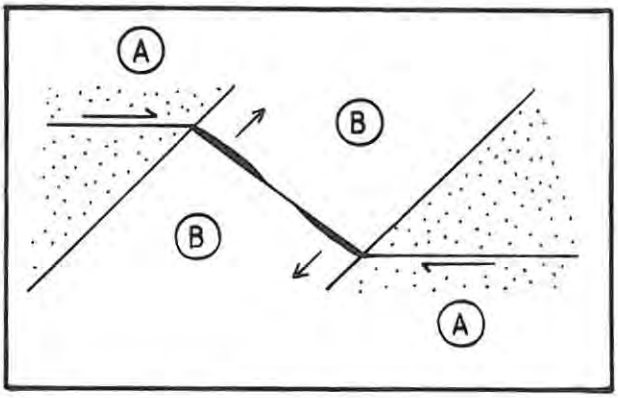

Figure 5.7 Schematic illustration demonstrating the development of dilational sites in the mineralized D_2 shear zone. The shear zone underwent refraction as it passed from less competent **(B)** to more competent (A) lithologies. Dilational sites developed in the less competent lithologies during movement along the non-planar shear zone.

Source of Fluids: Fluids of both magmatic and metamorphic origin appear to have played a role in the formation of the Harewood and Vira Au deposits. The evidence favouring a magmatic fluid input includes;

a) the close spatial and temporal association between the mineralization and the D_2 granodiorite pluton.
b) the extensive K metamsomatism which is particularly suggestive of a felsic source (Hodgson, 1985).
c) the presence of tourmaline (indicating fluids rich in B) which is common in some deposit types with magmatic affiliations, for example - Sn and W lodes and tourmaline breccia pipes of porphyry Cu environments (Hodgson ,1985).
d) the presence of haematite which suggests that the mineralizing fluids were, certainly in the early stages, oxidizing in nature.

Since the Au mineralization in the MGGR is related to the D_2 deformation event however, the mineralizing fluids were probably derived, in part, from devolatilization reactions occurring at depth. As previously mentioned (see section 3.5), Southern African greenstone belts rarely exceed 5 km in depth. Devolatilization reactions associated with amphibolite facies metamorphism in the MGGR would have occurred at shallow depths in

response to deformation **accompanied** by the intrusion of the D_2 granitoid.

The mineralogy of the auriferous quartz reefs supports the contention that the hydrothermal fluids were of both magmatic and metamorphic origin. Both haematite and pyrrhotite are present, yet the two minerals cannot co-precipitate from the same fluid. The principal controlling factor is fO_2 with haematite precipitating in response to higher O_2 fugacities and pyrrhotite in response to lower O_2 fugacities (Fig. 5.8). The evidence suggests therefore that the earlier fluids (those from which the silicate and oxide phases were deposited) were oxidizing in nature and the later fluids (those from which the sulphide phases and Au were deposited) were reducing in nature. The earlier fluids were thus probably magmatic in origin, being derived from the intruding D_2 granitoid during pressure release and magma crystallization. The extensive K^+ metasomatism evidenced at the Harewood deposit is ascribed to early magmatic fluids. In addition, base metal-chloride complexes may have been an important constituent of these fluids. The actual reduced, Au-bearing fluids were probably derived during the metamorphic dehydration of the greenstone pile, the heat source being the intruding D_2 granodiorite. These somewhat later fluids deposited sulphide phases (pyrrhotite and sphalerite) and finally **Au**. The generation of the oxidized and reduced fluids probably overlapped to a certain extent. The auriferous fluids were probably similar to those detailed by Ho *et al.* (1985) and others (refer to section 5.2), except that they were CO_2-poor.

Source of Au: The source of the Au remains uncertain. Since the fluids which deposited the Au were metamorphic in origin, it seems probable that the Au was derived from the greenstone sequence itself. Interflow sediments in the MGGR, now represented mainly by recrystallized chert, are not enriched with respect to Au (see Table 5.1), suggesting that Au liberated early from the volcanic pile **may** have been flushed completely from the system. Alternatively, Au may have been incorporated in the cherts during seawater metasomatism and then subsequently remobilized during deformation and metamorphism. However, the absence of any spatial relationship between the Au deposits and the recrystallized chert

layers suggests that the latter were unrelated to ore formation.

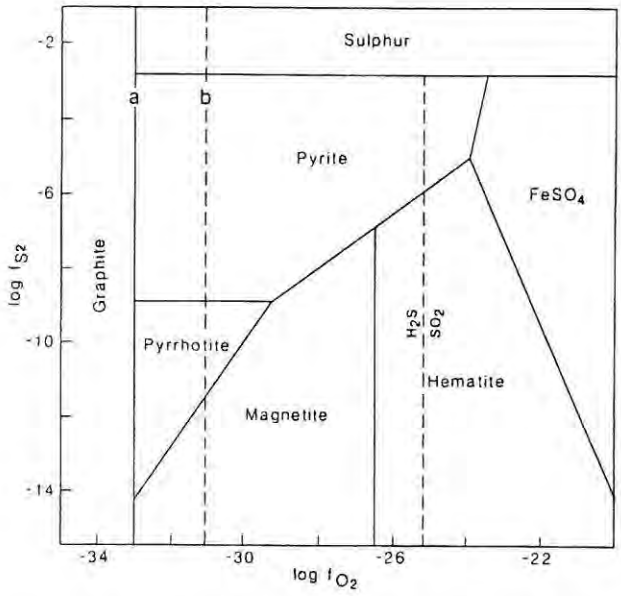

Figure 5.8 Log fS_2 - log fO_2 diagram showing the stability of Fe minerals at 350°C and fH_2O = 165 atm (after Cameron and Hattori, 1987). Note that the formation of haematite and pyrrhotite is dependant principally on O_2 fugacity. On the other hand, pyrite and haematite can occur at similar O_2 fugacities, pyrite precipitating in respose to higher S fugacities and haematite in response to lower S fugacities. Hence the fluids must have changed from oxidizing to reducing **prior** to Au deposition.

In igneous rocks, Au is readily scavenged by immiscible sulphide melts which remain at depth (refer to 5.1), and hence high temperature magmas (that is those in which sulphur saturation is inhibited) constitute the most likely source rocks. The Au was thus probably derived from the basaltic komatiites and/or serpentinite. The latter is a more likely source since it may not have been subjected to seafloor metasomatism (and hence Au loss) during the initial stages of deformation. Furthermore, talcification accompanying the introduction of hydrous fluids during D_1 and D_2 would have occurred under oxidizing conditions, allowing for the dissolution of Au and S during fluid/sulphide interaction. The close spatial association between the serpentinites and talc schists of the MGGR and the Au mineralization supports the contention that the Au was derived from serpentinite intrusions.

Mechanisms of Mobilization and Transport: The Au was liberated from the greenstone pile during prograde metamorphic reactions and dissolved into metamorphic fluids under **reducing** conditions. Hence the Au was almost certainly transported as a thio-complex [for example - $HAu(HS)_2$]. The instability of Au-chloride and Au-B-bearing complexes in reducing, near neutral pH fluids suggests that they were not important transporting agents.

"Abundant" Cu sulphides have been observed in quartz reef from the Times prospect (Gray, 1902), whereas none have been documented in the Vira and Harewood workings. Phillips and Groves (1983) pointed out that **base metals** in massive sulphide deposits are transported to the site of deposition (seafloor) as chloride complexes in oxidized, hydrothermal fluids. In addition, Hutchinson and Burlington (1984) noted that chloride complexes are important transporting agents in hydrothermal fluids of elevated oxidation potential and/or fluids containing very low reduced sulphur concentrations. Therefore the Cu observed at the Times prospect was probably transported as a chloride complex in oxidized fluids of magmatic origin. The absence of Cu sulphides in the Harewood and Vira workings may be due to the greater distance of the two workings from the D_2 granodiorite pluton.

Cause of Deposition: Au depostion probably occurred in response to a number of factors including: fluid/wall rock interaction; decreasing pressures and temperatures in dilational sites caused by shear zone refraction; decreasing fH_2S in response to sulphidation of the wall rocks; **increases** in the pH of the mineralizing fluids in response to argillic wall rock alteration adjacent to the auriferous quartz reefs (refer to section 5.5). Although fresh Fe-sulphides were not observed in wall rocks adjacent to the mineralized quartz reefs, this can ascribed to the extremely weathered nature of the rocks rather than to their absence. Fe-sulphides would almost certainly be present in unweathered wall rocks at depth. Evidence supporting Au deposition in response to decreasing pressures and temperatures rather than purely to fluid/wall rock interaction is provided at the Harewood deposit, where the auriferous reefs are hosted in Fe-poor rocks, in which extensive sulphidation is unlikely to have occurred.

Au deposition may have taken place in response to boiling although fluid inclusion studies would need to be undertaken in order to determine if phase separation actually occurred.

Timing of Mineralization: The Au mineralization in the MGGR has elsewhere been shown to have been deposited towards the end of the shearing event (refer to section 4.1) and can thus related to fluid ingress during the closing stages of D_2, therefore post-dating the peak D_1 metamorphism. In addition, Guha *et al.* (1983) pointed out that P shears (the fracture surfaces in which the mineralization in the D_2 shear zone occurs), develop during the **waning** stages of shearing.

The model is summarized in Fig. 5.9.

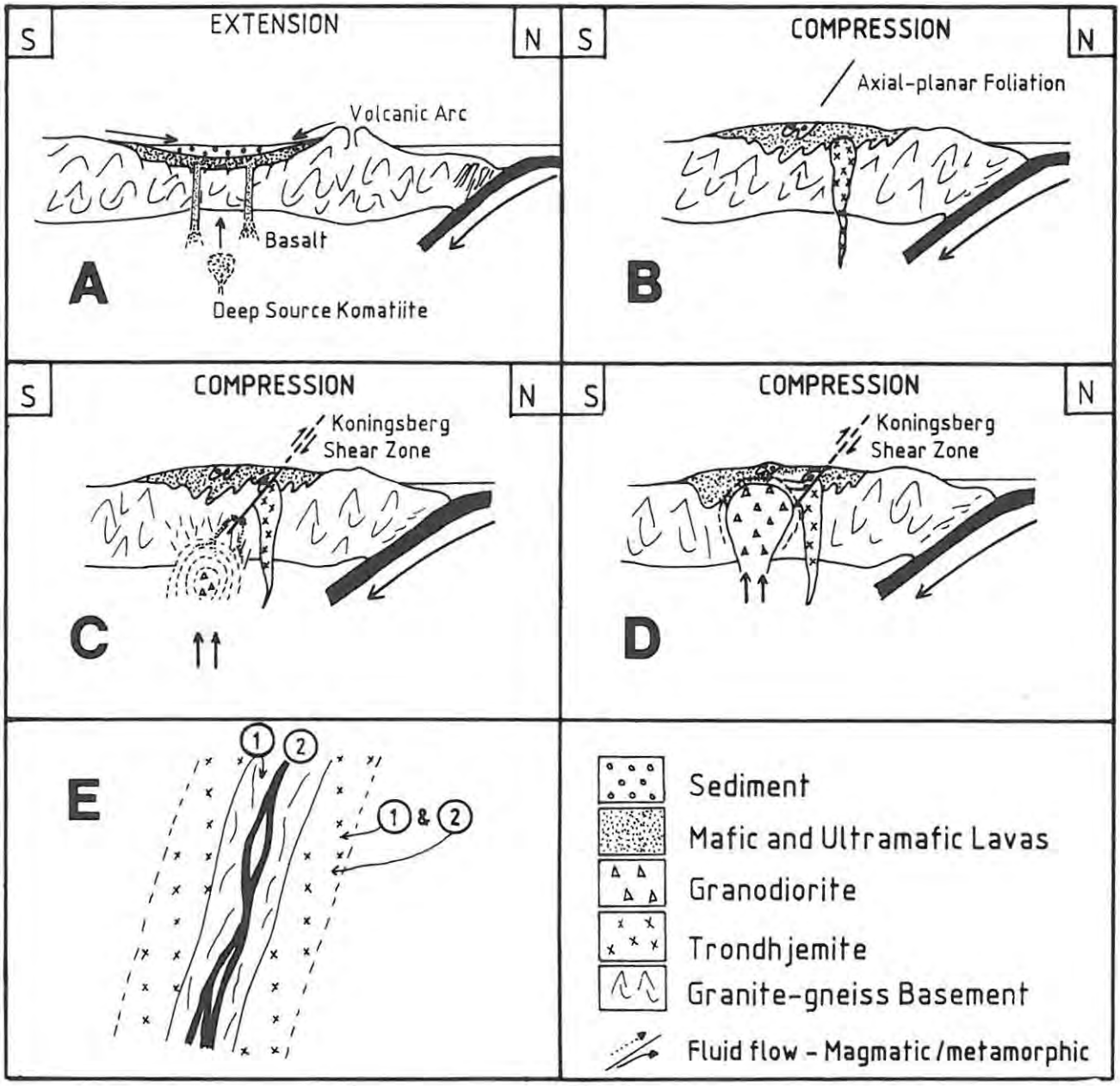

Figure 5.9 Highly schematic illustration depicting the geological evolution of the MGGR and the shear zone hosted Au mineralization.

A - Before deformation with the greenstone sequence accumulating in a back-arc basin setting.

B - Closure of the back-basin in response to the landward migration of the subduction zone coupled with the intrusion of trondhjemitic magmas. The magmas were derived from the partial melting of the subducting oceanic plate. The greenstone sequence underwent tilting and folding (with the development of a steep southerly dipping, penetrative, axial-planar cleavage - S1). Minor shear zones developed.

C - Continued deformation with development of the D_2 Koningsberg shear zone (of greenstone scale), in response the intrusion of granodioritic

magmas. Early magmatic fluids were channelled through fractures to the shear zone. Quartz, silicates and oxides (and to a lesser extent Cu-sulphides) were deposited in dilational sites.

D - Prograde metamorphism **near the base of the greenstone pile** in response to the emplacement of the granodiorite pluton generated metamorphic fluids. The fluids reacted with the host rocks dissolving Au (and Zn) and were subsequently channelled up the D_1 shear zone. Sulphides and Au were deposited in exisiting dilational sites. **E** - Close-up of a typical auriferous quartz vein from the Harewood working showing **(1)** early quartz, silicate and Fe-oxide deposition as well as K^+ metasomatism of the wall rocks and **(2)** later quartz, sulphide and Au deposition as well as sulphidation (pyritization) and argillic alteration of the wall rocks.

6. EXPLORATION MODEL

A typical **large-scale** exploration programme for the discovery of lode Au deposits in Archaean granite-greenstone terranes would involve:

a) Remote sensing - to identify crustal and greenstone-scale shear zones as well as lithologies which commonly host Au mineralization (for example - Fe-rich lavas, BIF).

b) Geochemical exploration - involving mainly lithogeochemical, stream sediment and soil sampling. Geochemical exploration may be used as a mapping tool although it is generally used as a direct guide to the Au mineralizion.

c) Geophysical exploration - electromagnetic, induced polarization and resistivity methods are used to define auriferous orebodies containing pyrite and pyrrhotite. Airborne magnetic surveys may be undertaken as an aid in geological mapping (for example to help identify Fe-rich, potentially Au-bearing lithologies.

d) Geological mapping - undertaken in areas of potential mineralization in order to detail the various rock types, structures, metamorphic grades and so on. Trenching would be undertaken at this stage.

e) Drilling - to investigate the nature of the mineralization at depth, to define the limits of the orebody and to calculate ore reserves.

f) Evaluation stage - to determine whether the Au may be extracted economically.

Known Au deposits in the D_2 Koningsberg shear zone in the MGGR have been shown however, by previous mining operations, to be restricted in size. Undiscovered deposits will probably also be restricted in size, suitable to exploitation by way of small-scale mining operations only. Hence the level of expertise and capital available for exploration purposes will be limited. In addition, it is probable that more than one shear zone of D_2 age is present in the inlier. An exploration programme has thus been specifically developed for the MGGR, taking these factors into account. The programme has been divided into a number of stages

in order to facilitate its application. **It must be emphasized however that the exploration model could probably be applied, with minor modifications, to shear zone-hosted Au deposits in other granite-greenstone inliers south of Swaziland.**

6.1 Stage I - Shear Zone Identification

A regional appraisal of the MGGR using aerial photographs is the first step that should be undertaken. A rough geological map must be constructed in order to identify any discontinuities (lithologic contacts, shear zones) and these must be checked in the field. The use of aerial photographs in the MGGR is however limited owing to poor exposure and thick vegetation cover. The area should therefore be traversed in order to locate shear zones not observed on the aerial photographs. Alteration (silicification, sericitization and chloritization) is a particularly useful exploration tool that should be used at this point. If available, simple geophysical techniques (such as magnetic and self-potential surveys) could be used to help identify structural discontinuities in areas of poor outcrop.

The second step involves distinguishing between D_1, D_2 and D_3 shearing utilizing Table 6.1. All D_2 shear zones must then be **mapped in detail**, particular attention being paid to the thickness of the shear zones and their strike extent. The Koningsberg shear for example is up to 150 m in thickness, is faulted out to the east against Natal Group sandstones but is open ended to the west, disappearing under Natal Group cover (refer to Fig. 3.1). In addition, the nature and intensity of the alteration must be documented.

6.2 Stage II - Delineation of Potential Orebodies

The D_2 shear zones must be now be investigated in order to determine which sections are mineralized. Investigations of the old Au workings in the MGGR revealed that:

a) the deposits are situated near lithological contacts, in the less competant rock type.

b) the shear zone thickens in the vicinity of the deposits.

c) the mineralization is located in the center of the shear

zone - that is in the most intensly sheared portion.

d) wall rock alteration facies (refer to section 4) are well developed.

e) two generations of quartz veins are present - namely an earlier phase of barren, foliation-parallel veins and a later phase of Au-bearing veins which **cross-cut** the s-fabric at a shallow angle.

Table 6.1 Criteria used to distinguish between D_1, D_2 and D_3 shear zones. The potentially mineralized D_2 shear zone is significantly different (and hence easily distinguished in the field) to D_1 and D_3 shear zones.

	D_1	D_2	D_3
Thickness	<2 m	>20 m, max 150 m, generally around 40 m	± 10 m
Orientation	071/40S	069-097/45-65S	119/± vert
Sense of Displacement	Dip slip	Oblique slip, s-c. lineations plunge 69 on 191 and 64 on 254 respectively	Oblique slip, lineations plunge 53° on 090
Ammount of Displacement	20 cm	> 20 m	≈10 m
Alteration	None	Sericitization, chloritization, argillization, silicification, pyritization	Silicification
Quartz Veining	Minor, foliation parallel veining	Two generations, early, foliation parallel veining and late oblique veining	Minor, foliation parallel veining
General Locality	In greenstone sequence only	In greenstone sequence and in trondhjemite	Spatially related to Hlagothi intrusive

Sections of the D_2 shear zones which display **at least one** of the aforementioned features must be demarcated and mapped on a scale of not less than 1:500. If exposure is poor however, soil geochemistry methods must be used to determine which portions of the shear zone warrant further investigation. The most rapid and

economical way of identifying Au anomalies would be by way of panning. For sufficiently accurate and consistent results, soil samples must be large (>1 kg). However, a number of factors need to be borne in mind when conducting soil surveys. For example, samples near old prospects may give spurious results owing to the effects of contamination. In addition, blind orebodies are likely to result in extremely subtle anomalies in the soil profile. Franey (1987) considered the use of probability graphs essential in identifying anomalous data.

6.3 **Stage III - Detailed Investigation**

The next step involves a detailed examination of potentially mineralized areas. Close attention must be paid to the **nature of wall rock alteration** and to the presence of **undeformed, oblique shear veins**. The strongest indicators of the presence of Au mineralization (as deduced from studies of the old Au workings) are argillization and (almost certainly) pyritization in wall rocks closest to the mineralization. However chloritization, which characteristically mantles the innermost zone of alteration, constitutes a far larger and hence more important exploration target. The old workings should be cleared out and mapped in detail in order to obtain an indication of the nature of the mineralization at depth (for example - orebody morphology). In addition, the remaining reefs must be sampled and possible extensions predicted.

Trenches must then be dug across potentially mineralized sections of the shear zone and a detailed lithogeochemical survey carried out. Samples of both oblique quartz veins and wall rock must be analysed since both have been shown to contain significant mineralization. The effects of Au depletion in the near-surface oxidized zone must be borne in mind. The "low" Au concentrations of up to 917 ppb in the mineralized zone at the Vira working are almost certainly an expression of the effects of near-surface depletion and hence grades can be expected to increase significantly with depth. As regards analytical methods, atomic absorbtion spectroscopy is favoured over fire assay owing to the lower detection limits of the former (although a combination of the two would provide excellent results).

At this point potentially economic, Au bearing reefs will have been identified on surface. The next step is to investigate the nature of the mineralization at depth, particularly below the near-surface zone of oxidation. This **must** be undertaken by diamond drilling (irrespective of the expense involved) in order to obtain a continuous and intact sample of reef for detailed analysis. Initially only a few, carefully sited holes (based on the detailed geological map) could be drilled to provide a rough idea of the grades at depth. A detailed drilling programme should then be initiated in selected areas in order to determine the size and extent of, and grade variations within, the orebody. Sampling must be undertaken systematically throughout the zone of argillization and pyritization with Au values being plotted on a histogram to facilitate the interpretation of the assay results. Care must be taken not to stop the drillholes prematurely. A clear understanding of the different wall rock alteration facies is fundamental in this regard.

6.4 Stage IV - Evaluation

Detailed feasibility studies must now be conducted on potential orebodies in order to determine their economic viability. This would entail a considerable ammount of further work and evaluation. Underground development coupled with extensive sampling would be necessary at this stage.

7. CONCLUSIONS AND RECOMMENDATIONS

The Harewood and Vira workings both show potential with regard to Au mineralization. Good grades obtained during recent sampling together with the fact that mining never proceeded below depths of 80 m and 40 m respectively, suggests that substantial quantities of ore may remain below these levels. Further work is however necessary in order to determine whether the remaining ore could sustain **small-scale** mining operations. The considerable extent of the Koningsberg shear zone in the MGGR, together with the probable existance of further shear zones of D_2 age (as yet undetected owing to poor outcrop), suggests that the MGGR may be host to a number of small, as yet undiscovered, economically viable ore deposits.

The development of an ore genesis model has enabled a **simple** exploration programme to be developed. The model was premised on the fact that if economically viable lode Au deposits were identified, their yields would probably be relatively small thus providing a limit on the amount of capital and hence geological expertise available for exploration purposes. The exploration programme was therefore devised in such a manner that it could be carried out in the field by only a few people, even if those people **were not necessarily versed in formal geologic principles**. In addition, the exploration model could probably be applied, with minor modifications, to the search for shear zone-hosted Au deposits in other granite-greenstone inliers in northern Natal.

The potential importance of small-scale mining operations should not be overlooked. Of the roughly 6000 operating Au mines in Zimbabwe for example, over 85% are defined as "small-scale" operations by the Ministry of Mines (Chenjerai, 1989). Although these small-scale mines each produce less than (often considerably so) 15 kg of Au per year, they account for 3-4% of Zimbabwe's annual Au production - a not insignificant amount considering that Zimbabwean Au production ranked 11th amongst the "non-communist" producing countries in 1982 (official production figures; cited in Foster *et al.*, 1986). Far more significant however are the socio-economic benefits provided by Zimbabwe's

small-scale mining industry, with the mines providing an income for thousands of people who would otherwise be unemployed.

If established, mining operations in the MGGR would probably be on a similar scale to those at the Dumisa Au mine near Umzinto, about 60 km southwest of Durban (see Thomas and Gain, 1989 and Figs. 7.1 and 7.2). Only one beneficiation plant would need to be established, the ore from all the workings being processed by the plant. The necessary capital and expertise could be provided by the State and/or Private sectors.

Finally, it is recommended that:

a) the Harewood and Vira Au deposits be cleared out and the old workings sampled.

b) a detailed drilling programme be carried out on the two deposits in order to determine the depth extent of the mineralization.

c) the Koningsberg shear zone be traced westwards (by way of mapping, geophysical methods and, if necessary, drilling) bearing mind that the Natal Group cover is, where present, of limited thickness and would pose no problems with regard to mining.

d) attention be paid to the discovery of further D_2 shear zones in the MGGR.

e) an attempt be made to apply the model to other granite-greenstone inliers in northern Natal.

Figure 7.1 Photograph showing a portion of the beneficiation plant at the Dumisa Au mine. The ore is passed through a jaw crusher into a ball mill (center).

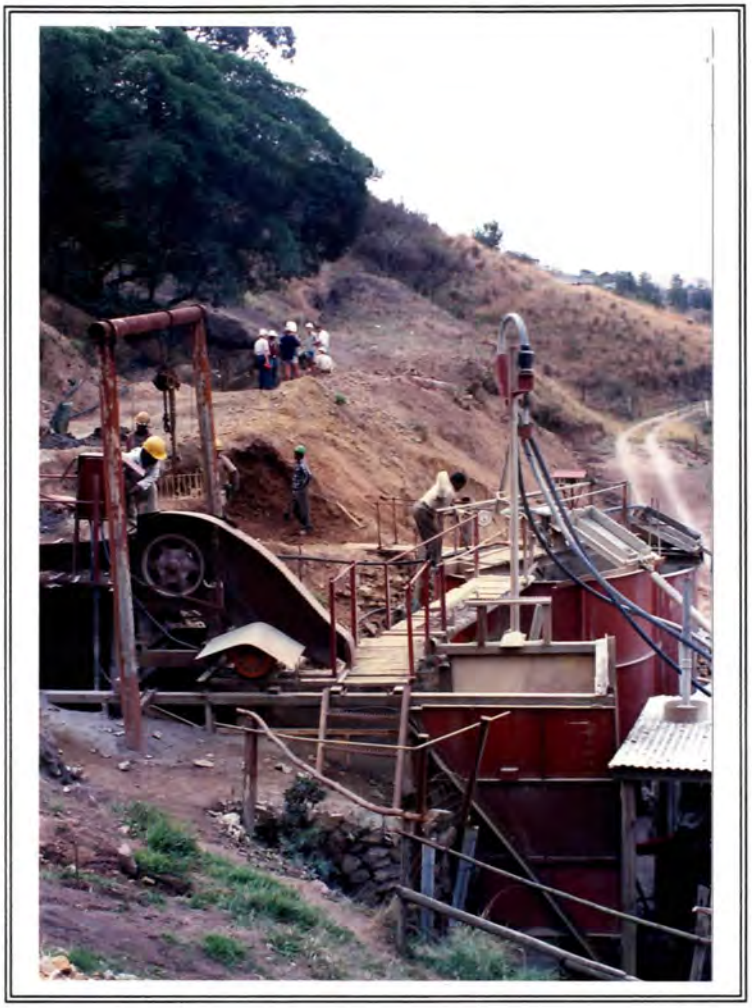

Figure 7.2 The crushed ore is slurried and then fed into tanks (right center) and cyanided. The jaw crusher (center left) and mine entrance (left background) are visible.

8. ACKNOWLEDGEMENTS

Firstly, I would like to thank the Chief Director, Geological Survey, for permission to undertake the MSc. (Economic Geology) degree at Rhodes University. Particular thanks are extended to Dr E Hammerbeck for allowing me to work uninterruptedly on this thesis following the period of full-time study at Rhodes. The constructive advice given by Mr P Wipplinger during field visits is gratefully acknowledged, as is his continued support and encouragement throughout.

Thanks are due to Professor F Pirajno and Mr C Mallinson of Rhodes University for the guidance and encouragement given throughout the duration of my studies. The former's enthusiasm was a continuous source of inspiration. Particular thanks are due to Mr C Malinson for reviewing, and thus helping to improve, the initial draft of this thesis.

Stimulating discussions with Dr R Thomas and Mr C Marshall provided much food for thought and their assistance in this respect is gratefully acknowledged. Mrs L Robertson is thanked for typing the Appendices and for helping to check spelling.

Special thanks are given to Tania Spencer who remained with me during some extremely trying times.

9. REFERENCES

Anhaeusser, C.R. 1973. The evolution of the early Precambrian crust of southern Africa. *Philos. Trans. R. Soc. London, Ser. A*, 273, 359-388.

Anhaeusser, C.R. 1976. The nature and distribution of Archaean gold mineralization in Southern Africa. *Minerals Sci. Engng.*, 8(1), 46-84.

Anhaeusser, C.R. 1983. Structural elements of Archaean granite-greenstone terranes as exemplified by the Barberton Mountain Land, Southern Africa. *Econ. Geol. Res. Unit*, Information Circular N° 162, Univ. Witwatersrand, pp 22.

Anhaeusser, C.R. 1986. Archaean gold mineralization in the Barberton Mountain Land, 113-154. *In* Anhaeusser and Maske (Eds.), *Mineral Deposits of Southern Africa*, I. Geol. Soc. S. Afr., 1020.

Anhaeusser, C.R. and Robb, L.J. 1981. Magmatic cycles and the evolution of the Archaean granitic crust in the Eastern Transvaal and Swaziland. *Spec. Publ. geol. Soc. Aust.*, 7, 457-467.

Anhaeusser, C.R. and Viljoen, M.J. 1986. Archaean metallogeny of Southern Africa, 33-42. *In* Anhaeusser and Maske (Eds.), *Mineral Deposits of Southern Africa*, I. Geol. Soc. S. Afr., 1020.

Anhaeusser, C.R. and Wilson, J.F. 1981. The granitic-gneiss greenstone shield, 423-453. *In* Hunter (Ed.), *Developments in Precambrian geology 2: Precambrian of the Southern Hemisphere*. Elsevier Scientific Publishing Co., Amsterdam, pp 882.

Barker, F. 1979. Trondhjemite : definition, environment and hypotheses of origin, 1-12. *In* Barker (Ed.), *Trondhjemites, Dacites and Related Rocks*, Elsevier, Amsterdam, pp 659.

Barley, M.E. and Groves, D.I. 1987. Hydrothermal alteration of Archaean supracrustal sequences in the central Norseman-Wiluna belt, Western Australia: A brief review, 51-66. *In* Ho and Groves (Eds.), *Recent Advances in Understanding Precambrian Gold deposits*. Geol. Dept & Univ. Extension, Univ. West. Aust., Publ 11, pp 368.

Barton, J.M., Robb, L.J., Anhaeusser, C.R. and Van Nierop, D.A. 1983. Geochronologic And Sr-isotopic studies of certain units in the Barberton granite-greenstone terrane, South Africa, 63-72. *In* Anhaeusser (Ed.), *Contributions to the Geology of the Barberton Mountain Land*, Spec. Publ. geol. Soc. S. Afr., pp 223.

Bonnemaison, M. and Marcoux, E. 1990. Auriferous mineralization in some shear-zones: A three stage model of metallogenesis. *Mineral. Deposita*, 25, 96-104.

Boyle, R.W. 1961. The geology, geochemistry, and origin of the gold deposits of the Yellowknife district. *Geol. Surv. Can., Mem. 310*, pp 193.

Boyle, R.W. 1979. The geochemistry of gold and its deposits. *Geol. Surv. Canada.*, Bull. 280, pp 584.

Brooks, C. and Hart, S.R. 1974. On the significance of komatiite. *Geology*, 2, 107-110.

Brown, K.L. 1988. Kinetics of gold precipitation from hydrothermal solutions, 199-204. *In* Bicentennial Gold '88 (compiled by A.D.T Goode and L.I. Bosma), *Geol. Soc. Aust., Abstracts Series N° 22*, Melbourne, Victoria, pp 369.

Burnham, C.W. 1979. Magmas and hydrothermal fluids, 71-136. *In* Barnes (Ed.), *Geochemistry of hydrothermal ore deposits*, J. Wiley, N.Y., pp 798.

Burrows, D.R., Wood, P.C., Thomas, A.V. and Spooner, E.T.C. 1986. A magmatic origin for Archaean gold-quartz vein mineralization in the Mink Lake granodiorite stock, NW Ontario, and from the Hollinger Au Deposit, Timmins, N Ontario, 283-286. Extended Abstracts, Geocongress '86 (Univ. Witwatersrand), *Geol. Soc. S. Afr.*, pp 1061.

Button, A. 1981. The Pongola Group, 501-510. *In* Hunter (Ed.), *Developments in Precambrian geology 2: Precambrian of the Southern Hemisphere*. Elsevier Scientific Publishing Co., Amsterdam, pp 882.

Cameron, E.M. 1988. Archaean gold: Relation to granulite formation and redox zoning in the crust. *Geology*, 16, 109-122.

Cameron, E.M. and Hattori, K. 1987. Archaean gold mineralization and oxidized hydrothermal fluids. *Econ. Geol.*, 82, 1177-1191.

Chenjerai, K.G. 1989. Small-scale gold production in Zimbabwe: Harare mining region 1980-1988, 78-83. *Annals Zim. Geol. Surv.*, 14, pp 89.

Colvine, A.C., Andrews, A.J., Cherry, M.E., Durocher, M.E., Fyon, A.J., Lavigne, M.J., Macdonald, A.J., Marmont, S., Pouslen, K.H., Springer, J.S. and Troop, D.G. 1984. An intergrated model for the origin of Archaean lode gold deposits. *Ontario Geol. Surv.*, Open File Report 5524, pp 99.

Compston, W. and Kröner, A. 1988. Multiple zircon growth within early tonalitic gneiss from the Ancient Gneiss Complex, Swaziland. *Earth Planet. Sci. Lett.*, 87, 13-28.

Condie, K.C. 1976. Trace-element geochemistry of Archaean greenstone belts. *E. Sci. Rev.*, 12, 393-417.

Condie, K.C. 1981. Developments in Precambrian geology 3: Archaean greenstone belts. *Elsevier Scientific Publishing Co.*, Amsterdam, pp 434.

Condie, K.C. and Hunter, D.R. 1976. Trace element geochemistry of Archaean granitic rocks from the Barberton region, South Africa. *Earth Plan. Sci. Lett.*, 29, 389-400.

De Beer, J.H. and Stettler, E.H. 1986. The deep structure of South African greenstone belts, 361-364. Extended Abstracts, Geocongress '86 (Univ. Witwatersrand), *Geol. Soc. S. Afr.*, pp 1061.

Dimroth, E., Cousineau, P., Leduc, M. and Sanschagrin, Y. 1978. Structure and organization of Archaean subaqueous basalt flows, Rouyn-Noranda area, Quebec, Canada. *Can. J. Earth Sci.*, 15, 902-918.

Du Toit, A.L. 1931. The geology of the country surrounding Nkandla, Natal: An explanation of sheet N° 109 (Nkandla). *Gov. Printer*, Pretoria, pp 111.

Eisenlohr, B.N., Groves, D. and Partington, G.A. 1989. Crustal-scale shear zones and their significance to Archaean gold mineralization in Western Australia. *Mineral. Deposita*, 24, 1-8.

Erzinger, J. 1989. Chemical alteration of the oceanic crust. *Geol. Rundsch.*, 78(3), 731-740.

Fouchè, J. 1986. The crustal framework and tectono-geological evolution of Southern Africa, 795-797. Extended Abstracts, Geocongress '86 (Univ. Witwatersrand), *Geol. Soc. S. Afr.*, pp 1061.

Foster, R.P. 1985. Major controls of Archaean gold mineralization in Zimbabwe. *Trans. geol. Soc. S. Afr.*, 88, 109-133.

Foster, R.P., Mann, A.G., Stowe, C.W. and Wilson, J.F. 1986. Archaean gold mineralization in Zimbabwe, 43-112. *In* Anhaeusser and Maske (Eds.), *Mineral Deposits of Southern Africa*, I. Geol. Soc. S. Afr., 1020.

Franey, N.J. 1987. A geological model of shear zone gold deposits in the Pietersburg greenstone belt. Unpbl. M.Sc. Dissertation, Rhodes Univ., pp 120.

Fyfe, W.S. and Kerrich, R. 1984. Gold: Natural concentration processes, 99-127. *In* Foster (Ed.), *Gold '82: The Geology, Geochemistry and Genesis of Gold Deposits, Geological Society of Zimbabwe*. A.A. Balkema, Rotterdam, pp 753.

Gélinas, L., Mellimger, M. and Trudel, P. 1982. Archaean mafic metavolcanics from the Rouyn-Noranda district, Abitibi greenstone belt, Quebec. 1. Mobility of the major elements. *Can. J. Earth Sci.*, 19, 2258-2275.

Glasson, M.J. and Keays, R.R. 1978. Gold mobilization during cleavage development in sedimentary rocks from the auriferous slate belt of Central Victoria, Australia: some important boundary conditions. *Econ. Geol.*, 73, 496-511.

Gray, C.J. 1900. Report on the mining industry of Natal for the year 1899, 15-16. *Times Printing and Publishing Co. Ltd*, Pietermaritzburg, pp 70.

Gray, C.J. 1902. Report on the mining industry of Natal for the year 1901, 35-36. *Times Printing and Publishing Co. Ltd*, Pietermaritzburg, pp 91.

Gray, C.J. 1904. Report on the mining industry of Natal for the year 1903, 15. *Times Printing and Publishing Co. Ltd*, Pietermaritzburg, pp 110.

Gray, C.J. 1907. Report on the mining industry of Natal for the years 1906, 1. *Times Printing and Publishing Co. Ltd*, Pietermaritzburg, pp 88.

Gray, C.J. 1910. Report on the mining industry of Natal for the year 1909, 9-10, 39-40. *Times Printing and Publishing Co. Ltd*, Pietermaritzburg, pp 121.

Groenewald, P.B. 1984. The lithostratigraphy and petrogenesis of the Nsuze Group northwest of Nkandla, Natal. Unpbl. M.Sc. thesis, Univ. Natal (Pmb.), pp 250.

Groenewald, P.B. 1988. The Hlagothi Complex : Layered Archaean mafic - ultramafic sills of Komatiitic affinity within the Pongola Sequence northwest of Nkandla, Natal, 215-218. Extended Abstracts, Geocongress '88 (Univ Natal, Durban), *Geol. Soc. S. Afr.*, pp 838.

Groves, D.I., Phillips, G.N., Ho, S.E., Henderson, C.A., Clark, M.E. and Woad, G.M. 1984. Controls on distribution of Archaean hydrothermal gold deposits in Western Australia, 689-712. *In* Foster (Ed.), *Gold '82: The Geology, Geochemistry and Genesis of Gold Deposits, Geological Society of Zimbabwe*. A.A. Balkema, Rotterdam, pp 753.

Groves, D.I., Phillips, G.N., Ho, S.E., Houstoun, S.M. and Standing, C.A. 1987. Craton-scale distribution of Archaean greenstone gold deposits: Predictive capacity of the metamorphic model. *Econ. Geol.*, 82, 2045-2058.

Groves, D.I. and Phillips, G.N. 1987. The genesis and tectonic control on Archaean gold deposits of the western Australian shield - A metamorphic replacement model. *Ore Geol. Rev.*, 2, 287-322.

Guha, J., Archambault, G. and Leroy, J. 1983. A correlation between the evolution of mineralizing fluids and the geomechanical development of a shear zone as illustrated by the Henderson 2 Mine, Quebec. *Econ. Geol.*, 78, 1605-1618.

Guilbert, J.M. and Park, C.F. 1986. The geology of ore deposits. *W.H. Freeman and Co.*, New York, pp 985.

Hamilton, P.J., Evensen, N.M., O'Nions, R.K., Smith, H.S. and Erlank, A.J. 1979. Sm-Nd dating of Onverwacht Group volcanics, southern Africa. *Nature*, 279, 298-300.

Hegner, E., Kröner, A. and Hoffmann, A.W. 1984. Age and isotopic geochemistry of the Archaean Pongola and Ushushwana suites in Swaziland, southern Africa: a case for crustal contamination of mantle derived magmas. *Earth Planet. Sci. Lett.*, 70, 267-279.

Ho, S.E., Groves, D.I. and Phillips, G.N. 1985. Fluid inclusions as indicators of the nature and source of ore fluids and ore depositional conditions for Archaean gold deposits of the Yilgarn Block, Western Australia. *Trans. geol. Soc. S. Afr.*, 88, 149-158.

Ho, S.E. 1987. Fluid inclusions: Their potential as an exploration tool for Archaean gold deposits, 239-263. *In* Ho and Groves (Eds.), *Recent Advances in Understanding Precambrian Gold deposits*. Geol. Dept & Univ. Extension, Univ. West. Aust., Publ 11, pp 368.

Hodgson, C.J. 1985. Precambrian lode gold deposits. Gold exploration 1985, Course notes, Queens Univ., Ontario, pp 316.

Hodgson, C.J. 1989. The structure of shear-related, vein-type gold deposits: A review. *Ore Geol. Rev.*, 4, 231-273.

Hunter, D.R. 1970. The Ancient Gneiss Complex in Swaziland. *Trans. Geol. Soc. S. Afr.*, 73, 107-150.

Hunter, D.R. 1988. A comparison of one billion years of earth history in the Pilbara and Southeastern Kaapvaal Province, 305-306. Extended Abstracts, Geocongress '88 (Univ Natal, Durban), *Geol. Soc. S. Afr.*, pp 838.

Hunter, D.R. in press [a]. Assegaai Formation, 5-6. *In* Johnson (Ed.), *Catalogue of South African Lithostratigraphic Units*, 2, South African Committee for Stratigraphy, Government Printer, Pretoria, pp 48.

Hunter, D.R. in press [b]. Anhalt Granitoid Suite, 3-4. *In* Johnson (Ed.), *Catalogue of South African Lithostratigraphic Units*, 2, South African Committee for Stratigraphy, Government Printer, Pretoria, pp 48.

Hunter, D.R. and Wilson, A.H. 1988. A continuous record of Archaean evolution from 3.5 Ga to 2.6 Ga in Swaziland and northern Natal. *S. Afr. J. Geol.*, 91(1), 57-74.

Hutchinson, R.W. and Burlington, J.L. 1984. Some broad characteristics of greenstone belt gold lodes, 339-371. *In* Foster (Ed.), *Gold '82: The Geology, Geochemistry and Genesis of Gold Deposits, Geological Society of Zimbabwe*. A.A. Balkema, Rotterdam, pp 753.

Jensen, L.S. 1976. A new cation plot for classifying subalkalic volcanic rocks. *Ontario Geol. Surv.*, Misc. Paper 66, pp 22.

Garrard, J.Jervis, 1895. Report on the mining industry of Natal for the year 1984, 16-20. *Gov. Printer*, Pietermaritzburg.

Garrard, J Jervis, 1898. Report on the mining industry of Natal for the year 1987, 16-18. *Gov. Printer*, Pietermaritzburg.

Keays, R.R. 1984. Archaean gold deposits and their source rocks: The upper mantle connection, 17-51. *In* Foster (Ed.), *Gold '82: The Geology, Geochemistry and Genesis of Gold Deposits, Geological Society of Zimbabwe*. A.A. Balkema, Rotterdam, pp 753.

Keays, R.R. and Scott, R.B. 1976. Precious metals in ocean-ridge basalts: Implications for basalts as source rocks for gold mineralization. *Econ. Geol.*, 71, 705-720.

Kerrich, R. 1984. Archaean lode gold deposits of Canada : A review, 13. *In* Pearton (Ed.), *Archaean Gold: Barberton Centenary Symposium: Abstracts and Guide Book*, pp 93.

Kerrich, R. 1986. Archaean lode gold deposits of Canada - Part II : Characteristics of the hydrothermal systems, and models of orogin. *Econ. Geol. Res. Unit*, Information Circular N° 183, Univ. Witwatersrand, pp 34.

Kerrich, R. 1989. Archaean gold: Relation to granulite formation or felsic intrusions? *Geology*, 17, 1011-1015.

Knight, C.L. 1953. Ore genesis - the source bed concept. *Econ. Geol.*, 71, 705-720.

Korobeynikov, A.F. 1988. Gold in volcanic rocks. Translated from *Geokhimiya*, 11, 1618-1626.

Kröner, A. 1985. Evolution of the Archaean continental crust. *Ann. Rev. Earth Planet. Sci. Lett.*, 13, 49-74.

Kwong, Y.T.J. and Crocket, J.H. 1978. Background and anomalous gold in rocks of an Archaean greenstone assemblage, Kakaigi Lake area, northwestern Ontario. *Econ. Geol.*, 73, 50-63.

Lindström, W. 1987. The geology of the Dundee area: Explanation of Sheet 2830. *Government Printer*, Pretoria, pp 52.

Locke, B.E. 1973. The Cape Supergroup in Natal and northern Transkei, 485-486. *Geol. Mag.*, 110.

Lowe, D.R. and Knauth, L.P. 1977. Sedimentology of the Onverwacht Group (3.4 billion years), Transvaal, South Africa, and its bearing on the characteristics and evolution of the early earth. *J. Geol.*, 85, 699-723.

Maalφe, S. 1982. Petrogenesis of Archaean tonalites. *Geol. Rundsch.*, 71, 328-346.

Martin, H. 1987. Petrogenesis of Archaean trondhjemites, tonalites and granodiorites from Eastern Finland: Major and trace element geochemistry. *J. Petrol.*, 28, 921-953.

Matthews, P.E. 1972. Possible Precambrian obduction and plate tectonics in southeastern Africa. *Nature*, 240, 37-39.

Matthews, P.E. 1981. Eastern or Natal sector of the Namaqua-Natal mobile belt in southern Africa, 705-715. *In* Hunter (Ed.), *Developments in Precambrian geology 2: Precambrian of the Southern Hemisphere*. Elsevier Scientific Publishing Co., Amsterdam, pp 882.

Matthews, P.E. 1988. Regional geology of the Melmoth area, northern Natal, 9-13. 1888 - Melmoth Zululand - 1988 (Melmoth Centenary Publication), *Kings Press*, Empangeni, pp 99.

Matthews, P.E., Charlesworth, E.G., Eglington, B.M. and Harmer, R.E. 1989. A minumum age of 3.29 Ga for the Nondweni greenstone complex in the south-eastern Kaapvaal Craton. *S. Afr. J. Geol*, 92(3), 272-278.

Meyer, M. and Saager, R. 1985. The origin of gold in Archaean epigenetic gold deposits. *Econ. Geol. Res. Unit*, Information Circular N° 172, Univ. Witwatersrand, pp 11.

Neall, F.B. 1987. Sulphidation of iron-rich rocks as a precipitation mechanism for large Archaean gold deposits in western Australia: Thermodynamic confirmation, 265-269. *In* Ho and Groves (Eds.), *Recent Advances in Understanding Precambrian Gold deposits*. Geol. Dept & Univ. Extension, Univ. West. Aust., Publ 11, pp 368.

Nesbitt, R.W. and Sun. S.S. 1976. Geochemistry of Archaean spinifex-textured peridotites and magnesian and low-magnesian tholeiites. *Earth Planet. Sci. Lett.*, 31, 433-453.

Nisbet, E.G. and Walker, D. 1982. Komatiites and the structure of the Archaean mantle. *Earth Planet. Sci. Lett.*, 60, 105-113.

Paris, I., Stanistreet, I.G. and Hughes, M.J. 1985. Cherts of the Barberton greenstone belt interpreted as products of submarine exhalative activity. *J. Geol.*, 93, 111-129.

Pearce, J.A. and Cann, J.R. 1973. Tectonic setting of basic volcanic rocks determined using trace element analysis. *Earth Planet. Sci. Lett.*, 19, 290-300.

Perring, C.S., Groves, D.I. and Ho, S.E. 1987. Constraints on the source of auriferous fluids for Archaean gold deposits, 297-306. *In* Ho and Groves (Eds.), *Recent Advances in Understanding Precambrian Gold deposits*. Geol. Dept & Univ. Extension, Univ. West. Aust., Publ 11, pp 368.

Perring, C.S., Barley, M.E., Bettenay, L.F., Cassidy, K.F., Golding, S.D., Groves, D.I., Hallberg, J.A., McNaughton, N.J. and Rock, N.M.S. 1988. The conjunction of linear mobile belts, mantle-crustal magmatism and gold mineralization in the Archaean greenstone belts of Western Australia. *In* Bicentennial Gold '88 (compiled by A.D.T Goode and L.I. Bosma), *Geol. Soc. Aust., Abstracts Series N° 22*, Melbourne, Victoria, pp 369.

Phillips, G.N. 1984. Carbonate alteration as a guide to greenstone gold deposits, 17. *In* Pearton (Ed.), *Archaean Gold: Barberton Centenary Symposium: Abstracts and Guide Book*, pp 93.

Phillips, G.N. and Groves, D.I. 1983. The nature of Archaean gold-bearing fluids as deduced from gold deposits of Western Australia. *J. Geol. Soc. Aust.*, 30, 25-39.

Phillips, G.N. and Groves, D.I. 1984. Fluid access and fluid-wall rock interaction in the genesis of the Archaean gold-quartz vein deposit at Hunt Mine, Kambalda, Western Australia, 389-416. *In* Foster (Ed.), *Gold '82: The Geology, Geochemistry and Genesis of Gold Deposits, Geological Society of Zimbabwe*. A.A. Balkema, Rotterdam, pp 753.

Pirajno, f and Jacob, R.E. 1984. A review of Archaean, Proterozoic tectonic provinces, and patterns of crustal evolution in Southern Africa. *Dept. of Geol.*, Rhodes Univ., pp 327. publication brought whilst at Rhodes)

Ramsay, J.G. and Graham, R.H. 1970. Strain variation in shear belts. *Can. J. Earth Sci.*, 7, 786-813.

Ramsay, J.G. and Huber, M.I. 1987. The techniques of modern structural geology. *Academic Press*, London, pp 700.

Ridler, R.H. 1973. Exhalite concept: a new tool for exploration. *The Northern Miner*, 59(37), 59-61.

Robb, L.J. and Anhaeusser, C.R. 1981. Chemical and petrogenetic characteristics of Archaean tonalite-trondhjemite gneiss plutons in the Barberton Mountain Land. *Econ. Geol. Res. Unit*, Information Circular N° 155, Univ. Witwatersrand, pp 16.

Robb, L.J., Barton, J.M., Kable, E.J.D. and Wallace R.C. 1986. Geology, geochemistry and isotopic characterisitics of the Archaean Kaap Valley pluton, Barberton Mountain Land, South Africa. *Precam. Res.*, 31, 1-36.

Roberts, R.G. 1987. Ore deposit models #11. Archaean lode gold deposits. *Geo. Sci. Canad.*, 14(1), 37-52.

Saager, R., Meyer, M. and Muff, R. 1982. Gold distribution in supracrustal rocks from Archaean grenstone belts of Southern Africa and from Paleozoic ultramafic complexes of the European Alps: Metallogenic and Geochemical implications. *Econ. Geol.*, 77 1-24.

Saager, R. and Meyer, M. 1984. Gold distribution in Archaean granitoids and supracrustal rocks from Southern Africa: A comparison, 53-70. *In* Foster (Ed.), *Gold '82: The Geology, Geochemistry and Genesis of Gold Deposits, Geological Society of Zimbabwe*. A.A. Balkema, Rotterdam, pp 753.

Seward, T.M. 1984. The transport and deposition of gold in hydrothermal systems, 165-181. *In* Foster (Ed.), *Gold '82: The Geology, Geochemistry and Genesis of Gold Deposits, Geological Society of Zimbabwe*. A.A. Balkema, Rotterdam, pp 753.

Seward, T.M. 1988. The hydrothermal chemistry of gold and its implications for ore formation, 197-198. *In* Bicentennial Gold '88 (compiled by A.D.T Goode and L.I. Bosma), *Geol. Soc. Aust., Abstracts Series N° 22*, Melbourne, Victoria, pp 369.

Seyfried, W.E. and Mottl, M.J. 1982. Hydrothermal alteration of basalt by seawater under seawater-dominated conditions. *Geochim. Cosmochim. Acta*, 46, 985-1002.

Skinner, B.J. 1979. The many origins of hydrothermal mineral deposits, 1-21. *In* Barnes (Ed.), *Geochemistry of hydrothermal ore deposits*, J. Wiley, N.Y., pp 798.

Smith, R.G. and Hunter, D.R. 1988. Archaean tonalitic gneisses - their geochemistry and relation to the supracrustal suites north of Paulpietersburg, 579-582. Extended Abstracts, Geocongress '88 (Univ Natal, Durban), *Geol. Soc. S. Afr.*, pp 838.

Starling. A., Gilligan, J.M., Carter, A.H.C. Foster, R.P. and Saunders, R.A. 1989. High-temperature hydrothermal precipitation of precious metals on the surface of pyrite. *Nature*, 340, 298-300.

Tankard, A.J., Jackson, M.P.A., Eriksson, K.A., Hobday, D.K., Hunter, D.R. and Minter, W.E., 1982. Crustal evolution of southern Africa - 3.8 billion years of Earth History. Springer-verlag, N.Y., pp. 523.

Tarney, J., Dalziel, I.W.D. and De Wit, M.J. 1976. Marginal basin "Rocas Verdes" complex from S. Chile: A model for Archaean greenstone belt formation. *In* Windley (Ed.), *The Early History of the Earth*, J. Wiley and Sons New York, N.Y., 131-146.

Thomas, R.J. 1989. A tale of two tectonic terranes. *S. Afr. J. Geol.*, 92(4), 306-321.

Thomas R.J and Gain, S.B. 1989. The geological setting of gold mineralization at Dumisa, Natal. *S. Afr. J. Geol.*, 92, 410-419.

Vearncombe, J.R., Barley, M.E., Eisenlohr, B., Grigson, M.W., Groves, D.I., Houstoun, S.M., Partington G.A. and Skwarnecki, M.S. 1988. Structural controls on gold mineralization : examples from the Archaean terranes of Western Australia and Southern Africa, 19-23. *In* Bicentennial Gold '88 (compiled by A.D.T Goode and L.I. Bosma), *Geol. Soc. Aust., Abstracts Series N° 22*, Melbourne, Victoria, pp 369.

Versfeld, J.A., Wilson, A.H. and Hunter, D.R. 1988. The geology of the Nondweni greenstone belt, 663-665. Extended Abstracts, Geocongress '88 (Univ Natal, Durban), *Geol. Soc. S. Afr.*, pp 838. Viljoen, M.J. 1984. Archaean gold mineralization in southern Africa, 595-627. *In* Foster (Ed.), *Gold '82: The Geology, Geochemistry and Genesis of Gold Deposits, Geological Society of Zimbabwe*. A.A. Balkema, Rotterdam, pp 753.

Viljoen, R.P., Saager, R. and Viljoen, M.J. 1969. Metallogenesis and ore control in the Steynsdorp goldfield, Barberton Mountain Land, South Africa. *Econ. Geol.*, 778-797.

Ward, J.H.W. 1987. Genesis of Barberton gold: The exhalite source-bed concept. *S. Afr. J. Geol.*, 90(3), 326-321.

Wilson, A.H. and Carlson, R.W. 1986. Geochronologic studies of the Archaean Nondweni supracrustal sequence, South Africa. *Terra Composite 6*, pp 147.

APPENDIX I

KEY

TS1..... Granodioritic gneiss from Locality 28
TS2..... Granite from Locality 34
TS3..... Quartz-muscovite schist from Locality 31
TS4..... Quartzite from Locality 92
TS5..... Meta-tholeiite from Locality 84
TS6..... Trondhjemitic gneiss from Locality 107
TS7..... Meta-tholeiite from Locality 52
TS8..... Talc schist from Locality 51
TS9..... Chlorite-quartz schist Locality 49
TS10..... Serpentinite from Locality 67
TS11..... Talc schist from Locality 67
TS12..... Quartz-fuchsite schist from Locality 45
TS13..... Meta-gabbro from Locality 39
TS14..... Basaltic Komatiite from Locality 69

TGM1..... Quartz reef from the Times prospect
TGM2..... Talc schist 1 m S of quartz reef
TGM3..... Talc schist 5 m S of quartz reef
TGM4..... Talc schist 7 m S of quartz reef
TGM5..... Talc schist 3 m S of quartz reef

HGM1..... Quartz-sericite schist 50 m N of the N° 3 Leader, Harewood Au working
HGM2..... Quartz-sericite schist 40 m N of the N° 3 Leader
HGM3..... Chlorite-quartz-sericite schist 15 m N of the N° 3 Leader
HGM4..... Quartz-clay rock 1 m N of the N° 3 Leader
HGM5..... Auriferous quartz reef from the N° 3 Leader
HGM6..... Serpentinite to the south of the Harewood working

VGM1..... Chlorite-quartz schist 7 m N of the Sericite-quartz-clay unit at the Vira Au working
VGM2..... Chlorite-quartz schist 3 m S of the clay-rich unit
VGM3..... Sericite-quartz schist overlying the orebody
VGM4..... Talc schist W of the working
VGM5..... Serpentinite S of the working

VGM A..... Sericite-quartz-clay unit from the Vira working
(see text for details)

VGM B..... As for VGM A

VGM C..... As for VGM A

VGM D..... As for VGM A

VGM E..... As for VGM A

MAJOR ELEMENT COMPOSITIONS - WEIGHT PERCENT

	SiO2	Al2O3	Fe2O3	FeO	MnO	MgO	CaO	Na2O	K2O	TiO2	P2O5	TOTAL
TS1 WEIGHT PERC OXIDE	67.40	14.22	0.71	5.71	0.09	1.23	2.33	5.04	2.52	0.65	0.12	100.02
TS2 WEIGHT PERC OXIDE	75.59	12.10	0.36	2.93	0.04	0.05	0.91	3.63	4.13	0.3223	0.05	100.13
TS3 WEIGHT PERC OXIDE	80.62	9.66	0.10	0.78	0.05	1.33	1.52	1.30	3.29	0.6721	0.14	99.46
TS4 WEIGHT PERC OXIDE	99.58	0.36	0.00	0.02	0.00	0.01	0.03	0.11	0.07	0.0044	0.01	100.19
TS5 WEIGHT PERC OXIDE	58.90	13.48	1.28	10.39	0.16	3.10	7.26	2.72	1.37	1.1933	0.20	100.06
TS6 WEIGHT PERC OXIDE	73.63	14.97	0.18	1.47	0.02	0.80	2.91	4.85	0.83	0.2582	0.09	100.01
TS7 WEIGHT PERC OXIDE	51.84	13.69	1.53	12.37	0.22	5.82	10.12	2.04	0.59	1.6914	0.22	100.13
TS8 WEIGHT PERC OXIDE	44.92	3.70	1.52	12.28	0.23	30.54	4.35	0.13	0.04	0.3063	0.04	98.05
TS9 WEIGHT PERC OXIDE	52.29	15.97	1.65	13.40	0.12	15.67	0.03	0.16	0.05	0.6903	0.06	100.10
TS10 WEIGHT PERC OXIDE	47.39	0.82	0.61	4.96	0.06	45.14	0.00	0.13	0.05	0.0102	0.01	99.18
TS11 WEIGHT PERC OXIDE	62.64	1.90	0.58	4.68	0.03	29.71	0.00	0.13	0.04	0.0452	0.01	99.77
TS12 WEIGHT PERC OXIDE	89.09	6.86	0.04	0.29	0.00	0.13	0.02	0.29	1.87	0.6064	0.01	99.21
TS13 WEIGHT PERC OXIDE	56.44	17.05	0.91	7.33	0.17	4.96	8.86	3.61	0.53	0.2984	0.06	100.22
TS14 WEIGHT PERC OXIDE	51.44	9.82	1.13	9.16	0.18	19.88	7.03	0.52	0.05	0.2487	0.02	99.49
TGM1 WEIGHT PERC OXIDE	99.39	0.19	0.03	0.23	0.02	0.02	0.02	0.08	0.05	0.0097	0.00	100.04
TGM2 WEIGHT PERC OXIDE	56.74	5.62	1.32	10.65	0.15	23.53	0.00	0.04	0.05	0.1369	0.03	98.27
TGM3 WEIGHT PERC OXIDE	68.78	16.03	1.52	12.29	0.17	0.69	0.02	0.06	0.06	0.7001	0.10	100.42
TGM4 WEIGHT PERC OXIDE	56.47	6.74	1.09	8.82	0.10	25.67	0.00	0.07	0.05	0.1408	0.02	99.15
TGM5 WEIGHT PERC OXIDE	56.32	6.46	1.09	8.82	0.06	26.70	0.00	0.11	0.04	0.2629	0.03	99.90
HGM1 WEIGHT PERC OXIDE	77.35	12.70	0.35	2.80	0.04	0.68	0.06	0.20	5.38	0.5002	0.08	100.12
HGM2 WEIGHT PERC OXIDE	85.30	9.58	0.04	0.36	0.03	0.32	0.03	0.18	4.07	0.1594	0.01	100.08
HGM3 WEIGHT PERC OXIDE	73.13	16.65	0.37	2.99	0.04	1.42	0.04	0.11	4.52	0.6657	0.04	99.96
HGM4 WEIGHT PERC OXIDE	90.71	3.73	0.34	2.72	0.39	1.07	0.09	0.08	0.78	0.2282	0.02	100.15
HGM5 WEIGHT PERC OXIDE	99.61	0.06	0.05	0.38	0.00	0.00	0.02	0.00	0.05	0.0007	0.00	100.18
HGM6 WEIGHT PERC OXIDE	48.68	1.04	0.90	7.30	0.07	41.49	0.00	0.08	0.04	0.0321	0.01	99.64
VGM1 WEIGHT PERC OXIDE	62.38	13.44	1.38	11.17	0.17	7.66	0.01	0.10	0.13	1.0556	0.09	98.49
VGM2 WEIGHT PERC OXIDE	53.59	19.18	1.34	10.88	0.30	10.27	0.07	0.20	2.64	1.5098	0.10	100.0
VGM3 WEIGHT PERC OXIDE	64.12	18.02	0.54	4.36	0.14	7.99	0.05	0.06	3.42	1.4212	0.03	100.14
VGM4 WEIGHT PERC OXIDE	62.26	2.22	0.66	5.36	0.08	28.33	0.00	0.01	0.05	0.0702	0.00	99.05
VGM5 WEIGHT PERC OXIDE	56.23	0.70	0.56	4.56	0.16	37.42	-0.02	0.14	0.04	0.0125	0.01	99.80

d

Trace Element Compositions (in ppm unless otherwise indicated)

Sample No.	Zr	Sr	Nb	Y	Rb	U	Th	Sc	Ba	Cr	V	La
TS1	30	374	11	18	28	1	0	36	174	2	117	12
TS2	300	82	16	38	111	2	14	7	542	0	0	40
TS3	114	39	5	19	123	0	2	12	3737	342	105	9
TS4	1	1	1	0	1	0	0	1	53	7	2	0
TS5	195	126	8	46	44	2	9	31	404	32	324	25
TS6	136	212	8	18	26	1	11	3	272	13	19	35
TS7	139	181	12	35	15	0	0	46	204	64	381	17
TS8	25	32	1	8	1	0	0	18	48	3213	85	0
TS9	48	2	1	12	1	1	0	49	53	860	284	1
TS10	1	0	0	2	0	0	0	6	45	1527	17	3
TS11	2	0	0	1	0	0	0	5	48	1948	22	0
TS12	73	91	3	9	49	0	0	38	1017	2490	228	0
TS13	51	372	1	12	13	0	0	27	192	111	121	4
TS14	24	9	0	10	1	0	0	34	51	3814	177	4
TGM1	0	0	0	0	0	0	0	1	57	11	2	0
TGM2	7	1	1	10	1	0	0	15	53	3619	124	4
TGM3	46	1	2	17	2	0	0	58	72	1185	392	6
TGM4	7	0	1	5	1	0	0	28	57	5462	112	5
TGM5	16	0	1	9	0	0	0	27	69	3943	142	5
HGM1	298	34	14	47	82	1	9	15	515	6	3	28
HGM2	236	17	14	9	64	1	7	6	459	2	6	12
HGM3	315	4	18	33	113	1	9	17	1019	21	77	24
HGM4	27	1	2	10	28	0	0	16	93	46	69	8
HGM5	0	0	0	0	0	0	0	1	33	6	1	0
HGM6	0	0	1	1	1	0	0	7	55	2029	28	0
VGM1	99	15	4	146	5	1	1	52	221	1899	294	49
VGM2	94	19	5	221	117	1	0	56	428	231	393	26
VGM3	96	12	4	32	131	1	0	59	416	147	248	3
VGM4	4	3	1	150	0	0	0	20	52	4546	32	44
VGM5	1	1	0	2	0	0	0	5	57	2618	30	1

Trace Element Compositions (in ppm unless otherwise indicated)

Sample No.	Ce	Nd	Pb	Ga	As	S %	L.O.I. %	Zn	Cu	Ni
TS1	27	8	13	22	46	0.07	0.39	123	37	0
TS2	75	27	15	16	6	0.00	0.27	41	0	0
TS3	15	7	0	9	5	0.00	0.84	20	0	33
TS4	0	0	0	0	1	0.00	0.55	5	5	17
TS5	48	20	8	17	5	0.02	0.78	101	127	53
TS6	66	18	12	13	6	0.01	1.04	19	51	11
TS7	28	13	0	18	6	0.12	1.39	109	122	52
TS8	0	0	0	4	8	0.02	13.89	82	3	1836
TS9	0	0	0	15	9	0.01	8.39	161	0	224
TS10	0	0	0	0	82	0.01	13.82	19	0	3182
TS11	0	0	0	3	9	0.01	5.19	62	1	2145
TS12	0	0	2	8	269	0.01	0.97	52	0	31
TS13	2	0	2	18	6	0.01	1.19	70	2	32
TS14	0	0	0	8	2	0.01	5.64	71	10	794
TGM1	0	0	0	0	0	0.00	1.19	1	0	3
TGM2	0	0	6	2	6	0.02	6.54	123	33	1659
TGM3	0	0	8	13	9	0.01	7.88	45	28	291
TGM4	0	0	0	3	3	0.01	6.58	119	0	1087
TGM5	0	0	5	4	1	0.00	6.36	111	0	544
HGM1	35	47	14	16	16	0.01	3.64	106	14	2
HGM2	48	7	10	14	4	0.00	1.37	14	0	3
HGM3	16	22	0	19	2	0.00	4.41	61	14	16
HGM4	23	5	0	2	10	0.02	1.97	53	9	30
HGM5	0	0	1	0	3	0.01	0.15	3	8	2
HGM6	0	0	15	0	28	0.01	11.06	54	0	3975
VGM1	21	68	165	14	135	0.01	6.70	855	95	870
VGM2	17	60	77	22	72	0.00	7.67	1481	23	1213
VGM3	0	0	4	15	12	0.00	5.95	520	6	332
VGM4	0	49	2	2	21	0.00	5.77	57	6	2129
VGM5	0	0	2	0	38	0.01	7.89	31	0	2668

APPENDIX II

GOLD AND SILVER COMPOSITIONS

	Au (ppb)	Ag (ppm)
HGM 1	219	0,4
HGM 2	‹5	-
HGM 3	‹5	-
HGM 4	11	1,4
HGM 5	5,6 (ppm)	0,2
HGM 6	‹5	-
HGM 7	6	0,2
TGM 1(A)	7	0,2
TGM 2	14	1,1
TGM 3	22	0,8
TGM 4	8	1,0
TGM 5	‹5	-
TS 1	‹5	-
TS 2	‹5	-
TS 3	‹5	-
TS 4	7	‹0,1
TS 5	‹5	-
TS 6	13	0,5
TS 7	16	0,9
TS 8	23	0,9
TS 9	‹5	-
TS 10	‹5	-
TS 11	‹5	-
TS 12	‹5	-
TS 13	‹5	-
TS 14	‹5	-
VGM 1	24	1,4
VGM 2	268	1,9
VGM 3	‹5	-
VGM 4	‹5	-
VGM A	257	-
VGM B	917	-
VGM C	695	-
VGM D	25	-
VGM E	208	-

Figur
Area.
and t
(Comp

31°18'

88
107
57
86
96
101
70
83
92
40
75
77
75
69
67
Times Prospect
83
64
63
60
61
81
52
56
28°35'
45
NYANI RIVER
41
40
50
37
?
31
34
?
35
28
70
19
27
24

TN

0 m

e 3.1 Geological Map of the Study
The Harewood and Vira Workings
he Times Prospect are Indicated.

iled by W Bullen)

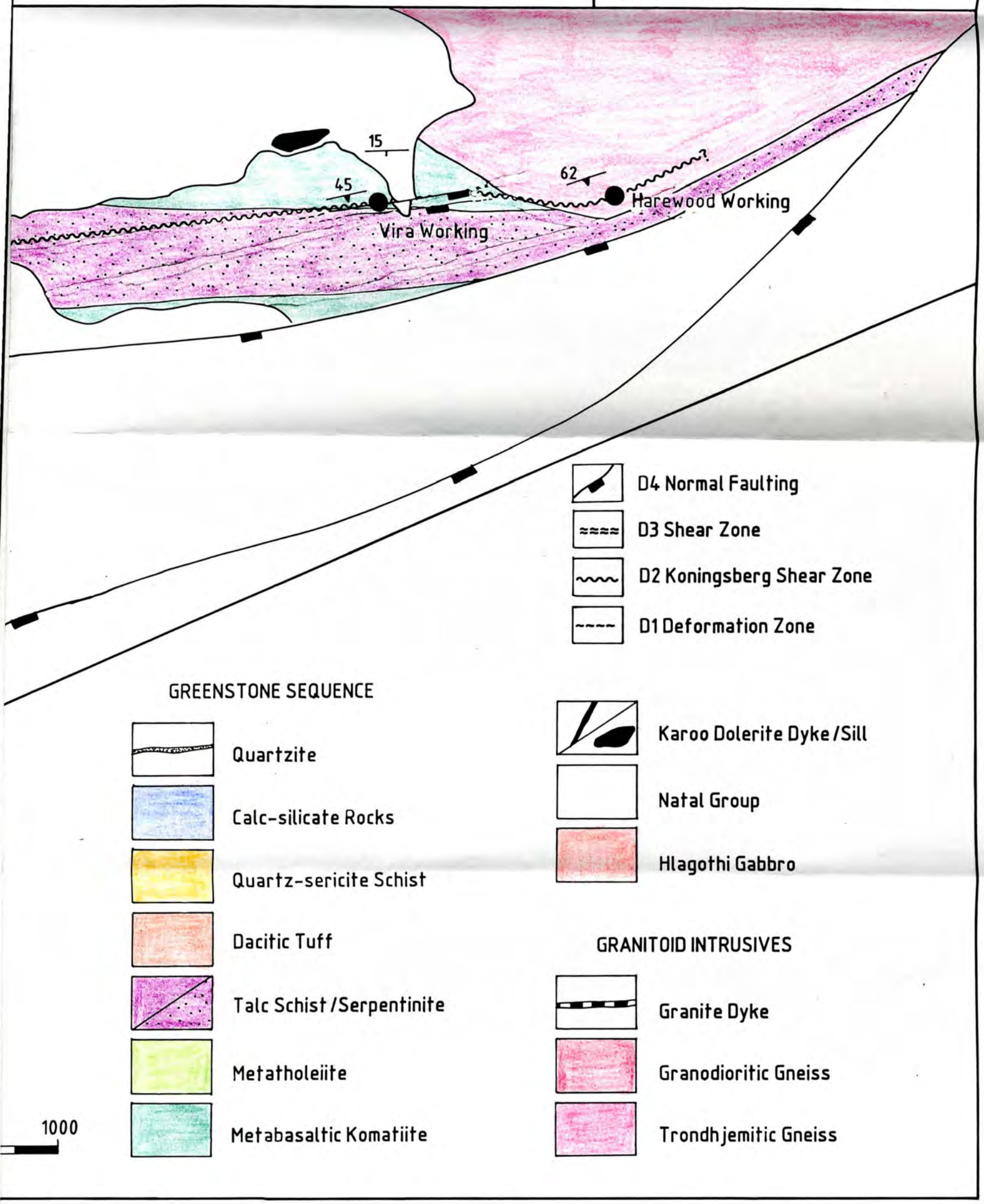

- Axial Trace of Syncline
- Axial Trace of Anticline
- 60 Crenulation Lineation
- 35 D2 Folding – Plunge of axial trace indicated
- 63 Locality Site and Number
- 75 Strike and Dip of Foliation
- 15 Strike and Dip of Bedding

- D4 Normal Faulting
- D3 Shear Zone
- D2 Koningsberg Shear Zone
- D1 Deformation Zone

GREENSTONE SEQUENCE

- Quartzite
- Calc-silicate Rocks
- Quartz-sericite Schist
- Dacitic Tuff
- Talc Schist/Serpentinite
- Metatholeiite
- Metabasaltic Komatiite

- Karoo Dolerite Dyke/Sill
- Natal Group
- Hlagothi Gabbro

GRANITOID INTRUSIVES

- Granite Dyke
- Granodioritic Gneiss
- Trondhjemitic Gneiss